2016

TOXICITY OF ENGINEERED NANOMATERIALS TO PLANT GROWTH PROMOTING RHIZOBACTERIA

Ricky W. Lewis
University of Kentucky, ricky.w.lewis@gmail.com
Digital Object Identifier: http://dx.doi.org/10.13023/ETD.2016.346

STUDENT AGREEMENT:

I represent that my thesis or dissertation and abstract are my original work. Proper attribution has been given to all outside sources. I understand that I am solely responsible for obtaining any needed copyright permissions. I have obtained needed written permission statement(s) from the owner(s) of each third-party copyrighted matter to be included in my work, allowing electronic distribution (if such use is not permitted by the fair use doctrine) which will be submitted to UKnowledge as Additional File.

I hereby grant to The University of Kentucky and its agents the irrevocable, non-exclusive, and royalty-free license to archive and make accessible my work in whole or in part in all forms of media, now or hereafter known. I agree that the document mentioned above may be made available immediately for worldwide access unless an embargo applies.

I retain all other ownership rights to the copyright of my work. I also retain the right to use in future works (such as articles or books) all or part of my work. I understand that I am free to register the copyright to my work.

REVIEW, APPROVAL AND ACCEPTANCE

The document mentioned above has been reviewed and accepted by the student's advisor, on behalf of the advisory committee, and by the Director of Graduate Studies (DGS), on behalf of the program; we verify that this is the final, approved version of the student's thesis including all changes required by the advisory committee. The undersigned agree to abide by the statements above.

Ricky W. Lewis, Student

Dr. Paul M. Bertsch, Major Professor

Dr. Mark S. Coyne, Director of Graduate Studies

TOXICITY OF ENGINEERED NANOMATERIALS TO PLANT GROWTH PROMOTING RHIZOBACTERIA

DISSERTATION

A dissertation submitted in partial fulfillment of the
requirements for the degree of Doctorate of Philosophy in the
College of Agriculture at the University of Kentucky

By

Ricky W. Lewis

Lexington, KY

Co-Directors: Dr. Paul M. Bertsch, Professor of Soil Chemistry

and Dr. David H. McNear Jr. Professor of Rhizosphere Science

Lexington, KY

2016

ABSTRACT OF DISSERTATION

TOXICITY OF ENGINEERED NANOMATERIALS TO PLANT GROWTH PROMOTING RHIZOBACTERIA

Engineered nanomaterials (ENMs) have become ubiquitous in consumer products and industrial applications, and consequently the environment. Much of the environmentally released ENMs are expected to enter terrestrial ecosystems via land application of nano-enriched biosolids to agricultural fields. Among the organisms most likely to encounter nano-enriched biosolids are the key soil bacteria known as plant growth promoting rhizobacteria (PGPR). I reviewed what is known concerning the toxicological effects of ENMs to PGPR and observed the need for high-throughput methods to evaluate lethal and sublethal toxic responses of aerobic microbes. I addressed this issue by developing high-throughput microplate assays which allowed me to normalize oxygen consumption responses to viable cell estimates. Oxygen consumption is a crucial step in cellular respiration which may be examined relatively easily along with viability and may provide insight into the metabolic/physiological response of bacteria to toxic substances.

Because many of the most toxic nanomaterials (i.e. metal containing materials) exhibit some level of ionic dissolution, I first developed my methods by examining metal ion responses in the PGPR, *Bacillus amyloliquefaciens* GB03. I found this bacterium exhibits differential oxygen consumption responses to Ag^{+}, Zn^{2+}, and Ni^{2+}. Exposure to Ag^{+} elicited pronounced increases in O_2 consumption, particularly when few viable cells were observed. Also, while Ni^{2+} and Zn^{2+} are generally thought to induce similar toxic responses, I found O_2 consumption per viable cell was much more variable during Ni^{2+} exposure and that Zn^{2+} induced increased O_2 utilization to a lesser extent than Ag^{+}. Additionally, I showed my method is useful for probing toxicity of traditional antibiotics by observing large increases in O_2 utilization in response to streptomycin, which was used as a positive control due to its known effects on bacterial respiration.

After showing the utility of my method for examining metal ion responses in a single species of PGPR, I investigated the toxicity of silver ENMs (AgENMs) and ions to three PGPR, *B. amyloliquefaciens* GB03*, Sinorhizobium meliloti* 2011*,* and *Pseudomonas putida* UW4. The ENM exposures consisted of untransformed, polyvinylpyrrolidone

coated silver ENMs (PVP-AgENMs) and 100% sulfidized silver ENMs (sAgENMs), which are representative of environmentally transformed AgENMs. I observed species specific O_2 consumption responses to silver ions and PVP-AgENMs. Specifically, *P. putida* exhibited increased O_2 consumption across the observed range of viable cells, while *B. amyloliquefaciens* exhibited responses similar to those found in my first study. Additionally, *S. meliloti* exhibited more complex responses to Ag^+ and PVP-AgENMs, with decreased O_2 consumption when cell viability was ~50-75% of no metal controls and increased O_2 consumption when cell viability was <50%. I also found the abiotically dissolved fraction of the PVP-AgENMs was likely responsible for most of the toxic response, while abiotic dissolution did not explain the toxicity of sAgENMs.

My work has yielded a straightforward, cost-effective, and high-throughput method of evaluating viability and oxygen consumption in aerobic bacteria. I have used this method to test a broad range of toxic substances, including, metal ions, antibiotics, and untransformed and transformed ENMs. I observed species specific toxic responses to Ag^+, PVP-AgENMs, and sAgENMs in PGPR. These results not only show the clear utility of the methodology, but also that it will be crucial to continue examining the responses of specific bacterial strains even as nanotoxicology, as a field, must move toward more complex and environmentally relevant systems.

KEYWORDS: engineered nanomaterial, plant growth promoting rhizobacteria, metal toxicity, nanotoxicology, respiration stress, high-throughput respiration assay

Ricky W. Lewis

July 28, 2016

TOXICITY OF MANUFACTURED NANOMATERIALS TO PLANT GROWTH PROMOTING RHIZOBACTERIA

By

Ricky W. Lewis

Dr. Paul M. Bertsch
Co-Director of Dissertation

Dr. David H. McNear Jr.
Co-Director of Dissertation

Dr. Mark S. Coyne
Director of Graduate Studies

July 28, 2016

Dedication

This work is dedicated to my father, George Elmer Lewis Sr. Throughout his life, my father worked tirelessly to ensure the well-being of his family and gave all he had so that we could better ourselves. It is also dedicated to my mother, Hallie M. Lewis, and to my wife, Tara L. B. Lewis. Without their encouragement and guidance, you would certainly not be reading this.

ACKNOWLEDGEMENTS

This dissertation represents the culmination of years of hard work that would have been impossible without a team of outstanding people. Firstly, I would like to acknowledge my advisors and advisory committee for their guidance and assistance throughout this process. Drs. David H. McNear Jr. and Paul M. Bertsch have assisted me greatly in experimental design and troubleshooting and in manuscript preparation. Drs. Mark Coyne and Daniel Pack assisted me with general questions regarding experimental troubleshooting and methodology.

Additionally, I would like to acknowledge Dr. Jason Unrine for assistance with ICP-MS and for his keen insights regarding the experiments and results presented here. Dr. Olga Tsyusko also generously provided many useful insights regarding experimentation and interpretation of the results. Through discussion, Zeinah Baddar assisted me with nanoparticle characterization and with general laboratory protocols. Others from the Ecotoxicology laboratory at the University of Kentucky I wish to acknowledge include, Jonathan Judy, Chen Chun, Anye Wamucho, Shristi Shrestha, Emily Oostveen, and Daniel Starnes. I would also like to acknowledge Joseph V. Kupper from the Rhizolab at the University of Kentucky for assistance with general laboratory practices and thought experimentation, and encouragement throughout my tenure at the University of Kentucky. Additionally, I acknowledge Ann Freytag for assistance with microbiological practices and her untiring encouragement, and Mark Maxey for technological assistance.

TABLE OF CONTENTS

LIST OF TABLES

LIST OF FIGURES

Chapter 1: Nanotoxicological Studies of Environmentally Relevant Engineered Nanomaterials and Beneficial Soil Bacteria – A Critical Review

1.1 Introduction

Engineered nanomaterials (ENMs), human made materials with at least one dimension between 1-100 nm[1], possess unique physical and chemical properties that emerge at the nanoscale[2], and this may be exploited to create new materials or to enhance a seemingly endless number of extant materials. The rapid increase in ENM containing products entering the market is coupled with an inevitable increase of intentional and unintentional releases to the environment[3]. Understanding the potential impact of ENMs to ecosystem and human health is critical[4-6].

Much of the research on the environmental toxicology of ENMs has focused on aquatic organisms[7, 8]; however, material flow analysis and risk evaluation suggests many ENMs will ultimately be deposited in the soil environment[9, 10]. There is growing interest in the study of ENM behavior in terrestrial systems, but research is ongoing and the complexities of working with nanoscale materials (i.e. system induced particle transformation) have posed significant challenges[1, 10-12]. Soil microorganisms are the primary drivers of ecosystem processes and functions, including nutrient and carbon cycling, and maintenance of soil health[13, 14]. An important subset of bacteria found to directly and indirectly promote the growth of plants are known as plant growth promoting rhizobacteria (PGPR), and they play key roles in various processes related to plant health, including, plant responses to pathogens, drought tolerance, and nutrient acquisition.

Given the importance of PGPR to plant health, terrestrial ecosystem function, and agricultural production, understanding potential impacts of ENMs to these organisms

should be a priority. Despite the obvious importance of PGPR, there is very little research examining the effects of ENMs on this key class of microbes. Additionally, as is the case with numerous nanotoxicological studies, the complex behavior of ENMs has posed a hurdle to understanding PGPR-ENM interactions. This is of particular concern in studies examining bacterial responses to ENM exposure in rhizosphere and bulk soils, where the heterogeneous soil environment and biological activity may lead to various ENM transformations. As such, a mechanistic understanding of ENM-bacteria interactions has primarily been pursued using pure-culture methods (where solution chemistry can be easily controlled) and "pristine" ENMs (which have not undergone environmental transformations).

However, pristine ENMs are still subject to media/matrix induced transformations in pure-culture systems, so it is necessary to thoroughly characterize ENMs, even in relatively minimal exposure media, for nanotoxicological studies. Along with primary particle size, important particle characteristics to consider are particle dissolution, aggregation status, size distribution, and zeta-potential/electrophoretic mobility, which should all be measured in the exposure medium. After particle characterization, one may design experiments including necessary positive and negative controls. In studies where nanomaterials remain uncharacterized or particle transformations are not controlled for, it is difficult to determine the role of nanoscale properties in the toxicity of the materials.

Still, a growing body of literature has examined the toxicity of several environmentally relevant nanomaterials to PGPR and related species. In this review, I critically examine the literature regarding PGPR-ENM interactions and suggest a path forward to clarify and identify toxicity mechanisms of ENM to bacteria. I also include

some key findings involving non-PGPR species of bacteria, when relevant to the discussion. Since metal containing ENMs are known to be toxic to bacteria and are expected to increase dramatically in all environmental compartments, this review focuses primarily on the responses of PGPR to metal containing nanomaterials.

1.2 AgENMs and PGPR

Silver containing nanomaterials are among the most highly produced nanomaterials commercially available, and environmental concentrations are expected to rise significantly[9]. While silver has been used by humans since antiquity as an antibiotic and, more recently, for its use as an electrical conductor and in the photography industry, the unique physiochemical properties of nanomaterials raise many questions regarding possible effects of environmental release. Understanding bacterial responses to AgENM both in pure-culture and in the environment remains difficult for a number of reasons, (i) AgENMs readily undergo dissolution in aerobic environments and the mechanisms of toxicity and resistance/tolerance of silver ions are still not clearly understood, (ii) there is uncertainty regarding the toxicity of environmentally transformed particles, namely, sulfidized AgENMs, (iii) AgENMs may interact with cells directly, (iv) AgENMs and Ag^{+} may generate ROS, (v) there is debate regarding the relative importance of particle size, shape, surface charge, and surface area on bacterial toxicity. Despite the difficulty in examining AgENM toxicity mechanisms, the abundant uses and expected environmental release of such particles has produced considerable research. However, very few studies have focused on the responses of PGPR to silver nanoparticles, or any other nanoparticles for that matter.

It is valuable to examine some of the most prominent publications regarding AgENM toxicity to bacteria to highlight what is currently known. While not a PGPR, many highly cited papers regarding the toxicity of AgENMs to bacteria use the model gram-negative bacteria, *Escherichia coli*, as a test organism. The work of Sondi and Sondi[15] examined the toxicity of AgENMs to *E. coli* by monitoring growth rates in Luria-Bertani (LB) medium or CFU counts on agar plates, where both media types were spiked with particles. On solid medium, they found roughly a 30 % reduction in CFU/mL in response to 93 μM AgENM, and observed 463 and 923 μM AgENM extended lag phases in liquid medium.

Another major finding of Sondi and Sondi[15], was that silver nanoparticles may attach to and cause "pitting" of the bacterial surface. A finding that has been confirmed by some studies[16], but not all[17], and there is no clear understanding of the mechanisms governing this phenomenon. Additionally, there is now evidence that many bacterial species may form nanoparticles extracellularly or intracellularly[18] and that nanoparticles may be formed from commonly used staining agents used in transmission electron microscopy[12].

Other studies have examined the role of nano-specific responses compared with responses to the dissolved fraction of AgENMs. One such study utilizes the fact that dissolution is minimal in anaerobic conditions and showed AgENMs were toxic to *E. coli* ATCC 25404 in aerobic conditions but not anaerobic conditions, while Ag^+ demonstrated similar toxicity in either condition [19]. While these results suggest the mechanism of toxicity in *E. coli* is driven primarily by dissolution of Ag^+, it is not clear how other alterations in microbial physiology may have affected the response to AgENMs in aerobic versus

anaerobic conditions. Additionally, others have found, in a well characterized system, that nano-specific patterns of global gene expression may occur in *E. coli* and that these patterns are altered by particle coatings[20]. Clearly, there is still much to understand regarding the toxicity of nanomaterials to bacteria compared with their bulk or ion equivalents; nonetheless, in the following sections, I review what is known concerning AgENM toxicity to PGPR.

1.2.1 AgENMs and the *Bacillus* genus

The *Bacillus* genus is utilized to generate most commercially developed PGPR, primarily because this genus forms endospores resulting in environmentally stable products with long shelf-lives[21]. *Bacillus subtilis* is a model bacterium[22] of great ecological, agricultural, and economic importance that possesses an intimate connection with the human, plant, and soil microbiomes. Many *B. subtilis* strains demonstrate plant growth promoting capabilities that have been primarily attributed to disease suppression and production of antibiotics, as discussed by Kokalis-Burelle et al.[21]. Additionally, *B. subtilis* and related species may induce systemic resistance in plants yielding enhanced resistance to many common pathogens[23].

Various strains of *B. subtilis* have been used to examine the toxicity of many ENMs[8, 11, 24]. Of all the studies examining ENM toxicity to *B. subtilis* as reviewed by Maurer-Jones et al.[8], one study examines the toxicity of particle-microbe interactions in pure water in the absence of potentially confounding medium constituents[25]. In this study, the authors specifically investigate assay dependent influences on toxicity measurements and found that either gram-positive or gram-negative bacteria appear to be more susceptible to ENMs depending on the assay used.

Ruparelia et al.[26], showed different strains of the same bacterial species may respond differently to silver and copper nanoparticles. For instance, the minimum inhibitory concentration (MIC) of silver nanoparticles to *E. coli* MTCC 443 was 0.37 mM, which was the same for *B. subtilis* MTCC 441, while *E. coli* MTCC 739 and MTCC 1302 had MIC's of 1.67 mM and 1.11 mM, respectively. Toxicity of AgENMs to the different strains of *Staphylococcus aureus* (NCIM 2079, 5021, and 5022) resulted in the same MIC value (1.1 mM). Feng et al.[27] found the gram-positive bacteria, *Staphylococcus aureus*, to be more resistant to silver ions than *E. coli*, while Yoon et al.[28] found *B. subtilis* to be more sensitive to both silver and copper nanoparticles than *E. coli*. Jin et al.[29] found *Pseudomonas putida* to be generally more resistant to $AgNO_3$ and AgENMs compared with *Bacillus subtilis*, but that mortality responses were greatly influenced by the presence of ions (i.e. Ca^{2+}, Mg^{2+}, Na^{+}, K^{+}, SO_4^{2-}, Cl^{-}, HCO_3^{-}) in solution. In another study, the toxicity of nano-colloidal silver to several gram-negative and gram-positive bacteria (including *Bacillus cereus*) demonstrated toxicity was independent of gram stain status[30]. These results clearly show that any generalizations made regarding the responses of gram-positive versus gram-negative bacteria in pure-culture are likely influenced by the test organisms and exposure media used in existing studies.

Suresh et al.[31] examined the toxicity of $AgNO_3$, biogenic AgENMs (prepared by incubating *Shewanella oneidensis* MR-1 in $AgNO_3$ solution), Ag colloids, and oleate-AgENMs to *B. subtilis* ATCC 9372, *S. oneidensis* MR-1, and *E. coli* ATCC 25922. They found $AgNO_3$ to be most toxic, but that biogenic particles were the most toxic of the ENM or colloids, even though the oleate-AgENMs were similar in size to the biogenic particles (Table 1.1). Atomic force microscopy (AFM) showed the biogenic particles were capable

of inducing significant membrane damage to ~10% of *B. subtilis* cells, but not *E. coli*. The Ag colloids were found to associate strongly with *E. coli,* but less so with *B. subtilis*. Notably, the authors measured dissolution of the particles in LB medium (the exposure solution) and found that the concentration of Ag^+ from dissolution did not explain the increased toxicity of the biogenic ENMs. Particle-cell interactions are known to enhance toxicity[32] and an increasing number of papers suggests AgENMs may not readily dissolve in some media, but after contact with the cell, may release Ag^+ ions, thus explaining much of the toxicity[33]. In some studies, biotic driven dissolution of AgENMs and intracellular silver concentrations appear to play a more important role in ENM toxicity than the abiotic dissolved fraction[20, 32]. However, it is clear from transcriptomic studies that the pattern of gene expression in *E. coli* was different for $AgNO_3$ compared to AgENMs[20, 34]; a pattern that was also influenced by particle coatings and size[20]. These studies show that, while intracellular Ag concentrations may sometimes be a good predictor of toxicity, there are certainly many other important aspects of particle-cell interactions influencing toxicity.

Table 1.1 Summary of nanotoxicology studies involving AgENMs and PGPR or related species

Species	Strain	Synthesis	Primary Particle Size (nm)	Suspended Particle Size (nm)	Coating/stabilizing agent	Surface Charge	Ion/Bulk Controls	Dissolution	Exposure Medium	Findings	Ref.
P. aeruginosa	n/r	commercial	16	n/r	n/r	n/r	n/a	yes	Luria-Bertani	695 µM inhibited growth on agar plates Particles ~10 nm to adhere to surface	16
B. subtilis	n/r	commercial	40	n/r	n/r	n/r	n/a	no	Nutrient Agar - unspecified composition	C_{90} = 297 µM	28
B. subtilis	ATCC6633	*in-house*	3	12 to 21	n/a	n/r	n/a	no	liquid: peptone + NaCl (5g/L each) yeast extract + beef extrack (1.5 g/L each) Solid: Liquid + 2% bacteriological agar	MIC = 370 µM, MBC = 556 µM, DIZ = 11 mm	
P. fluorescens	SBW25	commercial	65-100	n/r	sodium citrate	Electrophoretic mobility = -2.5 to -	Ions: $AgNO_3$	yes	MDM	Humic acid stablized particles, aggregates formed without	38
										Humic acid reduced toxicity of AgENM more than ion after 3 h	
										pH 7.5 decreased AgENM toxicity and dissolution after 24 h	
										pH 9 increased dissolution of AgENM, large reduction in growth at 19 µM, but not at pH 6 or 5.7	
P. putida	OUS82	commercial	65-100	n/r	sodium citrate	Electrophoretic mobility = -2.5 to -4 $cm^2/v/s$	n/a	yes	MDM	Biofilm biovolume per surface area reduced at pH 6 without fulvic acid at 0.19 to 19 µM AgENM	39
										Biofilm biovolume per surface area reduced at pH 7.5 without fulvic acid at 1.9 to 19 µM AgENM	
										Fulvic acid inreased Ag uptake in biofilms but reduced effect on biovolume per surface area	
P. putida	mt-2 KT2440	commercial	10 (supplier)	n/r	n/r	n/r	Ions: $AgNO_3$	no	sterile distilled water	>1.9 µM AgENM caused loss of light emission	47
							Bulk: Ag (44 µm , supplier)				
B. subtilis	ATCC9372	*in-house* (biogenic)	4	83	protein/peptide (FTIR)	Zeta-potential = 12 mV	Ions: $AgNO_3$	yes	liquid: LB Solid: LBA medium	MIC = 5 µM biogenic AgENM	31
		in-house	4	46	oleate	Zeta-potential = 45.8 mV				Not toxic ≤70 µM oleate-AgENM	
		in-house	9	63	pyridine	Zeta-potential = 42.5 mV				MIC = 19 µM pyridine-Ag colloid	
B. subtilis	n/r	commercial	15-35	10 to 100	n/r	Zeta-potential = -10 to -60 mV	Ions: $AgNO_3$	yes	Varied - testing influence of specific ions, pH not controlled	IC_{50} = 19-260 µM (*B. subtilis*)	29
P. putida	n/r				n/r					IC_{50} = 19 to > 460 µM (*P. putida*)	

Table 1.1 Summary of nanotoxicology studies involving AgENMs and PGPR or related species (continued)

Species	Strain	Synthesis	Primary Particle Size (nm)	Suspended Particle Size (nm)	Coating/stabilizing agent	Surface Charge	Ion/Bulk Controls	Dissolution	Exposure Medium	Findings	Ref.
P. putida	BS566::luxCDABE	commercial	35 (supplier)	n/r	citric acid	n/r	Ions: $AgNO_3$	no	Luria-Bertani	IC50 values were time and capping agent dependent	48
					bovine serum albumin (BSA)		Microparticles: Ag (0.6-1.6 µm, supplier)			Lowest IC_{50} for AgENM without stabilizer: 750 µM at 90 m	
										Lowest IC_{50} for AgENM with BSA: 324 µM at 90 m	
										Lowest IC_{50} for AgENM with citric acid: 1,200 µM at 90 m	
P. chlororaphis	O6	commercial	10 (supplier)	70-90	none	Zeta-potential = -33 to -35 mV	Ions: $AgNO_3$	yes	sterile deionized water		51
							Bulk: Ag (44 µm , supplier)				
B. subtilis	ATCC6633	*in-house* (biogenic)	9	36	protein/peptide (FTIR)	Zeta-potential = -1 mV	n/a	no	Luria-Bertani	≤ 1.4 mM sAgENM were not toxic	60
B. subtilis	NRS-744	commercial	< 100 (supplier)	n/r	polyvinylpyrrolidone	n/r	Bulk: Ag	no	medium (%, w/v): peptone(0.5), yeast extract (0.5), dextrose (1.0), NaCl (0.25)	ZnO ENMs were more toxic than AgENMs	67
B. subtilis	KACC10111	commercial	10 (supplier)	104-118	citrate	n/r	Ion: Ag^+ ($AgNO_3$)	yes	LB	0.23 uM AgENMs nearly led to complete inhibition of growth	25
										Dissolution did not explain response	
P. fluorescens	ATCC13525	commercial	Low stability: 30-50 (supplier)	20-600	polyvinylpyrrolidone	n/r	Ions: $AgNO_3$	yes	MDM	Stabilized AgENM penetrate biofilms, but aggregates do not	40
		in-house	High stability: 18.6 (previously characterized)		polyvinylpyrrolidone	n/r				EPS and humic acid limits penetration of silver ions into biofilms	
										Particle free suspension toxicity is driven by Ag ions	
										930 µM AgENM of low or high stability reduced viability by 70 and 90%, respectively	
S. meliloti	RM 2021	commercial	10-100	n/r	sodium citrate	n/r	Ions: $AgNO_3$	yes	Luria-Bertani	EPS overproducing strains are more resistant to AgENMs	86
	RM 7096								M9	80 µM AgENMs reduced viability to < 30% in RM 1021 and 7210, but only to 70% in RM 7096	
	RM 7210									Dissolution did not explain responses	

Table 1.1 Summary of nanotoxicology studies involving AgENMs and PGPR or related species (continued)

Species	Strain	Synthesis	Primary Particle Size (nm)	Suspension Particle Size (nm)	Coating/stabilizing agent	Surface Charge	Ion/Bulk Controls	Dissolution	Exposure Medium	Findings	Ref.
P. aeruginosa	CCM 3995	*in-house*	9-30	n/r	sodium dodecyl sulfate (SDS)	n/r	n/a	no	Mueller-Hinton Broth/agar plates	SDS stabilized AgENMs generated through reduction of $AgNO_3$ with hydrazine hydrate induced the greatest toxicity in *P. aeruginosa.*	49
										MIC = 62 µM	
P. aeruginosa	PA01	commercial	8 (supplier)	47*	citric acid	Zeta-potential = -42 mV	Ions: $AgNO_3$	no	Phosphate Buffered Saline	93 uM Ag+ or AgENMs equally inhibited biofilms with stirring	42
				*reported "ELS"						no toxicity was observed of AgENMS in static conditions	
P. aeruginosa	PA01	commercial	8.3	n/r	hydrolized casein peptides	n/r	Ions: $AgNO_3$	no	Nutrient Broth/Agar (Difco)	*P. aeruginosa* biofilm formation inhibited at 93 µM AgENM when stirred, no effect when static	41
P. chlororaphis	449									MIC = 74 µM AgENM for *P. aerugionosa* and *P. chlororaphis*	
P. putida	mt-2 KT2440	commercial	38.8	Stock: 82.2	n/r	n/r	n/a	no	minimal medium (mg/L): KH_2PO_4 (2000), Na_2HPO_4 (5583), $FeNH_4$-citrate (10), $MgSO_4 \times 7H_2O$ (200), $(NH_4)_2SO_4$ (1000), $Ca(NO_3)_2 \times 4 H_2O$ (50), $ZnSO_4 \times 7H_2O$ (0.1), $MnCl_2 \times 4H_2O$ (0.03), H_3BO_3 (0.3), $CoCl_2 \times 6 H_2O$ (0.2), $CuCl_2 \times 2 H_2O$ (0.01), $NiCl_2 \times 6 H_2O$ (0.02), $Na_2MoO_4 \times 2H_2O$ (0.03)	4.6 µM AgENMs completely inhibited biofilm growth n mt-2	44
P. putida	PaW340			Growth Medium: 254.1						0.74 and 4.6 µM inactivated cells of established biofilms	
P. aeruginosa	PG201	*in-house*	9	n/r	L-cysteine	MMD: Zeta-potential = -18 mV	Ions: $AgNO_3$	yes	Modified Minimal Davis (MMD) or LB medium	Dissolution of Ag+ explained toxic resposnes in either media	57
						LB: Zeta-potential = -6 mV				ROS generation and membrane damage induced by AgENMs	
Pseudomonas sp.	unspecified	commerical	20-30 (supplier)	n/r	n/r	n/r	n/a	no	minimal medium (g/L): K_2HPO_4 (10.5), KH_2PO_4 (4.5), sodium citrate ($2H_2O$) (0.5) , $(NH_4)_2 SO_4$ (1), $MgSO_4.7H_2O$ (0.25), and glucose (1)	AgENMs induced upregulation of proteins and mRNA transcripts of ribosomal proteins S2 and L9, alkyl hydroperoxide reductase/thiol-specific antioxidant (AhpC/TSA) family protein, and keto-hydroxyglutarate aldolase (KHGA)	58
										MIC = 1.9 µM	

Table 1.1 Summary of nanotoxicology studies involving AgENMs and PGPR or related species (continued)

Species	Strain	Synthesis	Primary Particle Size (nm)	Suspension Particle Size (nm)	Coating/stabilizing agent	Surface Charge	Ion/Bulk Controls	Dissolution	Exposure Medium	Findings	Ref.
P. putida	BS566::luxCDABE	commercial	15 (supplier)	LB: ~150	uncoated/dispersed in polyoxyethylene glycerol tioleate and Tween 20	n/r	Ion: Ag^+ ($AgNO_3$)	yes	LB	AgENMs had 4% dissolution in LB and 2% in AW after 60 min	71
				AW: <100					Artificial Wastewater (AW)	≥ 232 µM AgENMs reduced relative fluorescence to to near zero from 1-2 hours in LB or AW	
										AgENM toxicity driven by ions	
										IC_{50} of AgENMs was 37 - 574 µM	
P. putida	mt-2 (DSM6125)	commercial	10 (supplier)	n/r	sodium citrate	n/r	Ions: $AgNO_3$	no	mineral salt medium + 4 g Na_2-succinate /50 mL	3.25 µM AgENM completely inhibited growth	55
										1.75 µM Ag+ completely inhibited growth	
										Ag+ and AgENM increased trans:cis ratio of fatty acids (increased membrane fluidity)	
P. putida	DSM 50026	commercial	10 to 50	Stock: 53 (nanoparticle tracking analysis)	citrate, tannic acid, not specified (used various stabilizing agents)	n/r	Ions: $AgNO_3$	no	minimal medium (mg/L): $NaNO_3$ (500), KH_2PO_4 x $3H_2O$(120), KH2PO4 (60), $C_6H_{12}O_6$ (2000), $MgSO_4$ x $7H_20$ (200), Iron(III) citrate (0.5)	EC50 = 1.5 nM Ag+	59
										EC50 = 2.3 to30 nM AgENM	
B. subtilis	Cu1065	commercial	8.3 (supplier)	n/r	polyvinylpyrrolidone	Zeta-potential = -19 mV (supplier)	n/a	no	tryptic soy broth	Inhibited growth at 930 µM	17
										Intracellular ROS (planktonic cells), 9.3 µM reduced and 93 µM increased	
										Reduced protein biomass in biofilms at 93 µM	
										Biofilm ROS, AgENMs have no effect or decrease	
										Biofilm Polysaccharide content, increased by AgENMs	
										Phosphate solubilization increased with AgENMs addition	
										Intracellular AgENMs, but no membrane damage	
										No effect on swimming or swarming motility	

Table 1.1 Summary of nanotoxicology studies involving AgENMs and PGPR or related species (continued)

Species	Strain	Synthesis	Primary Particle Size (nm)	Suspended Particle Size (nm)	Coating/stabilizing agent	Surface Charge	Ion/Bulk Controls	Dissolution	Exposure Medium	Findings	Ref.
P. aeruginosa	PA01	commercial	10 (supplier)	105	polyvinylpyrrolidone	Zeta-potential = -25 mV	Ions: $AgNO_3$	yes	Davies minimal nutrient broth	0.2 µM AgENM increased protein and carbohydrate content	43
										0.2 to 1 µM AgENM induced quorum sensing	
										0.2 µM AgENM induced antibiotic resistance genes	
P. putida	mt-2 KT2440	*in-house*	n/r	40-60	polyvinyl alcohol	Zeta-potential = -2 to -6 mV	n/a	yes	Luria-Bertani	Stripping EPS from biofilms enhanced AgENM toxicity	46
										More mature biofilms were more resistant to AgENMs	
P. aeruginosa	ATCC 27317	laboratory supplied	18-40	n/r	citrate	n/r	Ions: $AgNO_3$	no	PBS	Citrate capped AgENMs were less toxic than 110mercaptoundecanoic acid capped particles	53
					11-mercaptoundecanoic acid						
P. aeruginosa	ATCC 10145	*in-house*	7	10 to 30	nitroxide coatetd	n/r	n/a	no	MH medium	MIC = 40 to 150 µM depending on synthesis procedure	54

n/r is “not reported”, n/a is “not applicable”, ref is “reference”

Perhaps the most extensive study on responses of a single PGPR species to AgENMs to date is the work of Gambino et al.[17]. The authors examined growth responses of planktonic cells of *B. subtilis* Cu1065 and *Azotobacter vinelandii* UW136 to commercially purchased AgENMs and found ~930 μM AgENM in Tryptic Soy Broth (TSB) was required to induce reduction in *B. subtilis* growth, while as little as ~0.93 μM AgENM significantly reduced generation times of *A. vinelandii*. Imaging via transmission electron microscopy (TEM) showed non-homogenous distribution of the particles on the surface and within planktonic *B. subtilis* cells, while no membrane damage was observed. This finding suggests particle dissolution followed by uptake of Ag^+ and intracellular formation of nanoparticles. The authors also utilized a number of assays to examine metabolic and functional responses of *B. subtilis* planktonic cells to AgENMs and found no effect on swarming or swimming motility, production of indole-3 acetic acid (IAA) or siderophores, but increased solubilization of inorganic phosphate. Intracellular ROS levels were significantly reduced by relatively low concentrations of AgENM (~9.3 μM), but increased in response to ~93 μM in planktonic cells, while intra/extracellular ROS levels were either unaltered or reduced by AgENMs in *B. subtilis* biofilms. Total protein levels were found to be reduced at 2-3 days of growth in biofilms by 93 μM AgENM while 9.3 μM increased total protein at 4 days; however, no influence on total protein was observed after 8 days of growth by either treatment.

Importantly, both 9.3 and 93 μM AgENM were found to markedly increase production of extracellular polymeric substances (EPS) in five-day old *B. subtilis* biofilms, while no significant effects were observed on concentrations of environmental DNA (eDNA – DNA released from the cells) or total protein. Increased EPS production in

response to AgENM exposure is particularly relevant given that addition of EPS to *E. coli* cultures exposed to Ag^+ led to reduction of ions to nanoparticles, which mitigated toxicity[35]. Gene ontology (GO) analyses showed upregulation of proteins from several annotated GO term groups in *B. subtilis* biofilms exposed to 9.3 and 93 μM AgENMs.

Stress response proteins were related to oxidative stress and redox status of the cell along with other stress responses. Proteins involved in primary metabolism, transcription, translation, and quorum sensing were also upregulated. While the work of Gambino et al.[17] is expansive and informative, there is a need to clarify the mechanisms underlying the observed responses by including silver ion controls, and characterization of AgENMs in the exposure medium in future studies.

1.2.2 AgENMs and the *Pseudomonas* genus

Fluorescent pseudomonads may provide plant growth promotion via biocontrol of soil borne fungal pathogens[36]. These microbes suppress growth of fungal pathogens in the rhizosphere by producing antifungal metabolites, which act upon the fungi, and iron chelators, which reduce the availability of Fe to other competing microbes, as discussed in Haas and Keel[36]. At least one strain of *Pseudomonas fluorescens*, CHA0, is capable of producing 2,4-diacetylphoroglucinol, a molecule exhibiting antifungal activity as well as bactericidal and phytotoxic activity[37].

Much research has been directed at understanding the effects of AgENMs on biofilm formation in the *Pseudomonas* genus. Fabrega et al.[38] examined the influence of organic matter and pH (6, 7.5, and 9) on the toxicity of AgENMs to *P. fluorescens* in Minimal Davidson Medium (MDM). An elevated pH of 9 greatly increased the toxicity of AgENMs to the bacterium at 18.5 μM. Suwannee River humic acids (SRHA) at 10 mg/L

completely mitigated the toxic responses after 24 hours of exposure and even induced growth after 3 hours of exposure relative to SRHA minus controls. Fabrega et al.[39] also examined the effect of pH and organic matter on AgENMs to *P. putida* OUS82 biofilms, also in MDM. Here the authors reported significant reductions in biovolume per surface area (BVSA) of the biofilms exposed to 0.185, 1.85, and 18.5 μM AgENMs at pH 6 and found similar reductions under 1.85 and 18.5 μM AgENMs at pH 7.5. Under both pH conditions 10 mg/L Suwannee River fulvic acid (SRFA) mitigated the effect on BVSA even as SRFA increased Ag uptake by biofilms at 18.5 μM silver. Given that only 18.5 μM AgENM was found to reduce viability at pH 6 by Fabrega et al.[38], these results indicate that biofilm BVSA may be a more sensitive end-point for AgENM toxicity.

Polyvinylpyrrolidone (PVP) coated AgENMs with either low or high stability effectively reduced biomass of established *P. fluorescens* biofilms in MDM, with the more stable particles exhibiting greater toxicity[40]. Natural organic matter (humic acid) was found to mitigate toxicity of both particle types and their particle free supernatants. Particle specific effects were more prominent in the highly stable particle type, as the particle-free supernatant explained less of the toxic responses compared with the low stability particles, particularly at higher tested concentrations (~93-930 μM AgENM).

In a study by Radzig et al.[41]. Biofilm formation of *Pseudomonas aeruginosa* PAO1 was significantly inhibited by 93 μM hydrolyzed casein stabilized AgENM in Nutrient Broth medium. Additionally, the Luxl/LuxR quorum sensing systems were not found to be involved in the response. Citric acid stabilized AgENM or Ag^{+} had equal inhibitory effects on *P. aeruginosa* PAO1 biofilms at 93 μM when the exposure solution (PBS buffer) was stirred, with no observed effect of the AgENMs in static conditions[42].

Yang and Alverez[43] found 0.2 or 1 μM PVP coated AgENMs (PVP-AgENMs) significantly induced the quorum sensing genes, LasR and Lasl, respectively in *P. aeruginosa* PAO1 in Davies minimal nutrient broth. LPS biosynthesis genes were also upregulated in response to 0.2 or 1 μM PVP-AgENMs, *sagS* and *pslA*, respectively, and 0.2 μM PVP-AgENMs was found to increase carbohydrate and protein concentrations in the biofilm matrix. Antibiotic resistance genes were induced by 0.2 μM PVP-AgENMs. Ion controls showed that often equimolar concentrations of PVP-AgENMs induced stronger responses than Ag^{+} (quorum sensing, LPS biosynthesis, and antibiotic resistance). Radzig et al.[41] also observed DNA damage in *E. coli* in response to AgENMs and increased resistance to AgENMs in mutant strains deficient in either OmpF or OmpC, both are outer membrane proteins.

Hartman et al.[44] developed a modified chip calorimetric method to examine effects of nanoparticles on growth inhibition and inactivation of *Pseudomonas putida* mt-2 KT2440 and PaW340 grown on agarose beads. Crystal violet staining of biofilms was insufficient to determine cell densities compared with traditional CFU counts. As little as 0.09 μM AgENM slightly inhibited biofilm formation, while 4.6 μM AgENM completely inhibited biofilm growth of *P. putida* mt-2. Both 0.74 and 4.6 μM AgENM significantly inactivated cells of established biofilms. Roughly 9.3 μM AgENMs were sufficient to damage biofilms of *Pseudomonas putida* PaW340. AgENMs were found to heavily aggregate in the minimal exposure medium (Table 1), demonstrating a mean diameter of 42 in stocks and 675 nm in solution. It is unclear what influence the exposure medium may have had on the toxicity of AgENMs as the minimal medium contained multiple sources of Cl^{-} (which has been shown to enhance availability of sAgENMs, sulfidized AgENMs,

in terrestrial environments[45]) and SO^{4-} (which could result in low solubility Ag_2SO_4 precipitates).

Growth stage of *P. putida* KT2440 biofilms was also found to influence responses to polyvinyl alcohol stabilized AgENMs in LB medium, with stage 3 (48 h) biofilms showing a greater tolerance to the particles than stage 1 (12 h) or 2 (30 h) biofilms[46]. Stripping EPS from biofilms was found to significantly enhance nanoparticle toxicity[46], adding to the growing body of literature showing the importance of the biofilm matrix in particle-biofilm interactions.

Many studies have also examined the effects of AgENMs on various planktonic *Pseudomonas* species. For instance, Radzig et al. found an MIC of 53 μM AgENMs in planktonic cultures of *P. aeruginosa* and *P. chlororaphis*[41]. Gajjar et al.[47] examined the toxicity of commercially available Ag, ZnO, and CuO nanoparticles to *P. putida* KT2440, which emits light as a measure of energy production, exposed in sterilized water. The authors found a good correlation between the loss of lux and CFU counts of exposed bacteria; however, AgENMs were uncharacterized and field flow fractionation revealed CuO and ZnOENMs had a broad size range of poly-dispersed nanoparticles, with some aggregates being greater than 300 nm. Similarly, Dams et al.[48] examined the toxicity of commercially available silver micro/nanoparticles to *P. putida* and showed citric acid stabilized AgENMs induced greater toxicity than microscale particles. Additionally, they demonstrated the utility of a bioluminescent strain, *Pseudomonas putida* BS566::luxCDABE, in nanotoxicological studies; however, the particles used in this study also remained uncharacterized, so future work should apply this method to examine

differences in responses to AgENMs and Ag^+ while measuring dissolution to place the findings in context.

In a well-cited study, the toxicity of sodium dodecyl sulfate stabilized AgENMs (SDS-AgENMs) to several gram-positive and gram-negative bacteria, including *P. aeruginosa* CCM 3955, was investigated in Mueller-Hinton Broth. SDS-AgENMs generated through hydrazine hydrate reduction were found to be the most toxic to *P. aeruginosa* (with an MIC of 62 μM), compared with particles generated through citrate/hydrate reduction without SDS (MIC = 133-267 μM) or with SDS (MIC = 2 mM)[49]. These hydrazine hydrate generated SDS-AgENMs were found to be the least toxic to *E. coli* and two different strains of *S. aureus*; however, the hydrazine hydrate generated SDS-AgENMs induced the largest zone of inhibition in all tested bacteria. Here, it is worth mentioning some researchers report similar findings in liquid vs. agar media[50], while others find assay-dependent responses [15, 25].

Demonstrating the importance of particle characterization, Dimkpa et al.[51], showed commercially available uncapped AgENMs reported to be 10 nm in diameter were composed of 10 nm particles, but also 70-90 nm particles in H_2O. Dimkpa et al. also showed that AgENMs had little influence on cell surface charge of *Pseudomonas chlororaphis* O6 (PcO6) cells suspended in distilled deionized water, whereas, Ag^+ ions neutralized surface charge. Likewise, the Ag^+ ions, but not AgENMs, neutralized the negative charge of PcO6 derived EPS. Addition of EPS to EPS-deficient and EPS-containing cells mitigated the toxicity of 14 μM AgENM and 14 μM Ag^+ ion, but not 93 μM AgENM. Interestingly, Badireddy et al.[52] showed that *P. aeruginosa* is capable of producing AgENMs from $AgNO_3$ and that particle formation and stability was enhanced

by the presence of EPS and NaCl, compared with natural organic matter (NOM). Intracellular ROS was not associated with AgENM toxicity but increased ROS was observed in cells exposed to 9.3-14 μM Ag^+ ions[51]. Addition of ROS scavengers during exposure reduced the toxicity of 14 μM AgENMs or ion, suggesting a role for extracellular ROS production. This is unlike the result of Gambino et al.[17], which showed AgENMs had no effect or reduced measured extracellular ROS.

Using atomic force microscopy and periplasmic and cytoplasmic enzyme leakage assays (alkaline phosphatase and cytoplasmically localized GFP, respectively), Dimkpa et al.[51] reported no significant damage to inner or outer membranes induced by AgENMs. This finding is similar to those of Gambino et al.[17] in *B. subtilis*; however, several studies show cell wall pitting and/or membrane disruption in response to nanomaterials[15, 38, 47, 50]. AFM micrographs of *P. aeruginosa* ATCC 27317 exposed to citrate or 11-mercaptoundecanoic acid-capped AgENMs or $AgNO_3$ showed no signs of membrane disruption in response to any of the metals[53]. These authors showed citrate-capped AgENMs were much less toxic than 11-mercaptoundecanoic acid-capped particles and that the latter were observed in higher numbers in association with the cell surface. Furthermore, AgENMs or $AgNO_3$ were not found to disrupt the membranes of *S. aureus* or *Saccharomyces cerevisiae*, while $AgNO_3$ led to cellular lysing and collapse of algal cells (*Euglena gracilis* and *Chlorella prototheciodes*). The authors speculate that citrate-capped AgENMs are more stable compared with 11-mercaptoundecanoic acid-capped particles and that the lower stability particles likely more readily released Ag^+ ions. However, estimates of dissolved Ag^+ were not reported. Still, it is unlikely that complete dissolution of the particles explains the observed toxicity, as equimolar concentrations of $AgNO_3$ were

generally more toxic. Additionally, it appears cells were exposed to AgENMs or $AgNO_3$ in water suspensions while controls were maintained in phosphate-buffered saline (PBS). It is unclear if the controls would have behaved the same in water (which would have been an adequate metal-free control).

Another study examined the toxicity of *de novo* synthesized nitroxide-coated AgENMs to *P. aeruginosa* ATCC 10145, *E. coli* AGCC 23546, *S. aureus* ATCC 29213, *S. epidermidis* ATCC 12228, or *Klebsiella pneumoniae* ATCC 13886[54]. The AgENMs were well characterized after synthesis and the most toxic particles synthesized yielded MICs in the low micromolar range in Mueller-Hinton Broth (37 μM for *P. aeruginosa*). However, future studies should fully characterize the particles in the exposure medium, and incorporate the necessary controls to examine the mechanism underlying the observed responses.

A study by Hachicho et al.[55] showed increasing trans/cis ratios of unsaturated fatty acids of *P. putida* mt-2 (DSM 6125) cells in response to Ag^+ ions and 10 nm sodium citrate stabilized AgENMs in supplemented mineral salt medium (Table 1.1), indicating possible decreased membrane fluidity. Total silver of either treatment appeared to at least partly explain observed responses; however, the total amount of AgENM silver necessary to completely inhibit growth was about twice that of $AgNO_3$ (3.2 vs 1.7 μM, respectively). Matzke et al.[56] examined the toxicity of many sized AgENMs with either tannic or citric acid or unspecified coatings and found no effect of size or coating on observed growth responses of *P. putida* DSM 50026 in minimal medium (Table 1). Surprisingly, EC_{50}'s of all tested materials were in the nanomolar range; however, particle characterization in the exposure medium (which contained significant amounts of K_2HPO_4/KH_2PO_4 $MgSO_4$ and

$NaNO_3$ and iron citrate) was not possible, so it is difficult to speculate regarding nano-specific effects. It is possible that size or coating effects were masked by changes to the AgENMs in the exposure medium. Future studies might clarify these results by characterizing the particles in the exposure medium and by incorporating particle size/coating combinations in a factorial experimental design.

Priester et al.[57] found *E. coli* to be much more tolerant to cysteine-capped AgENMs compared with *P. aeruginosa*, as measured by viability and membrane integrity. The authors suggest abiotic dissolution of the particles in the test media (LB, MMD) explained the observed toxic responses. However, it is known that biotic reactions are also involved in particle behavior, including dissolution. Unfortunately, researchers currently lack straightforward, cost-effective methods for accurately determining the role of biotic influences on particle behavior during exposure. Nevertheless, patterns in specific growth rate reduction induced by $AgNO_3$ or AgENMs were found to overlap in terms of dissolved Ag^+, insinuating the importance of the abiotically dissolved fraction of silver. It is worth noting that a strong correlation was found between the responses of *P. aeruginosa* to $AgNO_3$ and AgENMs in LB or MMD media, but only a weak correlation was found in the response of *E. coli* in MMD. Abiotic ROS and Ag^+ concentration were found to be positively correlated with reduction in membrane integrity, with the effect being more prominent in *P. aeruginosa*.

Proteins and mRNA transcripts of ribosomal proteins S2 and L9, alkyl hydroperoxide reductase/thiol-specific antioxidant (AhpC/TSA) family protein, and keto-hydroxyglutarate aldolase (KHGA) were upregulated in a soil isolated *Pseudomonas* sp. upon exposure to sublethal doses of AgENMs (0.93 μM) in minimal medium (Table 1.1)[58].

The MIC of AgENMs was found to be 1.9 μM. Metabolic activity and optical density at 600 nm correlated well and in a dose dependent manner in this study. However, particles were uncharacterized in media and no silver ion controls were used, so further studies are needed to determine the underlying chemical and biological mechanisms eliciting the molecular responses.

1.2.3 Sulfidized AgENMs and PGPR

Most engineered nanomaterials will enter terrestrial ecosystems via land applied biosolids enriched with nanoparticles that have been transformed during the waste water treatment process. In the case of silver, it is well accepted that most of these particles will be sulfidized during wastewater treatment and that these sulfidized particles are much less toxic than pristine ENM[59]. Indeed, Suresh et al.[60] found concentrations even up to 1.4 mM of ~9 nm sulfidized AgENM (sAgENM) were not toxic to *E. coli*, *S. oneidensis*, or *B. subtilis*; although, the tested particles had a capping protein/peptide which may have inhibited particle-cell interactions. Additionally, another study found a strong negative correlation between degree of AgENM sulfation and toxicity in *E. coli*[61].

1.3 ZnOENMs and PGPR

Zinc containing nanoparticles represent a large portion of the nanomaterials in consumer and industrial use and are expected to be enriched in biosolids amended soils at an exponential rate[9]. Several nanotoxicological studies have examined the effects of ZnOENMs on soil PGPR and related species (Table 1.2). In the soil bacterium, *Cupriavidus necator* JMP134, ZnO nanomaterials have been shown to elicit differential global protein expression profiles compared with Zn^{2+} supplied as zinc acetate (Zn-OAc)[62]. While it remains unclear what nanoscale properties may play a role in the observed

responses, ZnOENMs elicited expression of membrane proteins not associated with ion exposure. Unfortunately, the proteomic responses of bacteria to ZnOENMs remains virtually unexplored, so there is not much context for these results.

Another study addressed the difference in toxicity of 418 μM TiO_2, 741 μM Al_2O_3, 712 μM SiO_2 or 306 μM ZnO micro/nanoparticles to unspecified strains of *P. fluorescens*, *B. subtilis*, and *E. coli*[63]. Exposures were performed in 16.8 mM NaCl to avoid changes to particle characteristics; however, nearly all particles were either present as dispersed particles or aggregates with >200 nm hydrodynamic diameter, with the exception of SiO_2ENMs (46 nm)[63]. All Zn treatments (micro/nanoparticles and Zn^{2+} ions) caused mortality in *B. subtilis*, while the ZnOEMMs were most toxic to all other bacteria tested. Other studies have found various strains of *B. subtilis* were more sensitive to Zn containing ENMs than other bacteria, including, *P. putida* and *E. coli*[64], *S. aureus* ATCC 25923[65], *E. coli* DH5α[66], and others[67, 68]. However, Jones et al.[69] found *Staphylococcus epidermidis* 1487 and *Streptococcus pyogenes* NZ131 were both more sensitive to ZnOENMs in LB medium compared with *B. subtilis* 168 and the least sensitive tested organism, *S. aureus* N315. In at least one study, 1.3 mM ZnOENMs was required to reduce viability of *B. subtilis* (unreported strain) by 50 %[70].

Table 1.2 Summary of nanotoxicology studies involving ZnOENMs and PGPR or related species

Species	Strain	Synthesis	Primary Particle Size (nm)	Suspension Particle Size (nm)	Capping/stabilizing Agent	Surface Charge	Ion/Bulk Controls	Dissolution	Exposure Medium	Findings	Ref
B. subtilis	CB310	commercial	67	420-640	n/r	n/r	Bulk: ZnO (820-44.000 nM)	no	MDM: $K_2HPO_{4\,(0.7)}$, KH_2PO_4 (0.2), $(NH_4)_2SO_4$ (1), Nacitrate (0.5), $MgSO_4 * 7H_2O$ (0.1), glucose (1)	153 µM ZnOENMs (67 nm) reduced growth by 90%	66
B. subtilis	168	commercial	ZnO Nanoparticles = 8	n/r	n/r	n/r	Bulk: ZnO microparticles (> 1 µm)	no	Tryptic Soy Broth/Agar	Smallest particles were most toxic	69
			ZnO Nanopowder = 50-70							5 mM ZnOENMs (8 nm) resulted in 95% reduction in growth	
P. aeruginosa	PAO1	*in house*	13.7	n/r	n/r	Zeta-potential = 39 mV	Ion: Zn^{2+} ($ZnCl_2$)	no	LB	Cells with charged outer surfaces were most susceptible to ZnOENMs	72
	strains with differening outermembrane characteristics									3.25 to 4.25 mM ZnOENMs were required for large reductions in CFU/mL	
										Addition of Ca^{2+} reduced toxicity of ZnOENMs	
										Dissolution did not explain the observed the response	
P. fluorescens	n/r	commercial	20	1448		Zeta-potential = -5 mV	Ion: Zn^{2+} (unspecified form)	yes	NaCl (1 g/L)	306 µM ZnOENM resulted in total mortality of *P. fluorescens* and *B. subtilis*	63
B. subtilis	n/r						Bulk: ZnO (798 nm in suspension)			ZnOENMs associated with surface of *P. fluorescens*	
										306 µM ZnO microparticles or 31 µM ions resulted in complete mortality of *B. subtilis,* but not *P. fluorescens*	
B. subtilis	n/r	commercial	30.7 (XRD), 18.3 (BET)	Freshwater: 955	n/r	Freshwater: 0.47 (10^{-8} $m^2/V \cdot s$)	Ion: $ZnCl_2$	yes	model freshwater solution (mg/L): Na^+ (15), Mg^{2+} (7), Ca^{2+} (40), K^+ (2), Cl^- (22), SO_4^{2-} (104), HCO_3^- (29)	Zn dissolution explained toxic responses	64
P. putida	n/r	iron-doped (*in house*)	8.3-20 (XRD), 5.5-16 (BET)	Freshwater: 1510-1689		Freshwater: -0.14 to 0.75 (10^{-8} $m^2/V \cdot s$)				*B. subtilis* IC_{50}: 4.6-7.6 µM ZnOENM	
										P. putida IC_{50}: > 7.6 mM ZnOENM	
										Tannic acid mitigated toxicity more than humic, fulvic, or alginic acid	

Table 1.2 Summary of nanotoxicology studies involving ZnOENMs and PGPR or related species (continued)

Species	Strain	Synthesis	Primary Particle Size (nm)	Suspension Particle Size (nm)	Capping/stabilizing Agent	Surface Charge	Ion/Bulk Controls	Dissolution	Exposure Medium	Findings	Ref
B. subtilis	NRS-744	commercial	< 100 (supplier)	n/r	n/a	n/r	Bulk: ZnO	no	medium (%, w/v): peptone (0.5), yeast extract (0.5), dextrose (1.0), NaCl (0.25)	ZnO ENMs were more toxic than AgENMs	67
P. chlororaphis	O6	commercial	<100 nm (supplier)	n/r	n/r	Zeta-potential = -20 mV	Ion: Zn^{2+} (unspecified form)	yes	water	765 µM ZnOENMs slighlty reduced CFU/mL	77
							Bulk: ZnO (<1000 nm)			7.7 mM ZnOENMs was more toxic than bulk or ions at same concentration	
										ZnOENM exposure slightly increased charge on cell surface at pH 6, but not at pH 7	
										Membrane integrity was not compromised	
B. subtilis	n/r	commercial	50-70	n/r	n/r	n/r	Ion: Zn^{2+} ($ZnCl_2$)	yes	LB agar	EC_{50} ZnOENM = 1.3 mM	70
										Zn^{2+} dissolution did not explain response	
C. necatar	JMP134	commercial	1-3	n/r	acetate	n/r	Ion: Zn-acetate	no	10 mM Piperazine-1,4-bis(2-ethanesulfonic acid) buffer, 5 mM $Na(O_2CCH_3)_2$ (Na-OAc)	ZnOENMs elicited unique global protein expression compare to Zn-acetate	62
			2-6 (supplier)								
B. subtilis	KACC10111	commercial	n/r	315	n/r	Zeta-potential = 4.6 mV	Ion: Zn^{2+} ($ZnCl_2$)	yes	2.5 % w/v LB broth/LB agar plates	EC_{50} ZnOENMs = 688 µM (visible light)	68
										EC_{50} ZnOENMs = 474 µM (UVA illuminated)	
										EC_{50} ZnOENMs = 321 µM (UVB illuminated)	
S. meliloti	Rm 1021	commercial	10 nm	893-1302	n/r	Zeta-potential = -26 to -20 mV	Ion: Zn^{2+} ($Zn(OOCCH_3)_2 \cdot 2H_2O$	yes	yeast mannitol broth (YMB)	474 µM ZnOENMs resulted in complete inhibition of growth	85
										ZnOENMs were more toxic than Zn^{2+} ions	
										ZnOENMs changed protein and polysaccharide structures of EPS	
										ZnOENMs were found in periplasmic space	

Table 1.2 Summary of nanotoxicology studies involving ZnOENMs and PGPR or related species (continued)

Species	Strain	Synthesis	Primary Particle Size (nm)	Suspension Particle Size (nm)	Capping/stabilizing Agent	Surface Charge	Ion/Bulk Controls	Dissolution	Exposure Medium	Findings	Ref
P. chlororaphis	O6	commercial	<100 nm (supplier)	aggregated	n/r	Zeta-potential = -13.6 mV (MBB particles + ZnOENMs)	Bulk: ZnO (<1000 nm)		Mung Bean Broth (MBB)	ZnOENMs did not inhibit the inhibitory acitivity of *P. chororaphis* metabolites on *Fusarium* growth	76
P. chlororaphis	O6	commercial	<100 nm (supplier)	n/r	n/r	n/r	Ion: Zn^{2+} ($Zn(NO_3)_2$)	no	sand	7.7 mmol/kg ZnOENMs slightly reduced *P. chlororaphis* CFU/mL isolated from sand	75
										Dissolution of ZnOENMs correlated well with tissue concentrations of Zn in bean plants	
										7.7 mmol/kg ZnOENMs increased P. chlororaphis psiderophore production	
P. aeruginosa	PAO1	commercial	50 nm (supplier)	n/r	n/r	n/r	Ion: Zn^{2+} ($ZnCl_2$, $Zn(NO_3)_2$)	no	LB	5 mM $ZnCl_2$ or $Zn(NO_3)_2$ led to nearly complete inhibition of biofilm formation	73
	many mutant strains									1 mM ZnOENM lead to nearly complete inhibition of biofilm formation, though ions reduced formation to a greater extent at 0.5 mM compared with ZnOENMs at 0.5 mM	
										ZnOENMs induced the *czc* operon (involved in Zn efflux)	
										ZnOENMs repressed the *phz* operon (pyocyanin-related))	
B. subtilis	PB1831	*in-house*	ZnO nanorods: 20-40 nm (diameter), ≤ 4 µm (length)	n/r	n/r	n/r	Bulk: ZnO microrods	yes	PBS Suspension	0.15 µM ZnO nanorods resulted in ~80% reduction of *B. subtilis* CFU/mL	65
										Nanorods were more toxic than microrods	
										Membrane damage a likely mechanism of toxicity	

Table 1.2 Summary of nanotoxicology studies involving ZnOENMs and PGPR or related species (continued)

Species	Strain	Synthesis	Primary Particle Size (nm)	Suspension Particle Size (nm)	Capping/stabilizing Agent	Surface Charge	Ion/Bulk Controls	Dissolution	Exposure Medium	Findings	Ref
P. putida	BS566::luxCDABE	commercial	42 (supplier)	LB: 200	uncoated	n/r	Ion: Zn^{2+} ($ZnSO_4$)	yes	LB	ZnOENMs had 40% dissolution in LB and 2.5% in AW after 60 min	71
				AW: 1600					Artificial Wastewater (AW)	3.1 mM ZnOENMs reduced relative fluorescence to ~50 % after 1 h in LB media	
										Relative fluorescence increased with ZnOENM exposure in AW	
										ZnOENM toxicity driven by ions	
										IC_{50} of ZnOENMs was 0.9 - 1.5 mM in LB medium	
P. aeruginosa	PAO1	commercial	65	n/r	n/r	Zeta-potential = -11.1 mV	n/a	no	LB	1 mM ZnOENM exposure decreased biofilm formation, and elastase and	74

n/r is “not reported”, n/a is “not applicable”, ref is “reference”

Interestingly, Jiang et al.[63] found bulk ZnO was more toxic than Zn^{2+} in terms of survival percentage of *E. coli* and *P. fluorescens*. This is particularly important because the Zn^{2+} ion controls were representative of the dissolved fraction of ZnO-micro/nanoparticles. Aggregates of all particles found on the bacterial surfaces via TEM were generally smaller than those found in the medium without bacteria. Zeta-potential measurements suggested strong electrostatic attraction between the negatively charged bacterial surfaces and the positively charged Al_2O_3 and SiO_2 particles. To explain the strong association of the negatively charged ZnOENMs to the bacterial surfaces, the researchers speculated it was due to the "carboxyl, amide, phosphate, hydroxyl and carbohydrate related moieties in the bacterial cell wall"; however, no investigation into the biochemical or molecular mechanisms governing the particle-cell interactions was performed. Mallevre et al.[71] found increased aggregation and decreased dissolution of ZnOENMs suspended in artificial wastewater (AW) compared with LB media and attributed these differences in particle chemistry to decreased toxicity in the artificial wastewater-exposed *P. putida*. Additionally, the AW used by Mallevre et al. (2014) contained 0.1 mM $CaCl_2$ which has been shown to alter electrostatically driven interactions of ZnOENMs and *P. putida* cells[72].

Few studies have examined the influence of ZnOENMs on bacterial biofilm formation in soil bacteria. One relatively thorough investigation was that of Lee et al.,[73] which found Zn^{2+} supplied as either $ZnCl_2$ or $Zn(NO_3)_2$ equally inhibited biofilm formation to a greater extent than equimolar concentrations of ZnOENMs in *P. aeruginosa* PAO1. Additionally, sublethal ZnOENM exposure was also found to increase cellular hydrophobicity and reduce production of pyochelin (a siderophore), Pseudomonas quinolone signal (PQS), and toxin pyocyanin. Microarray analyses also revealed induction

of several genes associated with Zn efflux (czc operon) and transcriptional regulators involved in different biological processes (*opdT* – a porin, *ptrA* – Pseudomonas type III repressor A), while repressed expression was observed in pyocyanin-related genes. Some evidence for particle specific effects was found when either 0.1 mM ZnOENM or 1 mM $ZnCl_2$ resulted in ~40% reduction in hemolytic activity, but additional research is required to understand the underlying mechanism of this response. For instance, ion controls should be used in future microarray experiments to distinguish gene expression patterns driven by particle exposure from those induced by ions. Similarly, Garcia-Lara et al.[74] reported 1 mM ZnO ENMs reduced biofilm formation and production of elastase and pyocyanin in many tested strains of *P. aeruginosa*, including six clinical strains, two PA14 gallium resistant mutants, a C-30 resistant mutant, and four strains isolated from various non-terrestrial environments. Particles remained largely uncharacterized and no ion controls were used, so future work should attempt to clarify the mechanisms of the observed results.

An agriculturally relevant study showed ZnO treatment did not reduce *Phaseolus vulgaris* root colonization by *P. chlororaphis* O6[75]. Additionally, the antifungal behavior of *P. chlororaphis* O6 was not inhibited by ZnOENM exposure[76], but this was determined via growth inhibition tests of the fungal pathogen, *Fusarium graminearum*, cultured on agar plates (i.e. authors did not test the effects of ZnOENM exposure on biocontrol of the pathogen *in planta*). Still, this study draws attention to the broader issue of the need for more nanotoxicological investigations of plant-microbe interactions and provides a subject for future research. Dimkpa et al. also found *Pseudomonas chlororaphis* O6 was more susceptible to ZnOENMs than bulk or ionic zinc in another study[77]. Additionally, ZnOENMs reduced the surface charge of the bacteria at pH 6, but not at pH 7.

1.4 TiO_2ENMs and PGPR

Titanium containing nanoparticles are expected to represent the largest portion of environmentally released metal containing nanoparticles[9] and research is growing regarding the effects of TiO_2ENMs on PGPR (Table 1.3). Some studies suggest they elicit low toxicity even at high concentrations; however, this is likely because TiO_2ENM toxicity is enhanced by photo-activation (vide infra) and many studies do not explore this aspect of TiO_2ENM toxicity. Jiang et al. found the TiO_2 nano and microparticles (418 μM) were non-toxic to all tested bacterial species[63]. Similarly, Adams et al.[66] found 10.5 mM TiO_2 (330 nm) did not inhibit growth of *B. subtilis* and only moderately inhibited growth of *E. coli* (15% growth inhibition). A number of other pure bacterial culture studies found low toxicity of TiO_2ENMs compared with Ag or ZnOENMs, but some authors have noted significant toxic effects of TiO_2 to bacteria at relatively low concentrations.

Table 1.3 Summary of nanotoxicology studies involving TiO_2ENMs and PGPR or related species

Species	Strain	Synthesis	Primary Particle Size (nm)	Suspension Particle size (nm)	Capping/stabilizing Agent	Surface Charge	Ion/Bulk Controls	Dissolution	Exposure Medium	Findings	Ref.
B. subtilis	CB310	commercial	66	175-810	n/r	n/r	Bulk: TiO_2 (950-44.000 nM)	no	MDM (g/L): K_2HPO_4 (0.7), KH_2PO_4 (0.2), $(NH_4)_2SO_4$ (1), Na-citrate (0.5), $MgSO_4*_7H_2O$ (0.1), glucose (1)	21 mM TiO_2ENMs (66nm) reduced growth by 75%	66
B. subtilis	168	commercial	n/r	n/r	n/r	n/r	n/a	no	Tryptic Soy Broth/Agar	TiO_2ENMs were not toxic up to 10 mM	69
P. fluorescens	n/r	commercial	50 (supplier)	873	n/r	Zeta-potential = -21 mV	Bulk: TiO_2 (836 nm in suspension)	no	NaCl (1 g/L)	TiO_2 had no effect on bacteria	63
B. subtilis	n/r										
B. subtilis	KACC10111	commercial	n/r	828	n/r	Zeta-potential = 12.5 mV	Ion: Zn^{2+} ($ZnCl_2$)	no	2.5 % w/v LB broth/LB agar plates	EC_{50} TiO_2ENMs > 6.3 mM (visible, UVA illuminated)	68
										EC_{50} TiO_2ENMs = 4.8 mM (UVB illuminated)	
B. subtilis	ATCC21183	commercial	P25 = 22.9	P25 = 970 (after 120 m)		P25 Zeta-potential = -14.4 mV	n/a	no	Stream Water	104 µM TiO2ENM Exposure decreased viability nearly 80 % for PW6 and roughly 100 % for P25	79
			PW6 = 81.5	PW6 ~500 (after 120 m)		PW6 Zeta-potential = -19 mV			Lake Michigan Water (LMW)	photoactivation enhanced toxicity	
P. aeruginosa	PAO1	*in-house*	9	90 (in EVOH film)	ethylene-vinyl alcohol (EVOH)	n/r	EVOH, UV	no	LB (10 times diluted)	Gene/proteins downregulated (regulation, signalling, growth)	81
										Cellwall/membrane structure altered	
P. putida	BS566::luxCDABE	commercial	20 (supplier)	LB: >200	n/r	n/r	n/a	no	LB	TiO_2ENM exposure increased relative florescence	71
				AW: >600					Artificial Wastewater (AW)	≤ 4.2 mM had no toxic effect	
B. subtilis	VITLWS2	commercial	< 25 (supplier)	574-690 (varied over 24 hr)	n/r	n/r	n/a	no	Lake water from VIT Lake, Vellore, India (filtered and sterilized)	21 µM TiO_2ENM Exposure decreased viability >20 % after 24 h (in all tested bacteria)	78
B. altitudinis	VITLWS1									A consortium of all 3 bacteria responded similarly	
P. aeruginosa	VITLWS3										

n/r is “not reported”, n/a is “not applicable”, ref is “reference”

For instance, Kumari et al.[78] reported <21 μM TiO_2ENM exposure reduced viability of *Bacillus altitudinis* VITLWS1, *Bacillus subtilis* VITLWS2 , *Pseudomonas aeruginosa* VITLWS3 and consortia of all three tested species. Viability responses to exposures performed in light and dark were very similar, while Binh et al.[79] observed light-enhanced toxicity of TiO_2 in *B. subtilis* (ATCC 21183). The differences in observed responses is likely due to the use of visible light by Kumari et al.[78] versus simulated solar illumination (280 to 849 nm and 200 W/m2) by Binh et al.[79]. The importance of wavelength choice for illumination of TiO_2ENMs studies has been documented elsewhere[80] and the interaction of titanium with UV-light is well known. The studies by Binh et al. and Kumari et al. used particles which were in micron sized aggregates in the exposure media, nonetheless, Binh et al. also found low exposures of TiO_2ENM (52 μM) in simulated solar illumination reduced viability by ~40% in *B. subtilis*.

As discussed by Kubacka et al.[81] and the references within, the biocidal properties of TiO_2ENM containing materials emerge primarily from electron-hole carriers at the surface of photo-activated materials. Still, knowledge regarding bacterial responses to titanium-based ENM remains limited. Kubacka et al.[81] examined the responses of *P. aeruginosa* PAO1 to TiO_2 nanocomposites and observed several specific cellular responses. Microarray analysis revealed strong upregulation of genes related to detoxification, carbohydrate metabolism, transport, and amino acid metabolism, and strong downregulation of inorganic phosphate uptake genes. Cell-to-cell signaling was also inhibited by a reduction of spermidine biosynthesis via a decrease in an S-adenosylmethionine decarboxylase and a spermidine synthase. They also found several genes involved in maintaining cell wall structure to be upregulated or downregulated. The

authors suggested this finding (with others) shows UV activated TiO_2 exposure leads to a weakened cell wall which is compensated for by strengthening the underlying membrane with additional proteins and lipids. Additionally, changes in metabolism are likely, because coenzyme-independent respiratory chains were downregulated. Heme group biosynthesis and degradation were also both inhibited. These findings are the most in-depth analysis of titanium containing ENM toxic responses to date; however, they raise important questions such as, "Are these responses unique to *P. aeruginosa*?", and "To what degree does crosstalk exist among these seemingly disparate toxic responses?"

1.5 ENMs and Symbiotic Nitrogen Fixing Bacteria

Sinorhizobium meliloti is a soil bacterium capable of fixing N_2 through a symbiotic relationship with plant species from the *Medicago*, *Melilotus*, and *Trigonella* genera[82]. The symbiosis between *S. meliloti* and the model legume, *Medicago truncatula*, is currently being exploited to dissect the biochemical and molecular mechanisms of the legume symbiosis and much more. The plant growth promoting abilities of *S. meliloti* in non-leguminous plants (lettuce) have been known for some time now[83], but the mechanism remains unclear. Some strains of rhizobia have been shown to exhibit ACC deaminase activity which may lead to plant growth promoting activities, but it is not thought that *S. meliloti* 1021 possesses the ACC deaminase gene[84].

There are very few studies concerning nanotoxicity in *S. meliloti*, or any other N-fixing legume microsymbiont for that matter. One relatively thorough investigation assesses the toxicity of microscale aggregates of ZnO and CeO_2ENMs to *S. meliloti* Rm 1021[85]. This is particularly important because it is known that aggregates exhibit different levels of toxicity compared with nanoparticles. This could be why the authors found a weak

relationship between CeO_2ENM concentration and toxic response in terms of growth. Additionally, complexation of Zn^{2+} and Ce^{2+} was likely to occur in the yeast mannitol broth (YMB) medium used to expose the cells, which may also partially explain the weak correlation noted between ion concentration and growth response. Nevertheless, they found 0.5, 1, and 2 mM ZnOENMs to completely inhibit growth, while equimolar concentrations of Zn^{2+} did not. This is likely a result of the particles acting as a unique delivery mechanism of Zn^{2+} ions to the cell surface, whereas, any dissolved free Zn^{2+} ions in solution were likely rendered less bioavailable through complexation and possibly precipitation. Indeed, scanning-TEM micrographs along with EDX data showed clear association of both ZnOENMs and CeO_2ENMs with *S. meliloti* cells. FTIR analysis of EPS extracted from exposed cells showed CeO_2ENMs or ZnOENMs to alter shape and absorption intensities of absorption bands indicative of interactions of ENMs with proteins and polysaccharides. These changes in FTIR spectra appeared to be more dose dependent with ZnOENMs versus the less toxic CeO_2ENMs.

Another study investigated the role of EPS in modulating sodium citrate stabilized AgENM toxicity by exposing *S. meliloti* Rm 1021, Rm 7096 - an EPS overproducing mutant, and Rm 7210 – an EPS lacking mutant in LB medium[86]. Consistent with most literature, EPS over-producing mutants exhibited greater resistance to nanoparticle exposure. However, it appears that a considerable increase in CFU/mL was observed in no-metal controls of *S. meliloti* Rm 7096, suggesting either a greater initial starting viable cell number was used, or these mutants thrive in the exposure medium compared with the other test strains. Particle size was estimated in the medium and dissolution measurements, along with responses to silver ion controls, suggested abiotic AgENM dissolution did not

explain the observed responses. These authors also exposed *E. coli* JM109/pEdinbrick1, which produces low levels of colanic acid, and found addition of an EPS analog, xanthan, reduced toxicity of AgENMs. Furthermore, addition of EPS purified from *E. coli* JM109/pRscA2 reduced the toxicity of AgENMs to *E. coli*/BW25113/Δyhak, which produces low levels of polysaccharides.

A full review of the effects of ENM exposure on plant-microbe interactions is beyond the scope of this review; however, it is useful to provide highlights of what is currently known regarding N-fixing microsymbionts in the context of their host plants. There is relatively little known concerning the influence of ENM on root nodule development or function. From an environmental protection perspective, the most relevant study to date is that of Judy et al.[87], which examined the physiological responses of *Medicago truncatula* A17 grown in *S. meliloti* Rm 2011 inoculated soils amended with field composted biosolids containing Ag, ZnO, and TiO_2 ENMs or $AgNO_3$, $ZnSO_4$, and micron-sized TiO_2. In this study, the ENM enriched biosolids significantly reduced the number of root nodules observed after 30 days of growth compared with the no metal control and the dissolved/bulk enriched biosolids amended treatment. This effect did not appear to be a result of enhanced plant health, as fresh shoot biomass, dried root biomass, and shoot length were all significantly decreased only by the ENM treatment. There was a reduction in *S. meliloti* CFU estimates by bulk/dissolved and ENM treatments; however, reduced nodulation did not appear to be a result of decreased survival of *S. meliloti* in the ENM treatments as nodulation was not influenced by bulk/dissolved treatments. Regardless, it remains unclear if ENM specific stress responses may have influenced *S. meliloti* physiology, thereby, reducing the symbiotic capacity of the organism. The authors

suggest that enhanced Zn uptake observed in the ENM treatments is likely to explain much of the observed responses, but further research is required because plants were co-exposed to several metals at once. Furthermore, additional experiments should be duplicated using biosolids from multiple sources with varying compositions to determine the influence of biosolid specific factors.

Nevertheless, ENMs were also found to elicit distinct toxicogenomic responses in plants compared with the other treatments as determined via microarray analyses[88]. Importantly, the authors observed induction or downregulation of several nodulation related genes from various gene ontology categories, including, nodulation, nodule morphogenesis, and N-fixation. Additionally, the authors observed downregulation of several nitrogen metabolism related genes in roots and many other metabolic pathway GOs were identified in plants exposed to ENM, including those related to nodulation such as flavonoid metabolic/biosynthetic processes and phenyl-propanoid metabolic/biosynthetic processes.

Research with more agronomically relevant N-fixing legumes has also shown specific ENMs may disrupt the process of nodulation and negatively affect plant health. For instance, both ZnO and TiO_2 were found to inhibit nodulation and nitrogen fixation in hydroponically grown *Pisum sativum* L[89, 90]. In soybeans (*Glycine max*), ethylene reduction assays showed high concentrations of CeO_2 ENMs (3.6-7.1 mmol/kg) significantly reduced nitrogen fixation in root nodules[91] and ZnOENMs were found to hinder development and inhibit reproduction[92]. Additionally, ZnO and CeO_2 nanoparticles in soybeans are thought to differentially elicit genotoxicity as determined through RAPD analysis for DNA damage and mutations[93]. Another study examining responses of *Medicago sativa* L inoculated with

an unspecified strain of *S. meliloti* showed 11.5 mM bulk or ionic zinc decreased seed germination, while 11.5 mM ZnOENMs resulted in a non-statistically significant increase[94]. Furthermore, ZnOENM exposure reduced root and shoot biomass at 3.8, 7.7, and 11.5 mM, while equimolar concentrations of $ZnCl_2$ reduced shoot biomass, but only 11.5 mM reduced shoot biomass. Interestingly, 7.7 and 11.5 mM bulk Zn resulted in large increases in shoot biomass.

1.6 ENMs and Soil Microbial Communities

1.6.1 AgENMs and Soil Microbial Communities

As previous reviews have indicated, the influence of ENMs on soil microbial communities remains largely unexplored[95], but interest is growing[96]. Amendment of terrestrial mesocosms with biosolids containing ENMs or metals to a final metal concentration of 1.3 μmol/kg PVP-AgENM or 5.2 μmol/kg $AgNO_3$ resulted in no change in total plant biomass compared with biosolids only controls[97]. However, both metal treatments reduced aboveground biomass of *Microstegium vimineum* while increasing belowground biomass. Microbial community composition was found to be altered to a greater degree by AgENMs than Ag^+ when compared with biosolid-only controls at 1 and 50 days post exposure. The AgENMs reduced microbial biomass, leucine aminopeptidase activity (an extracellular proteolytic enzyme), and phosphatase activity, while N_2O production was increased. In another study, amendment of soils with AgENM resulted in decreased activities of urease, fluorescein diacetate hydrolase, arylsulfatase, β-glucosidase, dehydrogenase, and acid-phosphatase[98]. Silver ions at concentrations representative of the dissolved fraction of the AgENM treatments had no influence on soil enzyme activities; however, particle dissolution was estimated by sequentially filtering soil suspensions

through filter papers followed by nylon filters and it is unclear if the authors controlled for ion sorption to the membranes. Regardless, the enhanced chronic low-dose response of the microbial community to AgENMs when compared with ions, shows the complexity of econanotoxicological studies and the care needed when extrapolating laboratory results to environmental exposures.

In another study, relatively low doses of AgENMs (0.03, 0.3, and 3 μmol/kg) had no influence on soil enzyme activities, but a reduction in microbial biomass and net N mineralization coupled to an increased metabolic quotient were reported[99]. Arctic soils amended with 2 mmol/kg Ag, 3.5 mmol/kg Cu, and 7.8 mmol/kg Si ENMs had decreased microbial biomass after 6 months[100] and AgENM amendment alone was found to alter microbial community structure[101].

Recently, a study with tomato found a reduction in arbuscular mycorrhizal fungi (AMF) colonization in response to 930 μmol/kg PVP-AgENMs or AgNO3, or 93 μmol/kg sAgENM amended biosolids[102]. All tested concentrations of Ag^+ (9.3, 93, and 930 μmol/kg) and 93 or 930 μmol/kg PVP-AgENMs reduced total soil microbial biomass and abundance of gram-negative bacteria. Interestingly, 9.3 or 930 μmol/kg Ag_2S treatments reduced total microbial biomass and gram-negative bacteria abundance, but not 93 μmol/kg. Gram-positive bacteria abundance was reduced by 930 μmol/kg Ag^+, PVP-AgENMs, and sAgENMs and 93 μmol/kg Ag^+, while bacterial abundance was reduced across all treatments. Despite the noted effects on AMF colonization, total soil fungal abundance was only reduced by 9.3 μmol/kg Ag_2SENMs and 930 μmol/kg PVP-AgENMs. The 93 μmol/kg Ag^+ treatment resulted in doubling of the dry shoot biomass due to what the authors suggest could be potential hermetic responses; however, alternative hypotheses

might include possible suppression of plant pathogens in the biosolids amended soils due to the presence of Ag^{+}.

Also of note, mesocosm studies have shown even relatively low environmental concentrations of AgENMs, thought to likely be sulfidized (at least to some degree), altered microbial community structure, reduced plant shoot biomass, increased nitrous oxide production, and influenced several other ecologically relevant processes, often to a greater extent than $AgNO_3$ applied at 4-fold higher concentrations[97]. More recently, it was shown that sAgENMs may reduce root and shoot biomass in *Vigna unguiculata* L. Walp. and *Triticum aestivum* L., but this was only evident after prolonged exposure (2 weeks)[103]. While it is clear that sAgENMs are generally less toxic than pristine AgENMs, the long-term impact of these particles on terrestrial ecosystems has yet to be investigated.

1.6.2 Other ENMs and Soil Microbial Communities

Ge et al.[104] found soils amended with 10.5, 21, or 42 mmol/kg of TiO_2 or 8, 15, or 31 mmol/kg ZnOENMs had decreased substrate induced respiration (SIR) and extractable DNA. At 15 and 60 days of exposure, extractable DNA reductions were found to be concentration dependent, but were linear for TiO_2ENMs, and exponential for ZnOENMs. Both particle types were found to result in shifts in microbial community structure, but the impact of ZnOENMs was much more pronounced. Pyrosequencing revealed ZnO and TiO_2 led to a reduction in *Rhizobiales*, *Bradyrhizobiaceae*, *Bradyrhizobium*, and *Methylbacteriaceae* while increases were observed for *Sphingomonadaceae*, *Streptomycetaceae*, and *Streptomyces*[105]. Interestingly, others have noted Cu and Zn nanoparticles decreased abundance of the *Sphingomonadales* and *Flavobacteriales* orders [106]. Nogueira et al.[107] also found strong shifts in soil microbial community structure in

response to TiO_2ENMs or Au nanorods. A study examining the effects of soil properties on TiO_2ENMs toxicity found only one of six tested soils had decreased SIR (a soil with silty clay texture and high organic matter)[108]. Shifts in microbial community structure resulting from TiO_2ENMs exposure were also found to be more pronounced as soil moisture decreases, and may occur even though there are no changes in organic matter content, total N or C, C/N ratios, or bioavailable C[109]. Soil amendment with biosolids containing mixtures of ENMs (Ag, Zn, and Ti) led to unique shifts in microbial community structure compared with bulk/dissolved metal controls; where ENM treatment yielded significant reductions in most microbial groups as assessed via PLFA analysis compared with metal free controls[87].

Du et al.[110] found 2 mmol/kg TiO_2 or 0.7 μmol/kg ZnOENMs decreased wheat biomass and potential soil peroxidase and catalase activity, while ZnOENMs reduced protease activity and TiO_2ENMs slightly increased urease activity. Additionally, wheat root washings reduced the toxicity of CuO and ZnOENMs to *P. putida* KT2440[111], while root colonization by *P. chlororaphis* or co-exposure with ZnOENMs have been shown to reduce CuOENM toxicity to *Phaseolus vulgaris*[112]. Calder et al.[113] used sand and soil slurry microcosms to study the influence of soil components on AgENM and ion toxicity to *P. chlororaphis* O6. Sand and soil were autoclaved twice before inoculating with bacteria with and without AgENMs or ions. After 4 days of incubation, CFU counts were determined by serial diluting the slurry in water and plating. Despite the fact that many soil components were likely altered during autoclaving, up to 28 μM AgENMs or ions were both found to be essentially non-toxic in soil-microbe mixtures. In sand, roughly a 40% reduction in CFUs was observed in response to 9.3 μM AgENM. Addition of pore water

(isolated from metal free soil slurries; 0.083 mL isolated pore water/g sand) completely mitigated toxicity while humic acid (~8.3 mg humic acid/g sand) restored CFU counts to ~90%. Soil pore water and humic acid amendments restored CFU counts to >75% when applied with 28 μM AgENM which otherwise resulted in total loss of culturable cells. Interestingly, soil pore water was found to reduce the toxicity of 2.8 μM and 9.3 μM Ag^+, but humic acid was shown to enhance toxicity of 2.8 μM Ag^+. The difference in cell recovery observed in the presence of pore water or humic acid when AgENMs were supplied was largely found to be a function of measured free ion concentrations, where the presence of both of these substances reduced free Ag^+ concentrations, with the effect of the pore water being greater.

1.7 Conclusion and Path Forward

Considerable efforts have been focused on understanding nanotoxicity in bacteria, but soil bacteria have remained largely neglected. The complexities inherent to nanotoxicological studies (Figure 1.1) have also created uncertainty in the implications of the existing literature. Exposure solution pH, ionic strength, and general composition may all influence ENM behavior and bacterial physiology. Furthermore, ENM behavior in solution and in particle-cell interactions may be influenced by dissolution/aggregation status, ROS production, core/coating composition, surface chemistry, size, shape, and surface area. Bacteria may respond to ENM exposures in several ways, some of which may influence particle behavior (i.e. release of ROS and other exudates/metabolites/lysates, other general changes to solution chemistry), and bacteria may generate nanoparticles from ions or promote aggregation or dissolution of nanomaterials. Ideally, all of these

possibilities should be considered and tested for when designing nanotoxicity experiments, which highlights the cross-discipline collaborative nature of nanotoxicology.

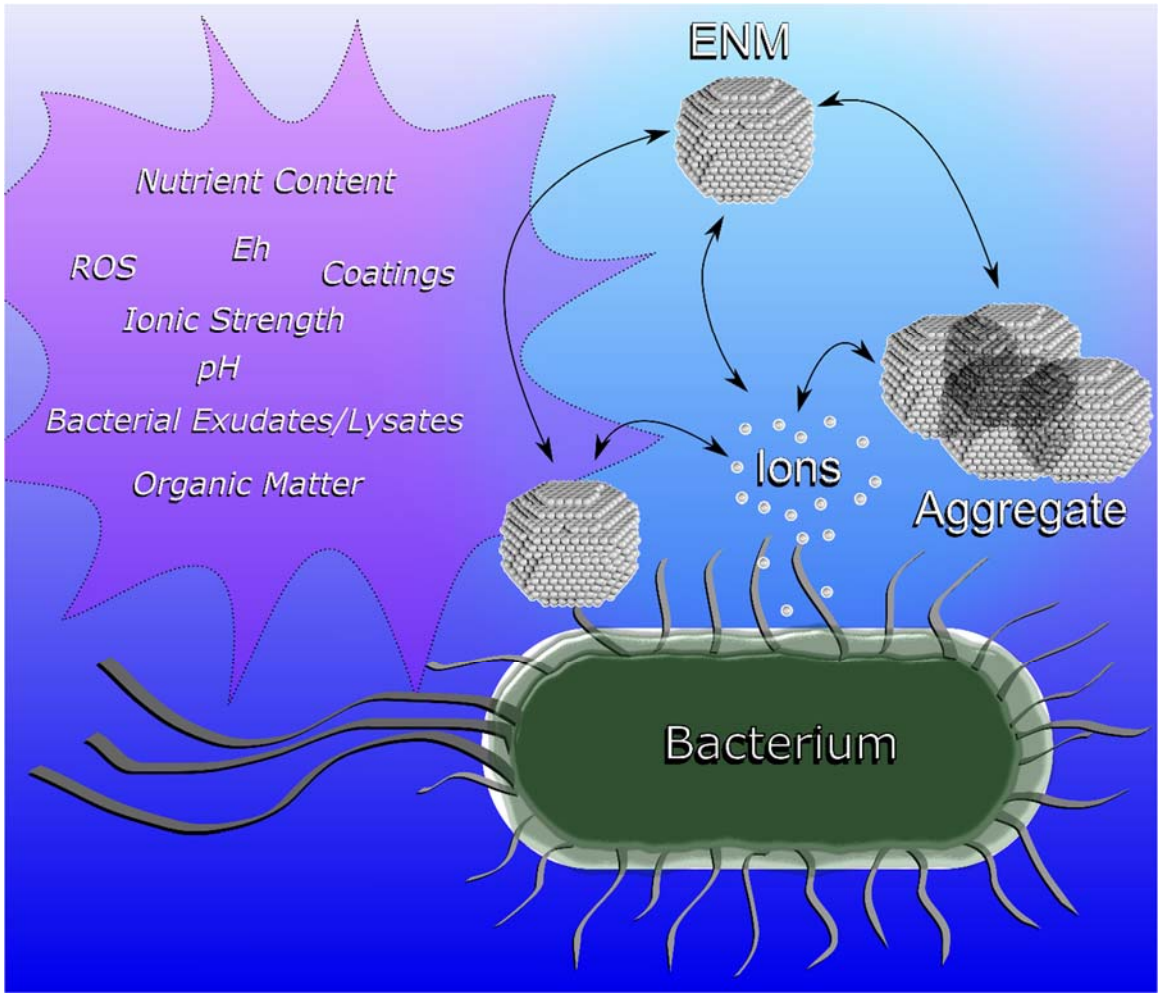

Figure 1.1 A depiction of the various aspects to be considered in pure-culture nanotoxicological studies of ENMs (engineered nanomaterials) and PGPR (plant growth promoting rhizobacteria). Arrows show particles may aggregate, dissolve, or remain dispersed, all forms may interact with the bacterium. The bacterium may also respond and influence the nature of the solution and ENMs. Key factors which may influence ENM-bacterium interactions are outlined in purple. ENM image modified from "A possible model for an ideal nanocluster is built from Pt atoms (draft version)" by Vadim A. Volochaev, licensed under CC BY0SA-4.0.

Future researchers working with pure-cultures should perform full particle characterization in experimentally relevant exposure media. This includes, dissolution measurements, aggregation status, surface charge measurements (zeta-potential or electrophoretic mobility) and size measurements (imaging and hydrodynamic radius). Without these basic, (yet, crucial) data, a mechanistic understanding of observed toxicological responses remains obscured. A multifaceted approach to experimental design must also be taken, where the effects of the toxicant on the organism are observed alongside the effects of the organism on the toxicant. It is now well known that abiotic and biotic driven reactions dictate particle behavior and particle-cell interactions during exposure. Again, neglecting these critical aspects of nanoparticle exposures inherently limits the ability to interpret the observed response and determine the underlying mechanisms.

Single organism and simplified plant-microbe interaction studies remain a valuable approach to understanding nano-specific effects in ENM-bacteria interactions and have provided a strong basis for future research. Lacking in pure-culture and in more complex media is an understanding of the toxicogenomic and proteomic responses of PGPR to ENMs. It is clear that nanomaterials can elicit specific genetic and proteomic responses in bacteria, but currently it is unknown how these responses may influence PGPR specifically, or alter their plant growth promotion activity and roles in other ecosystem services.

Additionally, microbes in the rhizosphere, and in the environment at large, are rarely (if ever), found alone. Future research should study multi-species interactions of ENMs with microbes that are both motile and present as biofilms on abiotic (e.g. mineral) and biotic (e.g. plant root) surfaces. As researchers attempt to clarify the results of the past

decade of pure-culture based nanotoxicological research, it is essential that future efforts are focused on more environmentally relevant conditions (i.e. soils).

Most research examining the responses of PGPR to ENM has been performed using single organisms in pure-culture, thus, there are large knowledge gaps regarding ENM-microbe-plant interactions. Examination of the effects of ENMs on plant-microbe interactions in meso/microcosms, and ultimately, actual field sites, will provide a rich research topic for future researchers. Findings regarding ENM induced changes in soil enzyme activities, nutrient cycling, and community interactions (reviewed by McKee and Filser[96]) should be examined with metagenomics, metatranscriptomics, and metaproteomics to elucidate the biological mechanisms governing these crucial responses.

As of now, nanoparticle characterization in more complex media (i.e. soil, sludge, or sediments) remains a challenge, but recent advances are helping make that possible[114]. This will be particularly important as the amount of nanomaterials entering terrestrial environments is increasing not only from current consumer and industrial uses, but also from emerging agricultural technologies (i.e. nanoparticle based fertilizers, pesticides, and herbicides). Because of the projected increase of nanotechnology-based agricultural products, PGPR and other beneficial microorganisms will encounter new ENMs at an ever increasing rate. Amongst these emerging nanotechnologies will also be hybrid materials composed of mixtures of bacteria and nanomaterials, the environmental risk of which remains virtually unexplored.

Chapter 2: A New Way of Assessing Viability and Respiration Responses in Aerobic Microorganisms

2.1 A Note on Method Development

The work presented in this chapter is based on methods I developed to rapidly assess viability and O_2 consumption responses in bacteria. While the work in this section shows the utility of the method for observing metal ion toxicity in *Bacillus amyloliquefaciens*, the goal was to develop a method also suitable for nanotoxicological tests. Development of the method required several preliminary steps, discussed below.

To limit the potential confounding effects of media on ENM properties, I tested the effects of several different media types on the optical density (600 nm) of *B. amyloliquefaciens*, *Pseudomonas fluorescens, Pseudomonas putida,* and *Sinorhizobium meliloti.* All bacteria were cultured and harvested as described in the methods section below (2.3), but without the MES (2-(N-morpholino)ethanesulfonic acid) in cases where other media were tested. Upon harvesting, cells were washed three times and suspended in the medium to be tested.

At 3 h post-harvest, KNO_3 reduced optical density in a concentration dependent manner (Figure 2.1). Cells washed and suspended in Spizizen medium with or without glucose[115] had no detectible optical density after 3 h (Figure 2.1). In another experiment, optical density of *Bacillus subtilis* was stable in sterilized double deionized water (DDI) over 20 h (harvested via filtration or centrifuged at 10,000 rcf for 10 m). Additionally, 0.85% NaCl, and 0.01 or 0.2 M KNO_3 led to reductions in optical density (Figure 2.2). It should be noted, these preliminary results are from studies where sample size = 1; however,

50 mM MES at a pH of 6 was found to be a useful exposure medium and viability was tested thoroughly for all tested bacteria in this medium (Chapter 3).

Optical density of *P. fluorescens* and *S. meliloti* filter isolated in sterilized DDI water (in triplicate) was found to be stable over a 2 h period across a range of starting optical densities (Figure 2.3). While, sterilized DDI water was suitable for maintenance of optical density over time, I found the high concentrations of $ZnSO_4$ and $NiSO_4$ required to induce toxic responses also reduced pH (Data Not Shown). Ultimately, 50 mM MES brought to pH 6 with NaOH and supplemented with 69 mM glucose was found suitable for metal ion exposures and to have minimal effects on bacterial viability and ENM properties (Chapters 2 and 3). It was also necessary to experiment with the starting cell density during exposure and dilution thereafter, for obtaining optimum results from the O_2 consumption and viability assays (Data Not Shown).

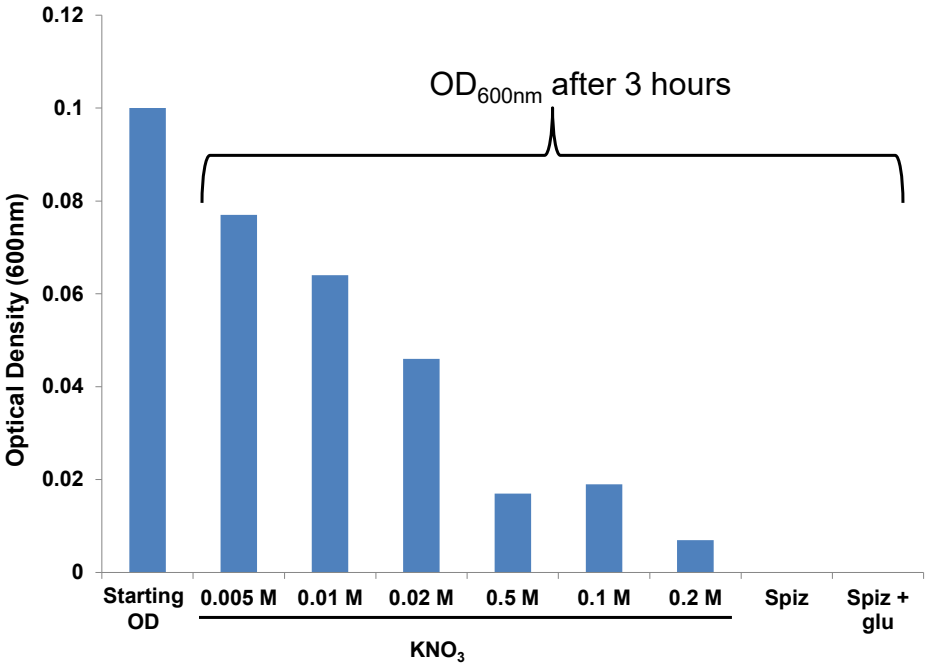

Figure 2.1 Measurement of *Bacillus amyloliquefaciens* optical density in KNO_3 and Spizizen medium. Optical density was measured at 600 nm. Starting OD indicates the optical density of the cells after harvesting and washing. KNO_3 is in molarity. Spiz = Spizizen medium without glucose, Spiz + glu = Spizizen medium with glucose. Optical density for KNO3 and Spizizen media was measured after 3 h (n = 1).

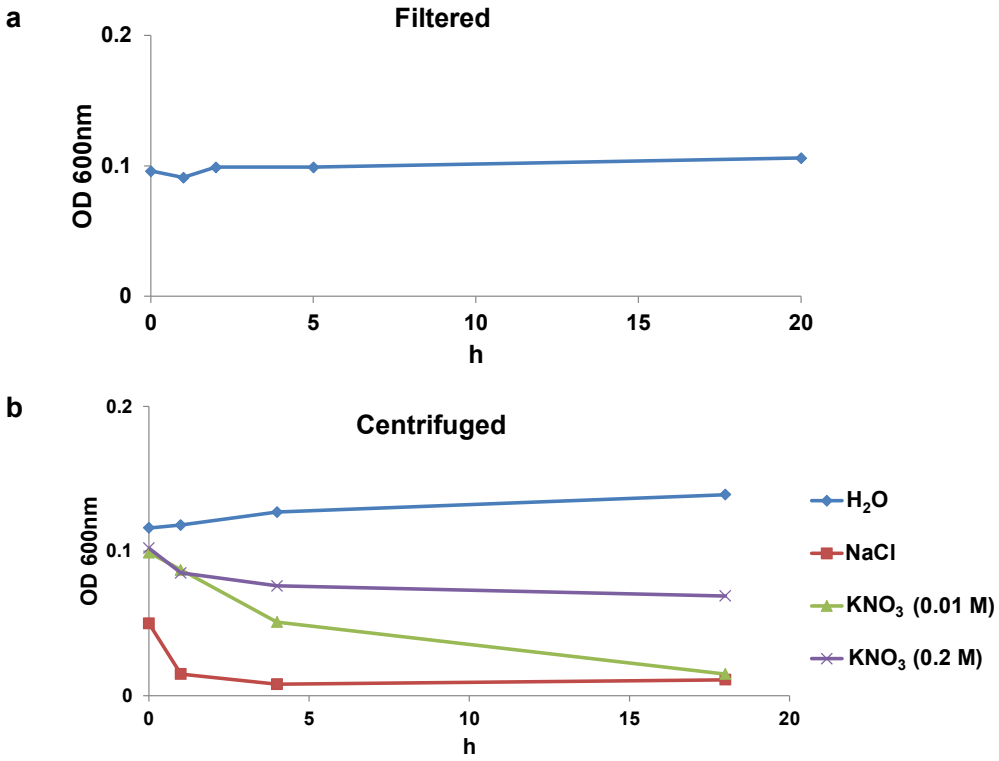

Figure 2.2 Measurement of *Bacillus amyloliquefaciens* optical density in H_2O, KNO_3 and NaCl. Optical density was measured at 600 nm. a) cells were harvested via filtration and suspended in sterilized double deionized water, b) cells were isolated via centrifugation (10,000 rcf, 10 min) and suspended in sterilized double deionized water (blue), 0.85% NaCl (red), 0.01 M KNO_3 (green), or 0.2 M KNO_3 (purple). n = 1 for each point.

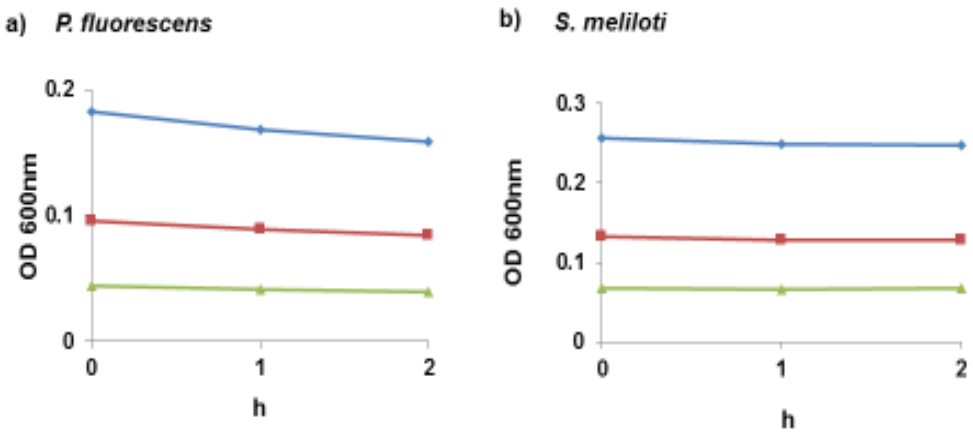

Figure 2.3 Measurement of *Pseudomonas fluorescens* and *Sinorhizobium meliloti* optical density in H_2O. Cells were harvested and suspended in sterilized DDI water. Optical density was measured at 600 nm. a) represents the response of *P. fluorescens.* b) represents the response of *S. meliloti*. Lines represent the average optical density (n = 3) over time of cell preparations with relatively high optical density (blue), medium optical density (red), or low optical density (green).

After exposure medium selection, it was possible to develop the high-throughput methods for assessing O_2 consumption and cell viability. The details of the cell preparation and methodology are provided in the methods section (2.3). For calibration of the O_2 consumption assay, mid-log phase cells were harvested to the desired cell density, diluted, and loaded into a 96 well microplate with embedded O_2 sensors (Oxoplate™). Cells were then supplemented with glucose and O_2 consumption curves were obtained over 1.5 h. Finally, the relationship between the area under the O_2 consumption curve and the starting cell density was determined (Figure 2.4).

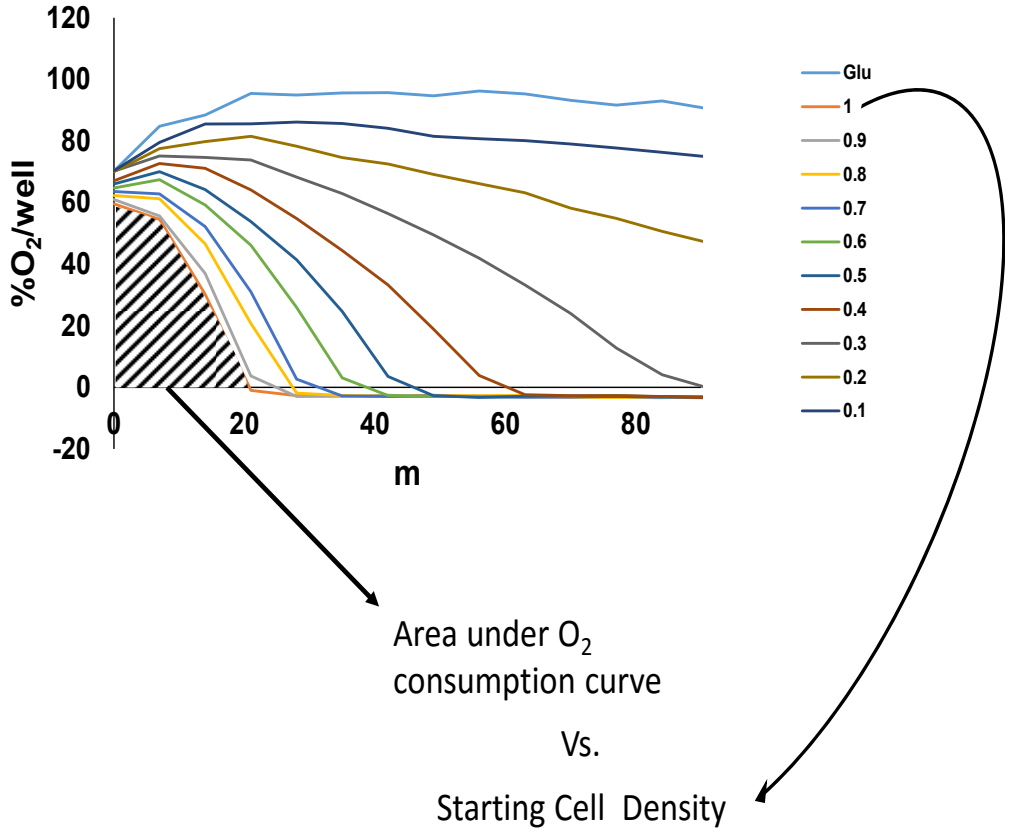

Figure 2.4 O_2 consumption assay calibration schematic. *Bacillus amyloliquefaciens* cells were cultured to mid-log phase then prepared in MES as in section 2.3, loaded into an Oxoplate at known dilutions (8 wells/dilution point), and O_2 consumption was measured. The area under the O_2 consumption curve was then related to the starting cell density for calibrating the assay. Color represent dilutions (1 = not diluted, 0.5 = 50 % diluted, Glu = glucose only). Stripes represent the area under the O_2 consumption curve of undiluted cells.

After the O_2 consumption calibration assay was completed the viability method could be developed. Cells were treated the same as in the O_2 consumption assay but after 1.5 h in the Oxoplate™, cells were diluted 500 times in microplates and then TY media was added 1:1 as in Section 2.3. Growth curves were then gathered by measuring absorbance at 450 and 600 nm (Section 2.3) or only 600 nm (section 3.2). For experiments using both 450 and 600 nm absorbance measurements (which was used to overcome spectral interference from condensation on microplate lids), absorbance was measured by subtracting the absorbance at 600 nm from that at 450 nm ($abs = abs_{450nm} - abs_{600nm}$). The relationship between starting cell density and the time at which the generated growth curves passed a cutoff absorbance of 0.005 was then determined (Figure 2.5).

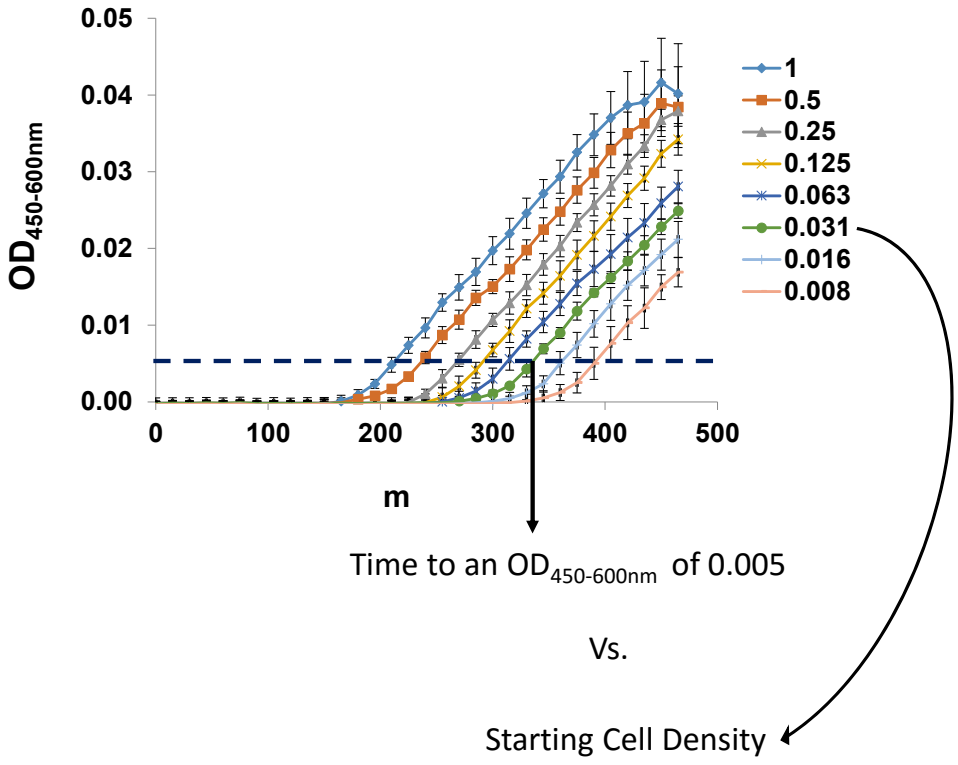

Figure 2.5 Viability assay calibration schematic. *Bacillus amyloliquefaciens* cells were cultured to mid-log phase then prepared in MES as in section 2.3, loaded into an Oxoplate at known dilutions (8 wells/dilution point). After 1.5 h cells were diluted and supplemented with tryptone-yeast media (Section 2.3). Optical density was estimated by measured as abs = absorbance at 450 nm – absorbance at 600 nm (media blanks were subtracted). The time at which growth curves passed $OD_{450\text{-}600nm}$ of 0.005 (dashed line) was recorded and related to starting cell density for assay calibration. Colors represent dilutions (1 = not diluted, 0.5 = 50 % diluted, etc.)

2.2 Introduction

Most approaches to examine toxic responses in bacteria rely primarily on mortality or growth assays. Mortality alone is a limited metric for assessing toxicity in microbes, as a wide range of stress responses occur prior to cell death[116]. For instance, sublethal concentrations of ZnOAc and ZnO nanoparticles have a significant influence on protein expression in *Cupriavidus necator*[62]. Likewise, sublethal concentrations of Ni^{2+} induce changes in protein expression in *Burkholderia vietnamiensis* $PR1_{301}$ and inhibit the constitutive degradation of a co-contaminant, trichloroethylene[117, 118]. Chronic exposure of bacteria to sublethal doses of toxic substances can also hinder ecologically significant processes, such as carbon and nitrogen cycling[119]. While these endpoints and others (including gene expression) may provide sensitive indicators of toxicity, a rapid method for examining respiration and viability stress responses of specific bacterial strains of interest and whole microbial communities would be a useful tool in several fields including, ecotoxicology, food science, and medical microbiology[120-122].

Observation of respiration stress in bacteria permits detection of sublethal responses to toxic pollutants and other compounds of interest. However, microbiologists currently lack a flexible, affordable, and high-throughput method of evaluating respiration stress in bacterial cultures. Respiration of soil microbes, frequently measured by O_2 consumption or CO_2 evolution, can be a relatively sensitive endpoint for observing metal induced toxicity[123]. Most high-throughput methods typically require special instrumentation and/or the use of potentially confounding reagents. For instance, many methods used for evaluating antimicrobial properties are conducted in media that may alter toxicant bioavailability due to the presence of complexing ligands, changes in oxidation

state, surface charge, or aggregation status of the toxicant (e.g. exposures in poorly characterized media), thus limiting the ability to ascertain the distinct chemical form of a contaminant involved in a toxic resaponse, or the toxicity mechanism. The requirement for carefully chosen exposure media in toxicological studies of bacteria[124] is generally neglected in the literature, which hinders cross study comparisons since differences in solution chemistry remain unknown/unreported.

One of the more prominent respiration assays, the Biolog Ecoplate™, while useful in examining utilization of various substrates, is experimentally restricted because the different substrates are pre-loaded on the plate in a non-customizable manner. This restricts exploration of additional carbon sources and in-depth study of any specific carbon source. There are also limitations on experimental design (e.g. the inability to randomize treatments), which complicates statistical analysis of the data. Another common respiration assay, Microtox™, is sensitive and flexible in terms of test substrates, but requires special equipment and is restricted to the use of a single test organism, *Vibrio fischeri*, which limits the scope of studies performed with this system. Recently, "extracellular flux analyzers" (Seahorse Biosciences) have been successfully adapted for microbial respiration assays[125-127], but these specialized instruments are relatively costly and not currently capable of high-throughput screening of toxic compounds.

Respiration stress experiments performed with the Microresp™ System show respiration, as measured by CO_2 evolution, to be useful for studying microbial community responses to various treatment conditions (e.g. metal exposure, antibiotic exposure, ecosystem management)[128-130]. The Microresp™ System was developed and has been utilized primarily for soil respiration assays, but has been more recently adapted for use

with pure microbial cultures[131]. A drawback of the Microresp™ assay is that respiration is measured only at the end of a defined exposure period, thus providing no real-time information. Importantly, respiration data gathered using this assay (or any other) must be interpreted in terms of viability over the course of the exposure to determine the relationship between CO_2 evolution and viable cell counts.

I report the development of a method for rapid and sensitive assessment of viability and respiration responses in aerobic microbes exposed to metals and antibiotics by combining two high-throughput 96 well microplate-based assays. The respiration assays are performed using Oxoplates™ (PreSens, Regensburg, Germany), which are 96-well microplates with O_2 sensing membranes embedded in the bottom of each well, allowing high-throughput real-time measurement of O_2 consumption *during* exposure. While Oxoplates™ have previously been used to evaluate respiration responses of bacteria to various substrates[132, 133], to my knowledge, respiration responses have not been normalized to viability responses. Here I combine an Oxoplate™ respiration assay with a high-throughput 96 well microplate viability assay similar to those previously described [134, 135], but which has been modified to simplify growth curve interpretation. By combining data from both assays, I express O_2 consumption in terms of viability, developing a method for visualizing changes in respiration as they correspond to viability. The new methodology is used to assess respiration and viability responses in the plant growth promoting rhizobacteria (PGPR), *Bacillus amyloliquefaciens* GB03 (formerly, *Bacillus subtilis* GB03)[136], to Ag^+, Zn^{2+}, and Ni^{2+}, all metals with known toxicity to bacteria. The incorporation of streptomycin as a positive control further demonstrated the utility of my methods for use in conventional antibiotic studies.

2.3 Materials and Methods

2.3.1 Maintenance and isolation of *Bacillus amyloliquefaciens* GB03

Bacillus amyloliquefaciens GB03 may be obtained from the *Bacillus* Genetic Stock Center (BGSCID: 3A37), where it is currently still referred to as *Bacillus subtilis* GB03. Vegetative cells were stored at -80 ˚C in glycerol stocks composed of 1:1 ratios of glycerol and bacterial cultures in tryptone/yeast extract media (TY media) consisting of 5 mg/mL tryptone + 3 mg/mL yeast extract + 0.01 M $CaCl_2$. Cultures made from the stocks were maintained on 1% agar plates containing TY media and incubated at 28˚C. For each experiment a single colony was used to inoculate 50 mL TY + 50 mM MES media and cells were cultured to mid-late log phase (OD_{600nm} ~0.86) at 28˚C and 200 rpm. After reaching the desired OD_{600nm} , ~ 30 mL were divided and filtered through two 1 µm Nuclepore membranes (GE Whatman, New Jersey, USA) seated on two separate glass filter holders and washed 3x with 7.5 mL of sterile 50 mM MES. A good seal was obtained by pre-wetting the glass filter holder with 50 mM MES before seating the membrane and funnel. The membranes holding the microbes were then transferred to 12 mL of 50 mM MES in a 250 mL sterile beaker and gently swirled to liberate the cells. The cell suspension was then brought to an OD_{600nm} ~1.15 (considered cell density proportion of 1) using 50 mM MES. Prior to culturing and isolation, MES solutions were brought to pH 6 with 5 M NaOH, resulting in 25 mM NaOH, and filter sterilized. All glassware was acid washed for a minimum of 2 hours in 12.5% HCL + 12.5% HNO_3.

2.3.2 Exposure procedure

Approximately 1 h prior to completion of cell isolation 50 µL of 50 mM MES was transferred to each well of an Oxoplate™. *B. amyloliquefaciens* cells prepared to an OD_{600nm} ~1.15 as described above were transferred to a 50 mL sterile, plastic reagent boat. During bacterial isolation, metal solutions at 8 times the target concentration (8x) were prepared using 50 mM MES pH 6 in a clear, sterile 96 well plate, and 10% glucose + 50 mM MES pH 6 was prepared and transferred to a 50 mL sterile, plastic reagent boat. Then, either 100 µL of the live cell suspension or 50 mM MES was transferred to each designated well of the Oxoplate™. Using a multichannel pipette, 25 µL of 8x metal solutions were added to each well, followed by 25 µL of 10% glucose + 50 mM MES. This results in exposure media containing the targeted metal concentration (*vide infra*) and a glucose concentration of 69 mM. The plate was then sealed with a clear, sterile PCR film, placed in the plate reader and the Oxoplate™ protocol described below was used to measure O_2 consumption with time. After 1.5 h the Oxoplate™ was removed from the reader, the PCR film was removed, and the cells were diluted 500x to a total of 100 µL in a clear, sterile 96 well plate. Then, 100 µL of 2x TY + 50 mM MES pH 6 was transferred to each well (resulting in 1000x dilution), the plate was sealed with a clear, sterile PCR film, and absorbance (450 nm and 600 nm) was measured as described below.

2.3.3 O_2 consumption assay calibration and measurement

The O_2 partial pressure (in terms of percent air saturation) per well with time was calculated using the methods described by the Oxoplate™ manufacturer. Briefly, fluorescence measurements for an O_2 sensitive indicator dye (excitation: 540 nm, emission:

650 nm) and a reference dye (excitation: 540 nm, emission: 590 nm) are incorporated into equation 1.

$$pO_2 = (100 \times \left(\frac{k_0}{I_R} - 1\right))/(\frac{k_0}{k_{100}} - 1) \quad (1)$$

Where, I_R is sample fluorescence intensity reading at 650 nm divided by the fluorescence intensity at 590 nm, k_0 is the I_R average of 4 wells loaded with 300 µL of 0.01 g Na_2SO_3/ml, and k_{100} is the I_R average of 4 wells loaded with 200 µL of 50 mM MES + 1.25% glucose shaken for 2 m before loading. Prior to the experiments, both k_0 and k_{100} were determined after allowing the solutions to incubate in a sealed Oxoplate™ for 1 h at 28 ˚C before measuring fluorescence intensity.

To calibrate O_2 consumption readings, cells were prepared as described above to an OD_{600nm} of 1.15 and diluted by 10% to a cell density <0.1% of the starting cell density using 50 mM MES in a clear, sterile 96 well plate. Then, 100 µL of the cells were transferred to an Oxoplate™ containing 50 µL 50 mM MES (loaded ~1 h prior). A mock exposure (an exposure simulating the actual exposure procedure but without any metals or streptomycin) was performed as above, and fluorescence intensity measurements at 540 nm/650 nm and 540 nm/590 nm were recorded every 5 m over a 90 m period. O_2 consumption curves for each well (8 wells/dilution point) were then constructed and the areas under the curves (AUC) were calculated using the “area below curve” macro in the Sigmaplot Software package (Systat Software, California, USA). The non-linear relationship between cell density (as a proportion) and log(AUC) was determined using

JMP® Version 10 (SAS Institute Inc., North Carolina, USA 1989-2007). The mathematical model derived from this relationship (NRMSE = 0.032) was used as a calibration equation to determine percent O_2 consumption. One caveat of the method, along with all common microbial respiration assays, is that dead cells may provide substances that are toxic to, or nutritive for, the remaining viable bacteria or serve as a sink for the chemicals being assessed for toxicity. This could influence respiration and/or growth, and will be captured in the measurements.

2.3.4 Viability assay calibration and measurement

Cells were prepared to the desired OD_{600nm} as described above and serially diluted (100 µL cell suspension: 100 µL 50 mM MES) in a clear 96 well plate (8 dilution points, 8 wells/dilution point). An Oxoplate™ was loaded with 50 µL of 50 mM MES ~1 h prior to transferring 100 µL of cells/well of the Oxoplate™. A mock exposure was performed by adding 25 µL of 50 mM MES followed by 25 µL 10% glucose + 50 mM MES. Once the Oxoplate™ was brought to 200 µL/well, the plate was sealed with a clear, sterile PCR film and placed in a Wallac Victor 2 microplate reader (Perkin-Elmer Life Sciences, MA, USA) for 1.5 h at 28 ˚C using the Oxoplate™ exposure protocol described below.

After the mock exposure the cells were diluted 500x using 50 mM MES to a volume of 100 µL. Then 100 µL of 2x TY + 50 mM MES was loaded to each well (resulting in 1000x dilution at 200 µL), the plate was covered with a clear, sterile PCR film, and placed in the plate reader at 28 ˚C. Dilution of cells provides the benefit of also diluting any added substrates. Hazan et al. [135] used similar methods and found the estimates of viability gathered from the microtiter plate corresponded well with CFU counts. Every 15 m the plate was shaken for 15 s and allowed to sit for 10 s before absorbance was measured at

450 and 600 nm. Dual-wavelength absorbance measurements were employed to overcome the problem of spectral interference resulting from the formation of condensation on the PCR film. Dual-wavelength spectroscopy was shown to provide accurate readings that reduce the influence of light scatter on absorbance/transmittance measurements in spectroscopic studies[137]. I found the dual wavelength method (abs = 450 nm – 600 nm) yielded low well-to-well variation in estimated absorbance of media controls (TY without metal or bacteria) over time (mean $abs_{450nm-600nm}$ = 0.02, standard deviation = 0.002). Condensation may not occur on the PCR films in all microplate readers, thus it is possible, and potentially optimal, for researchers using such instruments to rely upon a single absorption wavelength to generate growth curves. Preliminary tests should be performed to determine which method works best in a particular system.

The adjusted absorbance readings were used to construct bacterial growth curves from each well, where the background absorbance was subtracted from readings at each time point. Linear interpolation was applied to determine the time (m) at which each growth curve passed a critical threshold of 0.005 ($OD_{450nm-600nm}$). A mathematical relationship (R^2 = 0.98) between starting cell density (as a proportion) and time to threshold was determined using linear modeling of log(cell density) vs. log(minutes) using JMP® Version 10. This mathematical model is used as a calibration equation to estimate percent viability following exposure.

2.3.5 Experimental design of exposures

A randomized complete block design was used to evaluate the toxicity of Ag^+ (0.5, 1, 2, 3, 4, 6, 8, and 10 μM), Ni^{2+}, and Zn^{2+} (0.63, 1.3, 2.5, 5, 10, 20, 40 and 80 μM) using 7 experimental blocks/biological replicates. A metal free control was also used across all

experimental blocks. Treatments were randomized by column and control columns were randomized by row across all experimental blocks to control for variation due to plate placement of treatments and loading order of cells. Technical replicates of each treatment were performed in triplicate in each experimental block. Ions were supplied as either $AgNO_3$, $ZnSO_4$, or $NiSO_4$. Silver was chosen because its toxic effects are well documented and intracellular concentrations are not tightly regulated, whereas Zn^{2+} and Ni^{2+} were chosen because they are both tightly regulated essential nutrients that are also toxic at elevated concentration and both have been shown to display toxicity to *B. subtilis* (a relative of *B. amyloliquefaciens*) at similar concentrations under the same test conditions. Additionally, mechanisms governing intracellular Zn^{2+} concentrations are relatively well understood, while less is known regarding Ni^{2+} homeostasis. Streptomycin (2.6 μM) was used as a positive control, based on a preliminary study, where I found this concentration to significantly, but not completely, reduce viability. Stock metal concentrations were verified *via* ICP-MS analysis prior to exposures.

Distribution and variance of residuals were determined following linear regression using distribution plots, Q-Q plots, and Studentized residual plots. Treatment responses were normalized to metal free control wells, averaged within experiments, and the average of experimental means were compared to a hypothetical mean (H_O: $\mu = 100\%$, for viability and O_2 consumption measurements) using a two-tailed, one-sample t-test (n=7, alpha 0.05, assuming unequal variances). Mean O_2 consumption responses of each experiment were plotted against mean viability measurements and regression curves were fit using SoftMax Pro 6.4 (Molecular Devices, Wokingham, UK).

2.3.6 Chemical equilibrium modeling

Exposure media were modeled using Geochem-EZ[138] to determine the free ion activities of the metals of interest (Figures 2.6-7). It was necessary to update the ligand database to include stability constants for Zn-MES[139] and Ni-MES complexes[139, 140]. Taurine and MES share the same sulfonic acid functional group which is known to interact with Ag^+ ions. The stability constant for the Ag-MES complex was approximated with the published stability constant for Ag-taurine complexes found using the IUPAC Stability Constant Database[141]. All stability constants were input at infinite dilution. After concentrations of exposure media constituents were entered into Geochem-EZ, pH was fixed at 6, precipitates were allowed to form, and the ionic strength was calculated using an initial "guess" of 0.01 mol ionic strength, as recommended by the model developers. The standard convergence criteria were implemented.

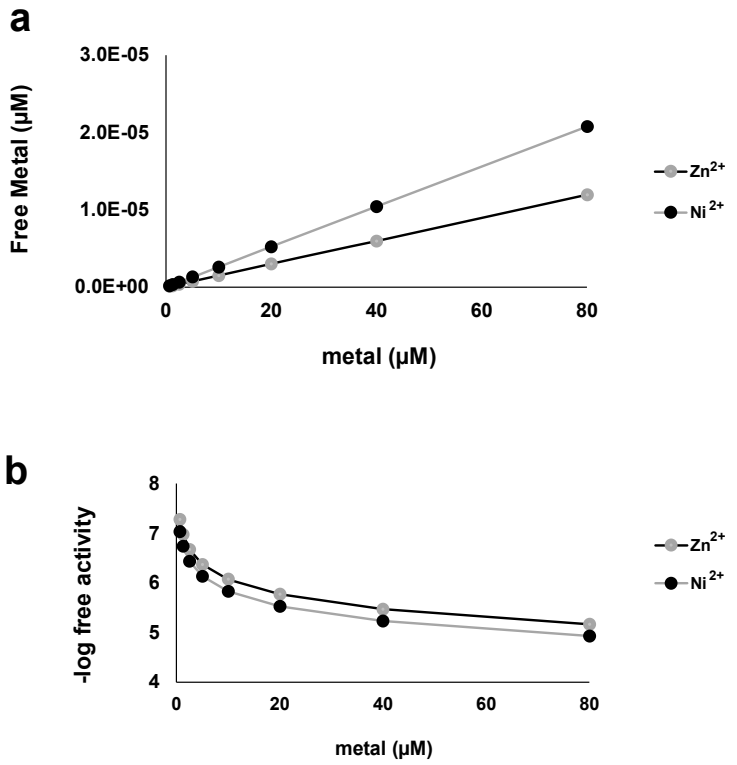

Figure 2.6 Predicted $Zn^{2+}$and Ni^{2+} free ion concentrations and activities in exposure media as calculated by GeoChem-Ez. Precipitates were allowed to form, pH was fixed at 6, and ionic strength was calculated as suggested by the developers. **a** Predicted free Zn^{2+} and Ni^{2+}(µM) in 50 mM MES at exposure metal concentrations used in this study. **b** –log free $Zn^{2+}$and Ni^{2+}activity in 50 mM MES at exposure metal concentrations used in this study.

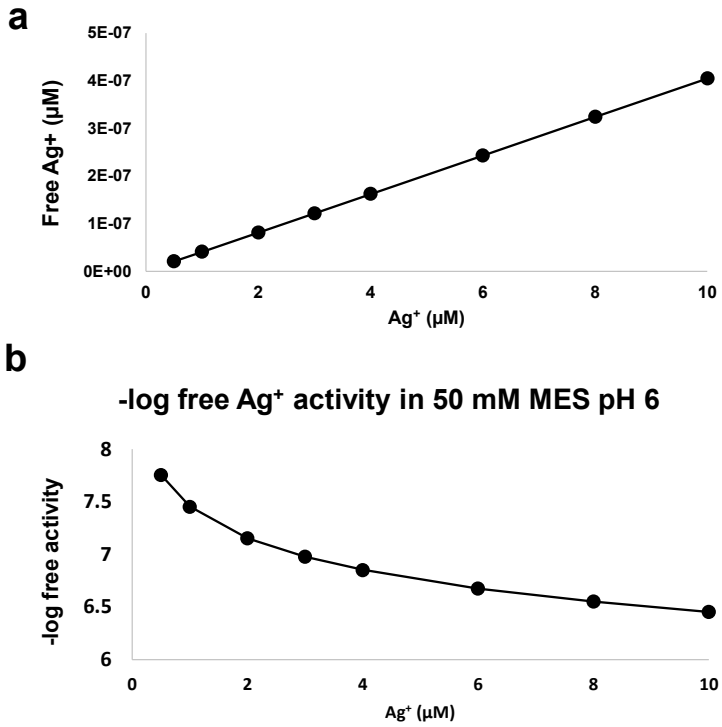

Figure 2.7 Predicted Ag^+ free ion concentration and activity in exposure media as calculated by GeoChem-Ez. Precipitates were allowed to form, pH was fixed at 6, and ionic strength was calculated as suggested by the developers. **a** Predicted free Ag^+ (µM) in 50 mM MES at exposure Ag+ concentrations used in this study. **b** –log free Ag^+ activity in 50 mM MES at exposure Ag^+ concentrations used in this study.

2.4 Results

2.4.1 *Bacillus amyloliquefaciens* response to streptomycin

When compared with the control, 2.6 μM streptomycin was found to significantly decrease the number of viable cells (~40%), while there was no statistically significant influence on O_2 consumed per well (Figure 2.8). This is reflected in the O_2 consumption-viability plots, which revealed highly elevated O_2 consumption in cells exposed to streptomycin (Figure 2.9).

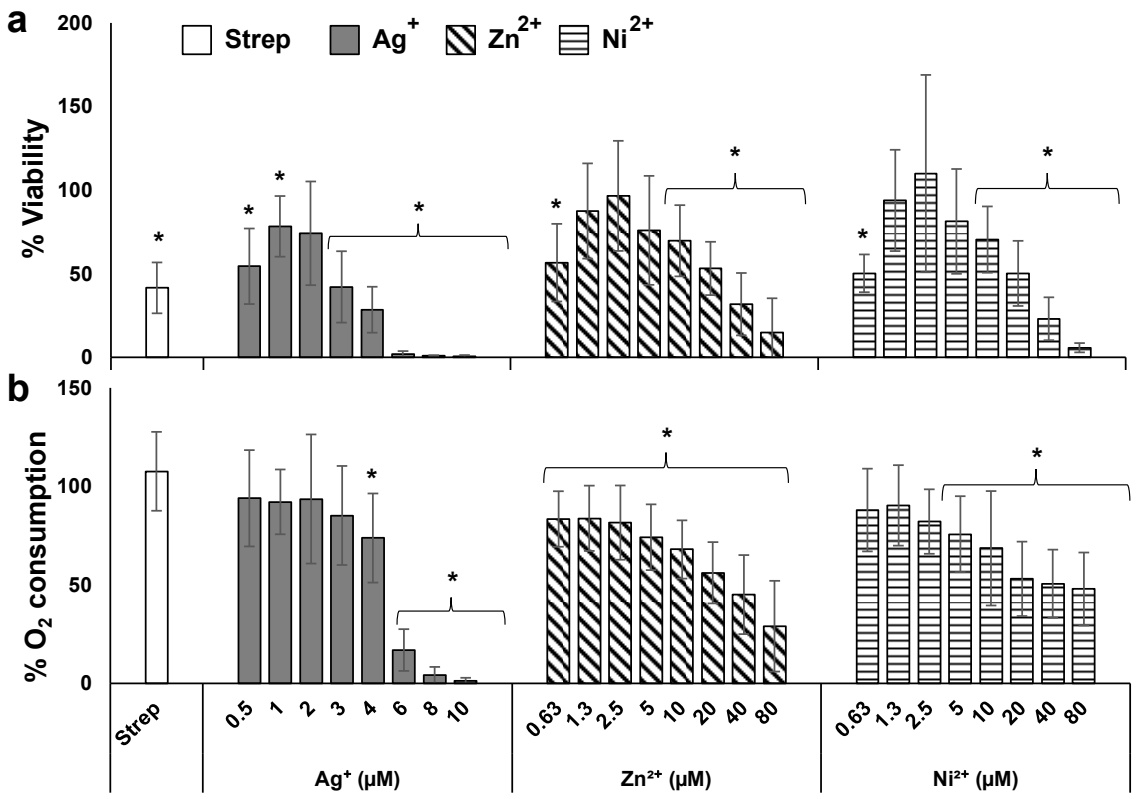

Figure 2.8 Response of *Bacillus amyloliquefaciens* GB03 to Ag^{+}, Zn^{2+} and Ni^{2+} metal ions. **a** Percent viable cells after exposure. **b** Percent O_2 consumption over the course of exposure. All bars are standard deviation of 7 experiments, * indicates response is statistically different from hypothetical mean (H_O: μ=100% for viability and respiration measurements) as determined using a two-tailed, one-sample t-test at alpha 0.05, assuming unequal variance.

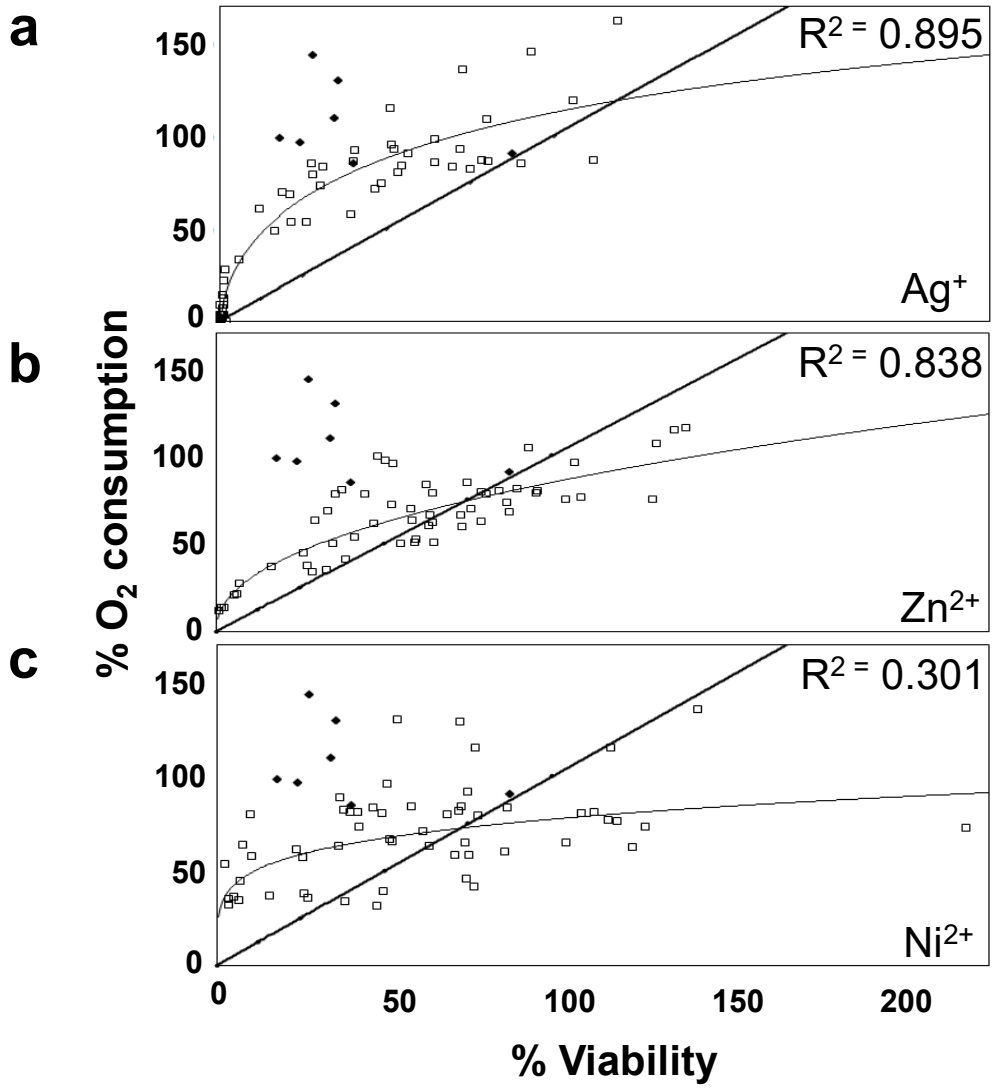

Figure 2.9 Regression plots of percent O_2 consumption versus percent viability showing the response of *Bacillus amyloliquefaciens* GB03 to Ag^+, Zn^{2+}, and Ni^{2+}. **a** Ag^+ (open boxes), **b** Zn^{2+} (open boxes), and **c** Ni^{2+} (open boxes). Black diamonds in all plots are the response in each experiment to streptomycin. Using Softmax Pro 6.4, a 4-parameter curve was fit to the Ag^+ induced responses and log-log curves were fit to the Zn^{2+} and Ni^{2+} induced responses.

2.4.2 *Bacillus amyloliquefaciens* response to Ag^+ ions

The O_2 consumption-viability plots revealed large increases in oxygen consumption per viable cell in response to Ag^+ exposure (Figure 2.9A), while I observed a statistically significant reduction in oxygen consumption per well at 4, 6, 8, and 10 µM Ag^+ (Figure 2.8B). A 4-parameter nonlinear curve yielded a relatively good fit ($R^2 = 0.895$), implying O_2 consumption and viability correlate in a nonlinear manner in response to silver ions. Only ~30% of the cells were viable after exposure to 4 µM Ag^+ (Figure 2.8A) and I observed nearly complete mortality after exposure to 8-10 µM Ag^+ (Figure 2.8A). There was a reduction in cell viability following exposure to all tested Ag^+ concentrations, most of which were statistically significant ($p= 0.05$) with the exception of the response at 2 µM ($p = 0.07$) (Figure 2.8A).

2.4.3 *Bacillus amyloliquefaciens* response to Zn^{2+} ions

I observed a decrease in O_2 consumption per well in response to all tested Zn^{2+} concentrations (Figure 2.8 B). The O_2 consumption-viability plots showed increased O_2 consumption when percent viability was low and decreased O_2 consumption when viability was high (Figure 2.9B). A log-log regression was used to generate a nonlinear curve with an R^2 of 0.838, supporting the notion that a nonlinear relationship exists between O_2 consumption and viability responses to Zn^{2+}. A statistically significant decrease in viability was induced by 0.63 and 10-80 µM Zn^{2+}, with viability gradually declining with increasing [Zn^{2+}] (Figure 2.8A). I found only ~15% of *B. amyloliquefaciens* cells exposed to 80 µM Zn^{2+} remained viable after exposure (Figure 2.8A).

2.4.4 *Bacillus amyloliquefaciens* response to Ni^{2+} ions

While a clear gradual decline in O_2 consumption per well was observed in response to 2.5-80 μM Ni^{2+} (Figure 2.8B), the O_2 consumption-viability plots showed high variability in O_2 consumption in terms of viability (Figure 2.9C). In fact, a log-log regression showed a nonlinear correlation between O_2 consumption and viability, but an R^2 value of 0.301 indicates this is a relatively weak correlation. Statistically significant declines in cell viability were observed in response to 0.63 μM Ni^{2+} and from 10-80 μM Ni^{2+} (Figure 2.8A).

2.5 Discussion

Widespread sublethal concentrations of antibiotics in the environment are thought to be a major contributor to selection of antibiotic resistant bacteria[120]. The sublethal effects of antibiotics are known to influence several important bacterial processes, such as biofilm formation and virulence, and may also be associated with increased mutagenesis[120]. The effect of streptomycin on respiration has been known for some time[142], and it proved to be a useful control in my studies. In fact, the response of *B. amyloliquefaciens* to streptomycin clearly illustrates the utility of plotting O_2 consumption responses by viability measurements and the careful interpretation required in bacterial respiration studies. Additionally, this finding is of particular importance given that accelerated respiration has recently been shown to potentiate bactericidal lethality of a range of antibiotics[127]. My method is applicable to screening potential antibiotic substrates and/or antibiotic resistance, simultaneously determining the effect on bacterial viability and O_2 consumption.

Like antibiotics, sublethal concentrations of heavy metals are known to select for antibiotic resistance in bacteria[143-145]. For instance, environmentally relevant sublethal concentrations of antibiotics (aminoglycosides, tetracycline, trimethoprim, *β*-lactams, sulfonamide, and macrolides) and heavy metals (silver, copper, and arsenic) were shown to select for multidrug resistance in *Escherichia coli*[143]. Such findings illustrate the importance of examining sublethal and sub-minimum inhibitory concentration (MIC; the minimum concentration of a substance required to completely inhibit bacterial division) responses in bacteria.

Exposure of *Escherichia coli* to Ag^+ concentrations similar to those in this study (<10 μM) has been shown to stimulate respiration in the presence and absence of glucose[146]. The authors suggest this is due to the uncoupling of the electron transport chain, which may at least partly explain the respiration responses to Ag^+ I observed. Jin et al. found the IC_{50} for Ag^+ and Ag nanoparticles to be highly dependent on the presence of specific ions for both *B. subtilis* and *Pseudomonas putida*44, with the Ag^+ 24 h IC_{50} for *B. subtilis* ranging from <1 to ~18 μM. Interestingly, my results show similarly low concentrations of Ag^+ induce toxicity in my minimal exposure medium in *B. amyloliquefaciens* (Figure 2.8A).

The toxicity of Ag^+ to bacteria has been studied extensively; however, differences in experimental procedures and measured toxicological endpoints has resulted in a wide range of reported toxicity concentration thresholds. Of paramount importance is the widespread lack of chemical equilibrium modeling of exposure media in microbial metal toxicology literature. Additionally, differences in bacterial strains play an important role in observed toxic responses. For instance, Suresh et al. found ~73 μM Ag^+ completely

inhibited growth of *B. subtilis* (ATCC 9372) in LB medium[31], while Kim et al. found ~463 μM Ag^{+} was required to completely inhibit the growth of *B. subtilis* (KACC10111) in LB medium[25]. Without consistent use of a specific test strain or an understanding of the speciation of metals in exposure media, it is difficult to make comparisons across the majority of metal toxicity studies performed with bacteria.

Because of the inconsistencies in exposure methodologies in metal toxicity studies and the novelty of my method, there are few studies with which I can directly compare my results. However, with these limitations in mind, it is instructive to compare the response data with those in the literature to emphasize its utility as a more sensitive platform for assessing respiration and viability responses. Gaballa and Helmann [147] found that 1.8 mM Zn^{2+} was required to completely inhibit growth of *B. subtilis* WT, while 1 mM Zn^{2+} led to only a 20% reduction in optical density (600 nm). Additionally, Kim and An[68] found CFU counts of *B. subtilis* KACC10111 were significantly reduced (~40% of the control) in response to 1 mM Zn^{2+}. Van Nostrand et al.[148] found a 64% reduction in growth of *Burkholderia cepacia* $PR1_{301}$ exposed to 3.8 mM Zn^{2+} at pH 6. It is also worth noting that a meta-analysis examining the toxicity of nanoparticles and associated ions to environmentally relevant test organisms estimated the average MIC of Zn^{2+} to be ~459 μM[149]. The MIC is a different test for toxicity because it requires complete inhibition of cell division. I did not measure the MIC of Zn, but my results indicate it would likely be well under 459 μM Zn for *B. amyloliquefaciens*. While the experiments cited above used various exposure conditions and toxicity endpoints, it is clear that the methodology is capable of detecting responses at comparatively low concentrations.

Compared with Ag^{+} and Zn^{2+}, little is known concerning the mechanisms governing Ni^{2+} toxicity and homeostasis. The toxicity of Ni^{2+} to *B. subtilis* WT was previously shown to be similar to Zn^{2+}. For instance, Gaballa and Helmann[147] found that 1.8 mM Ni^{2+} or Zn^{2+} were required to completely inhibit growth. I also found responses to Zn^{2+} and Ni^{2+} to be very similar in terms of O_2 consumption per well and viability in *B. amyloliquefaciens* (Figure 2.8). However, the O_2 consumption-viability plots clearly show Ni^{2+} induced large increases in O_2 consumption when percent viability is low (Figure 2.9C). Importantly, while the percent O_2 consumption and viability responses induced by Zn^{2+} and Ni^{2+} appear similar, the O_2 consumption-viability plots show a clear difference in the respiration stress induced by these metals (Figure 2.9). Modeling of my exposure solutions showed that, even at identical total molar concentrations, the estimated concentration and activity of free Ni^{2+} were greater than that of free Zn^{2+}, due to stronger interactions of Zn^{2+} with the MES buffer in my exposure solutions (Figure 2.6). The higher free ion activity of Ni^{2+} may be partially responsible for the notable difference I found in O_2 consumption-viability relationships compared with Zn^{2+}; however, the relationship between O_2 consumption and viability was weakly correlated under Ni^{2+} exposure and not Zn^{2+}, suggesting a different biological response to the metals.

The goal of this research was to develop a flexible, sensitive, and high-throughput method for evaluating responses of bacteria to substrates based on respiration and viability. The O_2 consumption-viability plots normalize respiration responses to viable cell numbers, allowing for a more accurate interpretation of the respiration response compared with examining results from each assay separately. This approach is similar to the metabolic quotient commonly used in ecological research[150], but different from the bacterial growth

efficiency (BGE) metric previously devised to interpret growth responses in terms of growth and respiration[151]. While highly useful for the interpretation of ecosystem or community level responses, neither of these metrics accurately or easily allow for the expression of O_2 consumption in terms of viable cell numbers and are, therefore, not as applicable when interpreting responses of an organism in pure culture. To demonstrate why it is important to account for viable cell numbers in respiration-based toxicity assays, I performed a series of experiments using a variety of substrates pertinent to medical, food, and environmental sciences. While my work focused on a PGPR species, the methodology reported is flexible and applicable to measuring O_2 consumption responses of most culturable aerobic bacteria.

Chapter 3: Silver Engineered Nanomaterials and Ions Elicit Species-Specific O_2 Consumption Responses in Plant Growth Promoting Rhizobacteria

3.1 Introduction

Engineered nanomaterials (ENMs), human designed and generated materials with at least one dimension between 1-100 nm[1], are now widely utilized in an array of consumer products and industrial applications. The antimicrobial properties of silver have been exploited by humans for centuries, but silver containing ENMs (AgENMs) and other ENMs are currently entering commercial and municipal waste streams and are subsequently being deposited at exponential rates in terrestrial environments through biosolids amendment of agricultural soils[9]. Debate still remains regarding predicted environmental concentrations of ENMs, which is at least partially explained by differences in models implemented to predict environmental concentrations and the lack of empirical data regarding them[9, 10, 152, 153]. While biosolids amended soils are predicted to have low µg/kg to mg/kg concentrations in the near term[9, 153], observed concentrations of total silver in biosolids can vary greatly, sometimes having extremely high concentrations ~856 mg Ag/kg dry biosolids[152]. Despite the debate regarding environmental concentrations of AgENMs, their exponential rate of release to the environment alone constitutes a clear need to explore AgENM responses of environmentally relevant test organisms. In addition, the effects of AgENMs (and other ENMs) on beneficial soil bacteria and other soil microbes remain largely neglected (Chapter 1), but interest is steadily growing[10].

Nanotoxicological studies concerning PGPR have been reviewed in Chapter 1; however, it is important to note that few studies have focused on physiological responses, such as O_2 consumption. This is crucial because a range of toxic responses can occur prior

to cell death, and antibiotic efficacy has recently been linked to modulation of respiration in medically relevant microbes[127]. Furthermore, microbial respiration may sometimes be a sensitive endpoint when examining metal/nanomaterial stress in microbes, especially when normalized to cell viability or biomass[154-156]. In fact, when respiration is not found to be sensitive to metal addition in soils, it is often not examined in terms of viable cells or biomass, so it remains unclear if any detectable changes in metabolism have occurred[154, 157]. Currently there are no widely accepted, cost-effective, and high-throughput methods of examining microbial O_2 consumption in a laboratory setting that do not rely on potentially confounding reagents.

I developed a high-throughput O_2 consumption assay and demonstrated the utility of the method by examining the response of *B. amyloliquefaciens* to streptomycin, Zn^{2+}, Ni^{2+}, and Ag^{+}. My method revealed metal and antibiotic specific O_2 consumption responses in *B. amyloliquefaciens.* My previous work, along with others[131, 155, 156], also highlights the need to normalize respiration responses to viable cell estimates or biomass. Here, I used the method to investigate the O_2 consumption responses of three PGPR species to silver ions and AgENMs.

Most microbial nanotoxicology studies have focused primarily on "pristine" or "as manufactured" ENMs (Chapter 1)[10, 102]. However, ENMs undergo various transformations during the wastewater treatment process and upon application to soils, which leads to sulfation (often referred to as sulfidation) and reduced toxicity of AgENMs[61, 97, 102, 158]. I examined viability and O_2 consumption responses to silver ions ($AgNO_3$), pristine PVP-AgENMs (untransformed polyvinylpyrrolidone-coated AgENM), and sAgENMs (100% sulfidized PVP-AgENMs) using three agriculturally and ecologically relevant plant growth

promoting rhizobacteria (PGPR), *Bacillus amyloliquefaciens* GB03 (formerly *Bacillus subtilis* GB03), *Sinorhizobium meliloti* 2011, and *Pseudomonas putida* UW4.

I hypothesized the unique biology (vide infra) of the PGPR may translate to distinct O_2 consumption patterns and viability responses elicited by Ag^+, AgENMs, and streptomycin exposure. *B. amyloliquefaciens* GB03 is a relatively rapidly growing gram-positive bacterium utilized as a fungicide[159] which promotes plant growth[160], and has never been the subject of a nanotoxicological study to my knowledge. *Sinorhizobium meliloti* 2011 is a relatively slow growing gram-negative bacterium capable of forming a nitrogen-fixing symbiosis with the model legume, *Medicago truncatula,* and related strains are known to promote lettuce growth[83]. Additionally, nodulation of *M. truncatula* A17 by *S. meliloti* 2011 was inhibited by biosolids enriched with nanoscale Ti, Zn, and Ag[87, 88]. *Pseudomonas putida* UW4 is a rapidly growing gram-negative bacterium capable of plant growth promotion and protection against many environmental/pathogen stresses, likely through modulation of plant physiology *via* the production of ACC deaminase[161]. While various strains of *P. putida* have been the subject of many nanotoxicological studies (Chapter 1), no study to date has reported the response of UW4 to nanomaterials. This is particularly important given that bacterial strains even of the same species sometimes exhibit very different responses to metals and nanomaterials (Chapter 1)[26].

3.2 Materials and Methods

3.2.1 Maintenance and Isolation of Bacteria

All bacteria were maintained at -80 °C as glycerol stocks containing a 1:1 mixture of glycerol and mid-log phase cells in tryptone yeast extract broth supplemented with 0.01 M $CaCl_2$ (TY). Single colonies were obtained from glycerol stock streaked TY 1% agar

plates incubated at 28 °C and were used to inoculate 50 mL mini-bioreactors containing 40 mL of TY + 50 mM MES + 0.01 M $CaCl_2$ at pH 6. After inoculation the bioreactors were shaken (horizontally) at 100 rpm and 28 °C. When *B. subtilis* and *S. meliloti* cells reached mid-log phase (OD_{600nm} ~0.64), the bioreactors were centrifuged at 2000 rcf and 28 °C for 5 m (3220 rcf, 28 °C, and 10 m for *P. putida*), medium was removed and cells were washed 3 times with 10 mL of 50 mM MES using the same centrifugation settings. Cells were then suspended to the desired optical density (reported below) and used for either calibrating the respiration and viability assays or in the toxicological experiments.

3.2.2 Assay Calibration

Cultures were prepared in mini-bioreactors as described above to an optical density at 600 nm (OD_{600nm}) of 0.64 ± 0.006 (one standard deviation) and then prepared to OD_{600nm} = 1.19 ± 0.004 (one standard deviation) or 1.045 for *P. putida* (see section 3.3.1). These washed cell preparations were used to calibrate the O_2 consumption and viability assays. Approximately 1 h prior to harvesting, 50 µL of 50 mM MES was added to each well of the Oxoplate™ to condition the membrane. Cells were then diluted to known cell density proportions (1.0, 0.75, 0.5, 0.25, 0.125), with a proportion of 1 equal to the prepared cell density above. Following dilution, 100 µL of cells was loaded in wells of the Oxoplate™ (n = 8 for each cell density proportion). Then 25 µL of 50 mM MES was added to each well of the plate, followed by 25 µL of 10% glucose + 50 mM MES. The Oxoplate™ was sealed with a clear, sterile film, the lid was seated, and fluorescence was measured at 590 and 650 nm (excitation: 540 nm) every 5 minutes for 1.5 hours using a Spectramax i3 microplate reader (Molecular Devices). The film was then removed from the plate and cells were serial diluted (1:500) in 50 mM MES using sterile 96 well plates to a volume of 100

μL, after which 100 μL of a double strength TY broth was added to each well of the plate, resulting in further dilution (1:1000). The plate was sealed with a clear, sterile PCR film and loaded in the reader where it was shaken 15 s and allowed to rest 20 s prior to measurement of absorbance at 600nm every 10 m using the same microplate reader. Strong correlations were found between starting cell density proportions and either the area under O_2 consumption curves or time at which growth curves passed OD_{600nm} 0.09 (after subtracting background absorbance) (Table 3.1). Cell viability was determined in control conditions (no metal) in terms of CFU/mL as assessed *via* a drop plate method[162] before and after the O_2 consumption assay procedure (Table 3.2).

Table 3.1 Calibration curve fitting results of the O_2 consumption and viability assays.

	O_2 Consumption Assay		**Viability Assay**	
PGPR	**Curve Fit**	**R^2**	**Curve Fit**	**R^2**
B. amyloliquefaciens	4-parameter	0.999	log-log	0.987
S. meliloti	linear	0.998	log-log	0.994
P. putida	4-parameter	0.999	log-log	0.999

PGPR, plant growth promoting rhizobacteria

Softmax Pro 6.4 was used to regress O_2 consumption (area under curve) or viability (time to $OD_{600nm} = 0.09$) against cell density proportion.

Table 3.2 CFU/mL before and after O_2 consumption assay

		CFU/mL ± S.D.			
Culture	**OD_{600nm}**	**Before**	**S.D.**	**After**	**S.D.**
B. amyloliquefaciens	1.159	1.05E+08[a]	8.33E+06	1.01E+08[a]	2.28E+07
S. meliloti	1.189	1.63E+09[a]	1.46E+08	1.98E+09[b]	1.22E+08
P. putida	1.191	1.13E+09[a]	2.13E+08	6.67E+08[b]	1.15E+08
P. putida	1.045	6.35E+08[a]	3.82E+07	6.58E+08[a]	2.96E+07

CFU, colony forming unit; PGPR, plant growth promoting rhizobacteria, S.D., one standard deviation of the mean; OD_{600nm}, optical density at 600 nm

OD_{600nm} is the optical density of the isolated cells prior to diluting 1:1 with medium for the O_2 consumption assay. Letters represent significant differences at α 0.05 as determined *via* a Studentized t-test comparing CFU/mL before and after the O_2 consumption assay. All CFU/mL estimates are from n = 6 plates, excluding *B. amyloliquefaciens* (n = 3 plates).

3.2.3 Exposure Procedure

After culturing to mid-log phase, cells were harvested as described above in 50 mM MES (pH 6) and suspended to OD_{600nm} ~1 (*B. subtilis*: OD_{600nm} = 1.08 ± 0.02; S. meliloti: OD_{600nm} = 1.06 ± 0.02; *P. putida*: OD_{600nm} = OD_{600nm} = 1.07 ± 0.02, error is one standard deviation). Prior to cell harvest, 50 µL of 50 mM MES pH 6 was added to each well of an Oxoplate™ and all the metals, glucose and streptomycin were prepared to 8 times the target concentration. Upon cell harvest, 100 µL of cells or MES was added to each designated well of the Oxoplate™, followed by 25 µL of metals, streptomycin, or MES and then 25

μL of 10% glucose/50 mM MES. Finally, the O_2 consumption and viability assays were performed as described in the assay calibration section, and O_2 consumption of blank wells was subtracted from all other wells.

3.2.4 Metal and ENM Characterization

Concentrations of stock metals were determined *via* ICP-MS analysis prior to exposure. PVP-AgENMs and sAgENMs were characterized in the exposure medium at ~300 μM total silver and 28 °C using a Zetasizer Nano ZS (Malvern). Hydrodynamic diameter and electrophoretic mobility were estimated using direct light scattering and electrophoretic light scattering, respectively. The particles used were previously characterized and PVP-AgENMs had a primary particle size of 53-58 nm[114, 163], while sAgENMs had a primary particle size of ~65 nm[163], both determined *via* transmission electron microscopy (TEM).

A mock exposure (without bacteria) was scaled up to 2 mL to examine the abiotic dissolution of PVP-AgENMs and sAgENMs in the exposure medium. Briefly, PVP-AgENM (29, 115, and 230 μM) and sAgENM (~300 μM) were prepared in the exposure medium with glucose to 2 mL in ultracentrifuge tubes. Samples were gently vortexed to ensure mixing and 100 μL was immediately removed for total metal analysis, before centrifuging for 90 m at 28 °C and 246,000 x *g*. According to Stoke's law, these conditions were sufficient to sediment spherical particles ≥ 2 nm. After centrifugation, 1 mL was removed and acidified to 1% HCl for dissolved metal analysis. Total metal samples were microwave digested at 100 °C and 400 watts for 35 m (20 m ramp, 10 m hold, 5 m cooldown) in 13% HCl/40% HNO_3 before diluting 15 times in pure double deionized water, yielding 1% HCl/3% HNO_3.

3.2.5 Chemical Speciation Modeling

Free ion concentrations and activities were modeled using GeoChem-Ez[138], as previously described (Chapter 2). *Briefly,* $AgNO_3$ concentrations or expected dissolved Ag^+ concentrations from AgENM were modeled in GeoChem-Ez with 50 mM MES, 25 mM NaOH, pH fixed at 6, and precipitates were allowed to form. A "guess" of 0.01 M/L was used to calculate ionic strength, as recommended by the software developers. See the previous work in Chapter 2 for the necessary additions to the GeoChem-EZ ligand database.

3.2.6 Experimental Design and Data Analysis

A randomized complete block design was used to assess toxicity in each of the test organisms, with 3 experimental blocks and 3 replicates per block. Microplate columns were randomized across experiments and controls were randomized across rows. *B. amyloliquefaciens* and *S. meliloti* were exposed to 2.6 µM streptomycin, $AgNO_3$ (0.5, 1, 2, 3, 4, 5, 6, 10 µM), 296 µM sAgENM, and PVP-AgENM (4.6, 37, 55.6, 111, 148, 185, 222, and 296 µM). The same concentrations of $AgNO_3$, streptomycin, and sAgENM, but 4.3, 34.5, 43, 46, 115, 144, 172, and 230 µM PVP-AgENM were used for *P. putida* exposures. Molarity is expressed in terms of total silver concentration. Viability and O_2 consumption estimates were normalized to the no metal controls and were found to be non-normally distributed. The data were ranked and ANOVA was used to examine experiment by treatment interactions. Because no experiment by treatment interactions were found, observations were pooled across experiments (n = 9) and a two-tailed Wilcoxon signed rank test was used to compare the observations to a hypothetical mean of 100% viability or O_2 consumption (H_0: $\mu = 100$, α 0.05) using JMP.

Sigmaplot was used to generate non-linear, 4-parameter dose response curves and extrapolate LC_{50} values for viability responses to PVP-AgENM and $AgNO_3$. LC_{50} values were compared using an unpaired t-test with a Bonferroni correction. Additionally, Sigmaplot was used to perform regression analyses on O_2 consumption-viability plots for interpreting O_2 consumption responses in terms of relative viable cell numbers. Dissolution measurements were used to generate predicted viability responses to the dissolved fraction of AgENMs by extrapolating responses from $AgNO_3$ dose response curves for the average dissolution estimate ± one standard deviation (n = 3).

3.3 Results and Discussion

3.3.1 Assay Calibration and Particle Characterization

Cell viability of PGPR was not negatively affected in the control conditions without metals or antibiotics, but *P. putida* exhibited mortality at an OD_{600nm} = 1.191 (before dilution in the Oxoplate™) (Table 3.2); this was the highest cell density used in the initial calibration curves, so this point was removed from the curve. Fortunately, at cell densities similar to those used in the exposure conditions, *P. putida* exhibited no significant change in cell viability (Table 3.2). *S. meliloti* showed modest levels of growth during the O_2 consumption assay. I found strong log-log correlations between starting cell density and time to OD_{600nm} of 0.09 (Table 3.1). I also found a strong relationship between starting cell density and area under the curve of O_2 consumption measurements which was linear for *S. meliloti* and explained by a 4-parameter curve in the other PGPR (Table 3.1). Hydrodynamic diameter and electrophoretic mobility of PVP-AgENMs and sAgENMs were stable in the exposure medium over the course of the study in the absence of bacteria

(Table 3.3). I observed minimal dissolution of sAgENM (0.14% ± 0.02) and moderate dissolution of PVP-AgENM (6.15% ± 0.23, error is one standard deviation).

Table 3.3 Particle characterization of PVP-AgENM and sAgENM in exposure medium

ENM	**time (m)**	**Z-avg d. nm (± S.D.)**	**Electrophoretic mobility µmcm/Vs (± S.D.)**
PVP-AgENM	0	84.6 (± 0.9)	-0.24 (± 0.1)
	90	85.4 (± 1.5)	-0.29 (± 0.1)
sAgENM	0	142.7 (± 28)	-1.45 (± 0.3)
	90	144 (± 28)	-1.85 (± 0.1)

ENM, engineered nanomaterial; PVP-AgENM, polyvinylpyrrolidone-coated silver ENM; sAgENM, 100% sulfidized AgENM; z-avg d. nm, average hydrodynamic diameter in nanometers; µmcm/Vs, electrophoretic mobility; S.D., one standard deviation; m, minutes

Diameter and electrophoretic mobility values are averages of 3 replicates as assessed *via* dynamic light scattering and electrophoretic light scattering. Significant differences were evaluated at α 0.05 as determined *via* a Studentized t-test comparing measurements at 0 and 90 m, no differences were observed.

3.3.2 PGPR Viability Responses

In terms of viability, PVP-AgENMs were far less toxic than ions on a molar basis across all organisms (Figure 3.1). Others found ~65 μM PVP-AgENM (10 nm) was required for 50% reduction in viability of *S. meliloti* 1021, whereas I observed an LC_{50} for AgENM of 207 μM in *S. meliloti* 2011[86]. While there were differences between studies, such as the use of Minimal Davidson Medium (MDM) in their study versus glucose supplemented MES in ours, it is likely the large difference in primary particle size at least partially explains the differences in observed LC_{50}'s (smaller nanoparticles are generally more toxic); however, strain specificity in AgENM responses may occur even in the same bacterial species[26] and exposure medium mediates the toxicity of ENMs[164].

The relatively higher CFUs/mL used for *S. meliloti* exposures compared with *B. amyloliquefaciens* and *P. putida* (Table 3.5) does not completely explain the relatively high LC_{50}'s I observed; as *S. meliloti* and *P. putida* were both exposed at much higher CFUs/mL than *B. amyloliquefaciens,* yet *P. putida* and *B. amyloliquefaciens* exhibited similar LC_{50}'s for $AgNO_3$ and PVP-AgENM (Table 3.4). *B. subtilis*, which is closely related to *B. amyloliquefaciens*, was generally found in previous studies to be more susceptible than *P. putida* to exposure to presumably uncapped AgENMs; however, viability responses depended on the presence of specific ions (i.e. Ca^{2+}, Mg^{2+}, Na^{+}, K^{+}, SO_4^{2-}, Cl^{-}, HCO_3^{-})[29]. A study using a comparable exposure procedure showed ~0.23 μM citrate capped-AgENM (10 nm) was sufficient for nearly complete mortality of *B. subtilis* KACC10111 after 1-2 h of exposure[25]. Another study showed ~300 μM AgENM (32 nm) yielded a ~50% reduction in light emission of *P. putida* BS566::luxCDABE after 1.5 h exposures[48].

Table 3.4 LC_{50}'s of Ag^+ and AgENM

Culture	Ag^+ LC_{50} (µM ± S.E.)	AgENM LC_{50} (µM ± S.E.)
B. amyloliquefaciens	2.64 (± 0.1)[a]	89.7 (± 6.3)[a]
S. meliloti	6.62 (± 1.1)[b]	206.5 (± 18)[b]
P. putida	3.39 (± 0.2)[c]	86.4 (± 7.0)[a]

LC_{50}, the lethal concentration yielding a 50% decrease in viability; PGPR, plant growth promoting rhizobacteria; S.E., standard error of regression

LC_{50}'s were extrapolated from 4-parameter dose response curves in Sigmaplot. Letters represent significant differences at α 0.05 using an unpaired t-test with a Bonferroni correction. LC_{50}s were compared within treatment (Ag+ or AgENMs).

Table 3.5 CFU/mL used in toxicity experiments

PGPR	CFU/mL	S.D.
B. amyloliquefaciens	1.59E+07	1.60E+05
S. meliloti	1.10E+09	3.31E+07
P. putida	7.17E+08	2.73E+07

CFU/mL, colony forming units in one mL of bacterial suspension; S.D., one standard deviation of colony forming units

CFU/mL is estimated from absorbance measurements

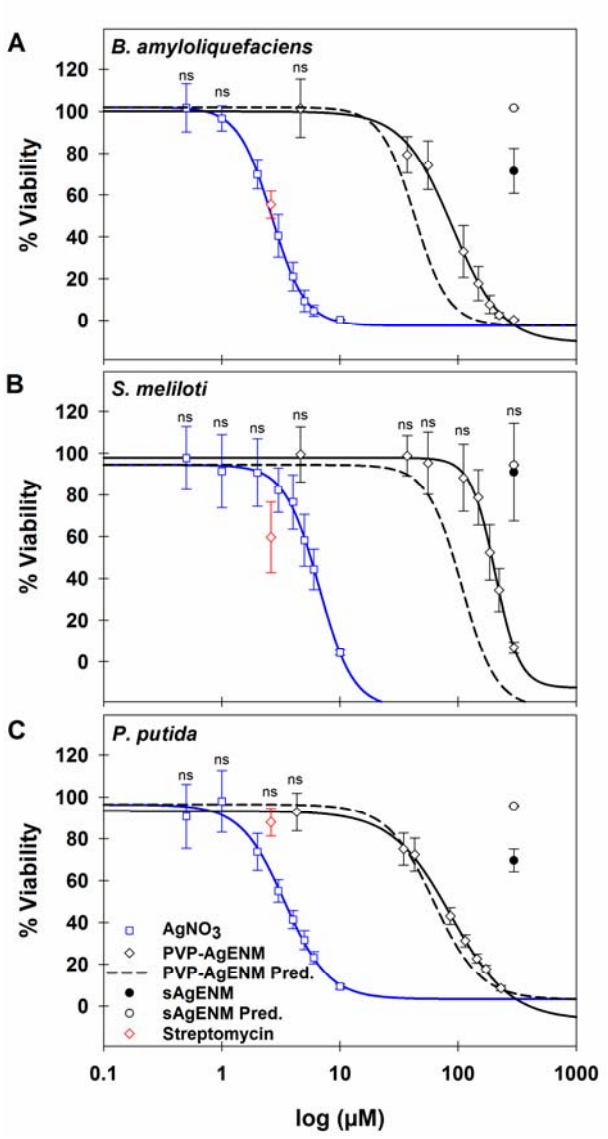

Figure 3.1 Viability responses of PGPR to Ag^{+}, PVP-AgENM, and sAgENM

Viability responses to $AgNO_3$ (Ag^{+}), PVP-AgENM, and sAgENM expressed as percentage of no-metal controls in (A) *B. amyloliquefaciens,* (B) *S. meliloti*, and (C) *P. putida.* Lines represent 4-parameter dose response curve fits performed in Sigmaplot. The blue line represents $AgNO_3$ treatment, the solid black line is PVP-AgENM, and the dotted black line and open circle are predicted response based on abiotic dissolution estimates. Bars are one standard deviation (n = 9). ns = not significant as determined *via* a Wilcoxon signed rank test (H_0: μ = 100, α 0.05).

Bacillus amyloliquefaciens and *P. putida* both exhibited significant decreases in % viability starting at 1 µM $AgNO_3$ and 37 µM PVP-AgENM, with significant reductions continuing with increased concentrations (Figure 3.1). Interestingly, both *P. putida* and *B. amyloliquefaciens* viability was reduced by ~30% in response to 300 µM sAgENM exposure, while there was no significant effect on *S. meliloti* viability (Figure 3.1). The finding that *S. meliloti* is generally more resistant to Ag^+, PVP-AgENMs, and sAgENMs has environmental and agricultural implications, given that amending soil with Ag, Ti, and Zn ENMs enriched biosolids significantly inhibited nodulation of *Medicago truncatula* A17 by *S. meliloti* 2011[87]. My results suggest silver induced reduction in bacterial viability is likely not the mechanism of toxicity observed in my previous study; however, the previous study was performed in biosolids amended soils and with plants, so further work is needed to determine the translatability of the findings between these two systems.

Predicted free Ag^+ activities were higher in PVP-AgENM treatments than $AgNO_3$ treatments, which induced similar viability reductions (Figure 3.1, Figure 3.2). Accordingly, abiotic dissolution of PVP-AgENM generally over-predicted observed reductions in viability, but correlated well with the observed mortality in *P. putida* (Figure 3.1). Abiotic dissolution is only an estimate of the dissolved fraction present during exposure; however, my findings suggest the <2 nm fraction likely explains most of the observed response to PVP-AgENM exposures, but dissolution is likely suppressed in the presence of the bacteria. I found abiotic dissolution estimates under-predicted sAgENM viability responses in *B. amyloliquefaciens* and *P. putida*, implying particle-specific toxicity of these particles in the presence of these bacteria (Figure 3.1). Previously, Colman et al.[97] observed shifts in microbial community structure, decreased microbial biomass, and

increased N_2O production in long-term terrestrial mesocosms treated with AgENM containing biosolids slurries (133g biosolids/L deionized H_2O) relative to slurry only treatments. The ENM were reportedly sulfidized to some degree and the effects of AgENMs were similar or greater than those observed with $AgNO_3$ treatment. This finding, along with ours, shows sulfation of AgENMs may result in nano-specific delivery of ions leading to prolonged toxicity, likely due to enhanced dissolution at the nano-bio interface. Indeed, dissolution at the nano-bio interface has been correlated with toxicity of AgENMs in previous studies[33]. Additionally, sAgENMs were found to induce phytotoxic effects in the crop plants, *Vigna unguiculata* L. Walp. and *Triticum aestivum*, that were only observable after weeks of exposure[103], and AgENM enriched biosolids were found to inhibit mycorrhizal-plant associations, including sAgENMs at environmentally relevant concentrations[102].

Streptomycin reduced cell viability in *S. meliloti* and *B. amyloliquefaciens by* ~40-45%, while *P. putida* showed only a 10% reduction in viability (Figure 3.1). The modest streptomycin induced viability response in *P. putida* UW4 is important, as others have found antibiotic resistance is an exploitable trait when examining root colonization by *P. putida* strains in the field[165]. The similarities in viability reduction between *S. meliloti* and *B. amyloliquefaciens* along with the minimal reduction in viability of *P. putida* also shows any observed differences in toxicity between the species are not likely purely driven by the differences in cell densities used in my study.

3.3.3 PGPR O_2 Consumption Responses

Previously, I demonstrated the importance of normalizing O_2 consumption responses to viable cell estimates and the current findings further support this. For instance, O_2 consumption/well of *P. putida* suggests no treatment effect (Figure 3.3C); however, it is clear from O_2 consumption-viability plots that oxygen consumption increased per viable cell under most treatment conditions (Figure 3.4C). This is particularly important as some have questioned the utility of basal soil respiration (a related assay) for assessing metal toxicity in soils based on finding CO_2 evolution was often not heavily affected by metal addition to soils[157]; however, respiration estimates were not normalized to active microbial biomass or viable cell estimates, so it's unclear what such findings imply concerning the metabolic response of the soil microbial community.

While it was possible to fit 4-parameter curves to *B. amyloliquefaciens* O_2 consumption/well measurements (Figure 3.3A), meaningful 4-parameter curve fits for the response in the other organisms were not possible (Figure 3.3). Furthermore, the results suggest the PGPR demonstrated species-specific trends in O_2 consumption in response to $AgNO_3$ and PVP-AgENM, which become clear when O_2 consumption is normalized to viable cell estimates (Figure 3.4).

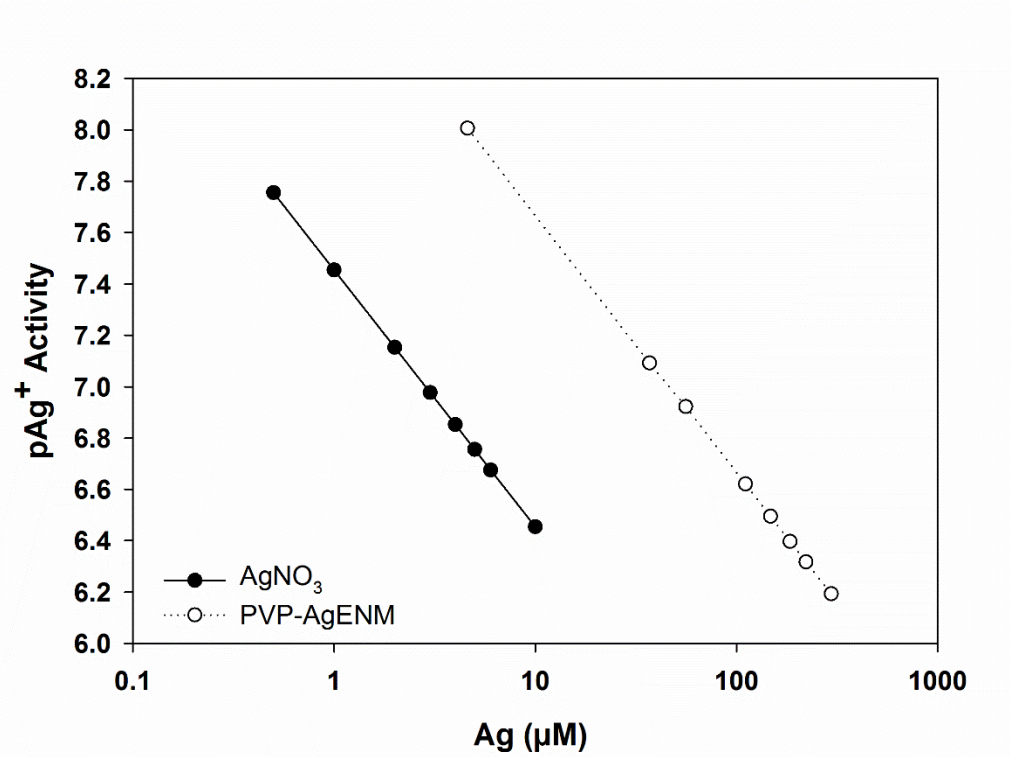

Figure 3.2 –log free Ag^+ Activity in $AgNO_3$ and PVP-AgENM Exposures

-log free Ag^+ activities (pAg^+) in $AgNO_3$ and PVP-AgENM in 50 mM MES as predicted using GeoChem-EZ. The pH was fixed at 6, precipitates were allowed to form, and ionic strength was calculated as suggested by the developers.

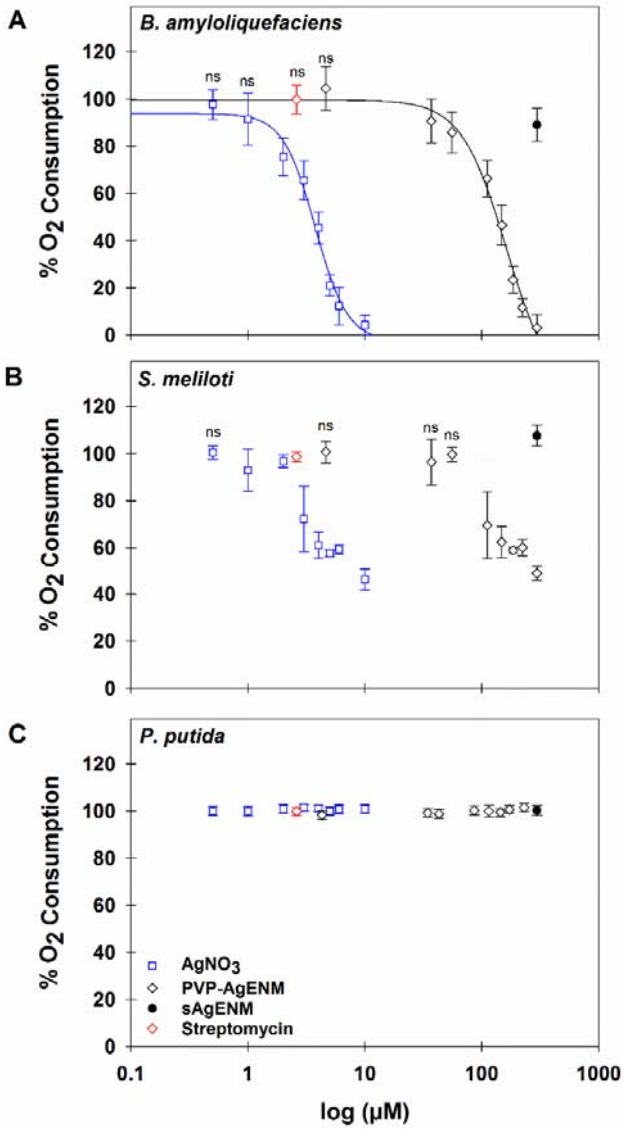

Figure 3.3 O_2 consumption/well responses of PGPR to Ag^+, PVP-AgENM, and sAgENM O_2 consumption/well responses to $AgNO_3$ (Ag^+), PVP-AgENM, and sAgENM expressed as percentage of no-metal controls in (A) *B. amyloliquefaciens,* (B) *S. meliloti*, and (C) *P. putida.* Lines represent 4-parameter dose response curve fits performed in Sigmaplot. The blue line represents $AgNO_3$ treatment, the solid black line is PVP-AgENM. Bars are one standard deviation (n = 9). ns = not significant as determined *via* Wilcoxon signed rank test (H_0: μ = 100, α 0.05)

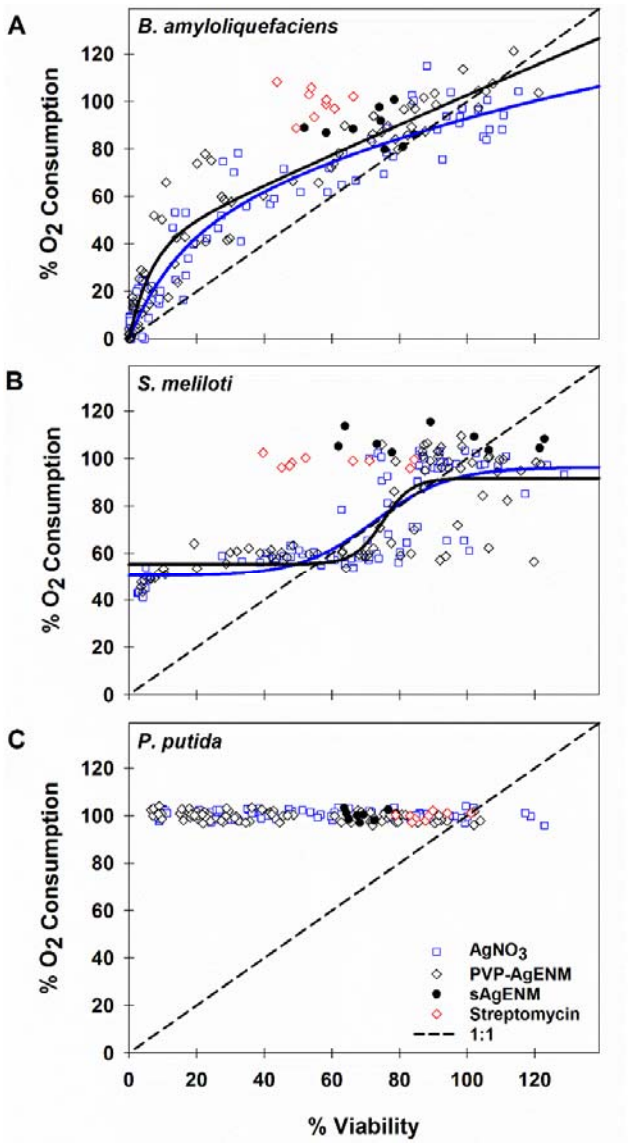

Figure 3.4 O_2 consumption-viability responses of PGPR to Ag^+, PVP-AgENM, and sAgENM

O_2 consumption-viability responses to $AgNO_3$ (Ag^+), PVP-AgENM, and sAgENM expressed as percentage of no-metal controls in (A) *B. amyloliquefaciens,* (B) *S. meliloti*, and (C) *P. putida.* Lines represent regressions performed in Sigmaplot, (A) 3-parameter, (B) 4-parameter. The blue line represents $AgNO_3$ treatment, the black line is PVP-AgENM. The dotted line is hypothetical 1:1 relationship between % O_2 consumption and % Viability.

Bacillus amyloliquefaciens generally showed similar increases in O_2 consumption in response to $AgNO_3$ and PVP-AgENM exposure, with the effect being exaggerated at <50% viability (Figure 3.4A). I observed similar trends in O_2 consumption-viability plots of *B. amyloliquefaciens* exposed to $AgNO_3$ at higher cell densities in the previous work (Chapter 2). PVP-AgENM and ion exposure of *S. meliloti* also yielded increased O_2 consumption at viable cell densities <50%, but decreased O_2 consumption was observed when % viability was ~50-80% (Figure 3.4B). PVP-AgENM and ion exposure of *P. putida* yielded increased O_2 consumption at all viable cell densities <100% (Figure 3.4C). These distinct bacterial responses in O_2 consumption reflect unique metabolic responses of each organism to PVP-AgENM and $AgNO_3$ exposure, which exhibits the significance of examining bacterial species-specific responses to potentially toxic substances. All PGPR demonstrated increased O_2 consumption in response to sAgENM exposure, though responses were more variable in *S. meliloti* (Figure 3.4B).

Previously, it was found that silver ions increased respiration of *E. coli* in the presence of glucose[146]. The authors suggest this may arise from uncoupling of the electron transport chain from ATP synthesis. My results suggest, if this is the general underlying mechanism of Ag^+ toxicity in aerobic microbes, it must lead to very different physiological responses in each of the tested PGPR, meaning uncoupling must occur at different concentrations and/or induce specific metabolic responses in the tested bacteria. Determining the exact biological mechanism of the observed respiration responses was beyond the scope of this study; however, the results are promising for future researchers wishing to probe the mechanisms of metabolic responses of bacteria to ENMs, metal ions, and antibiotics. Because the method is very cost effective, simple, and high-throughput, it

may easily be paired with other assays (i.e. molecular biology assays), providing a robust platform for studying metabolic aspects of ENM-bacteria interactions and the effects of other substances on microbial metabolism.

Streptomycin exposure increased O_2 consumption in all PGPR, though the effect was small in *P. putida* (Figure 3.4). The stimulatory effects of streptomycin on bacterial respiration was observed long ago[142]. In my studies, it was a useful treatment for observing increased O_2 consumption and examining species-specific responses to a medically relevant antibiotic (Figure 3.4). Future studies may utilize the method to examine respiration and viability responses to both conventional and novel antibiotics. For instance, medical microbiologists may incorporate antibiotic tolerant/resistant bacteria along with my method for swiftly screening metabolic responses to antibiotics, allowing rapid identification of distinct patterns in O_2 consumption.

3.4 Conclusion

Using my method, I have shown silver ions and PVP-AgENMs elicit similar respiration responses, which are unique in each of the studied PGPR species. This finding, along with others[26], illustrates the importance of examining the ENM responses of specific bacterial species/strains under identical exposure conditions. This will be even more important as nanotoxicologists further explore the responses of microbial communities. Interestingly, ENMs containing CeO_2, Fe_3O_4, and SnO_2 were also shown to induce increased respiration as assessed by the metabolic quotient (qCO_2 = basal CO_2 evolution rate/microbial biomass-C) in ENM treated soils in a time and spatial (soil horizon) dependent manner[156].

In agreement with a growing body of literature[19, 164], abiotic dissolution estimates of PVP-AgENM suggest the dissolved fraction likely plays a large role in the observed toxic responses. Importantly, estimates of abiotic dissolution of sAgENM suggest PGPR-sAgENM interactions enhance the toxicity of these environmentally relevant materials. Others have shown particle-cell interactions may lead to delivery of ions in a nano-specific manner (reviewed in Chapter 1). Because my results indicate that the abiotically dissolved fraction of sAgENM explains little of the toxic responses, these particles may be useful for examining the process of particle dissolution at the nano-bio interface along with other particle specific responses.

My findings highlight the significance of examining bacterial species-specific responses to ENMs. Given the role of microbial respiration in antibiotic efficacy, the distinct % O_2 consumption-% viability patterns I observed in the PGPR in response to Ag^+ and PVP-AgENMs have implications with respect to agricultural application of biosolids and microbial amendments. It is clear that ENM accumulation in biosolids amended soils is occurring exponentially; concurrently, there has been an increased utilization of microbial amendments for biocontrol of pathogens/pests and to enhance agricultural production. Thus, it is crucial to understand how the distinct respiration responses observed in my study translate to observed toxicity in more realistic scenarios where PGPR and plants are co-exposed to AgENMs in test-plots.

Additionally, my method could be used to screen for more effective antibiotics which may induce increased respiration in terms of cell viability. Upon identifying unique trends in respiration responses, future studies may investigate the biological mechanisms underlying species-specific O_2 consumption responses, like those found in this work. Such

an approach could rapidly increase the discovery of novel antibiotics that influence respiration, potentially assisting researchers in combatting antibiotic resistance in pathogenic bacterial species.

Chapter 4: Conclusion and Perspective

Researchers in the field of nanotoxicology have generally struggled to overcome the complexities of working with materials on the nano-scale in the context of traditional ecotoxicological approaches (Chapter 1). Indeed, the challenges of nanotoxicological studies have often led to, what appear to be, inconsistent findings, which has limited the ability to ascertain meaningful mechanistic information of ENM toxicity. Upon reviewing the literature, I observed the need for a high-throughput, cost-effective means of assessing metabolic responses of bacteria without the use of confounding reagents.

To address this methodological gap and to probe metabolic responses of PGPR to ENMs, I developed two high-throughput assays to examine O_2 consumption responses and viability responses in aerobic bacteria. Developing the methods required fine tuning of several experimental parameters, including selection of the appropriate buffer and carbon source (at the appropriate concentrations) along with determining adequate cell densities to use in the studies.

Many metal containing ENMs undergo dissolution, so I chose to initially develop my method examining the toxicity of Ag^+, Zn^{2+}, and Ni^{2+} to *B. amyloliquefaciens* (Chapter 2). I found the metals induced differential O_2 consumption responses, even when viability responses were similar; this was particularly interesting when comparing Zn^{2+} and Ni^{2+}, where viability responses were similar, but O_2 consumption responses were much more variable in response to Ni^{2+}. I also observed large increases in O_2 consumption induced by streptomycin. These results clearly show the usefulness of my method for examining metal and antibiotic toxicity in terms of viability and O_2 consumption.

After demonstrating the effectiveness of my method using metal ion exposures, I expanded my studies to examine the response of several PGPR to streptomycin, $AgNO_3$, PVP-AgENMs, and sAgENMs (Chapter 3). I found the silver ions and PVP-AgENMs elicited very similar O_2 consumption responses in the PGPR. However, each PGPR responded very differently to the silver ions and ENMs in terms of O_2 consumption. This was especially clear when I observed similar LC_{50}'s for $AgNO_3$ and PVP-AgENM in *P. putida* and *B. amyloliquefaciens*, but O_2 consumption was significantly increased by metal exposure in *P. putida* cells compared with *B. amyloliquefaciens*.

As the field of nanotoxicology attempts to keep pace with emerging nanotechnology it will be necessary to implement high-throughput screening techniques which allow robust examination of toxic responses in bacteria. I have developed a robust method for rapidly assessing viability and O_2 consumption responses of aerobic bacteria to metal ions and ENMs. Additionally, I have used my method to probe antibiotic responses in PGPR, and found it useful for comparing metabolic responses of *B. amyloliquefaciens* to L-cysteine and D-cysteine (Data Not Shown).

Furthermore, given the flexible and simple nature of the method, it should find utility in many fields of microbiology, including ecotoxicology, food microbiology, and medical microbiology. In the field of nanotoxicology, much is still unknown regarding basic responses of bacteria to ENMs. I have found respiration responses to ENMs may be very different between organisms when exposed under identical conditions, highlighting the challenge in extrapolating individual nanotoxicological studies using either single organisms or microbial communities. Upon identifying unique O_2 consumption responses, molecular biology assays may be incorporated to investigate the biological mechanisms

underlying differences in O_2 consumption patterns. Such research could potentially assist understanding not only how microbes metabolically respond to ENMs, but also if resistant/tolerant bacteria exhibit differential O_2 consumption responses to ENM exposure. With the recent advances in understanding the relationship between antibiotic efficacy and respiration, research implementing my methods could also be highly valuable in the field of medical microbiology.

References

1. Pan, B.; Xing, B., Applications and implications of manufactured nanoparticles in soils: A review. *European Journal of Soil Science* **2012,** *63*, (4), 437-456.

2. Verma, A.; Stellacci, F., Effect of surface properties on nanoparticle–cell interactions. *Small* **2010,** *6*, (1), 12-21.

3. Nowack, B.; Bucheli, T. D., Occurrence, behavior and effects of nanoparticles in the environment. *Environmental Pollution* **2007,** *150*, (1), 5-22.

4. Klaine, S. J.; Koelmans, A. A.; Horne, N.; Carley, S.; Handy, R. D.; Kapustka, L.; Nowack, B.; von der Kammer, F., Paradigms to assess the environmental impact of manufactured nanomaterials. *Environmental Toxicology and Chemistry* **2012,** *31*, (1), 3-14.

5. Unrine, J.; Bertsch, P.; Hunyadi, S., Bioavailability, trophic transfer, and toxicity of manufactured metal and metal oxide nanoparticles in terrestrial environments. *Nanoscience and nanotechnology: Environmental and health impacts* **2008**, 345-366.

6. Oberdörster, G.; Oberdörster, E.; Oberdörster, J., Nanotoxicology: An emerging discipline evolving from studies of ultrafine particles. *Environmental Health Perspectives* **2005,** *113*, (7), 823-839.

7. Klaine, S. J.; Alvarez, P. J. J.; Batley, G. E.; Fernandes, T. F.; Handy, R. D.; Lyon, D. Y.; Mahendra, S.; McLaughlin, M. J.; Lead, J. R., Nanomaterials in the environment: Behavior, fate, bioavailability, and effects. *Environmental Toxicology and Chemistry* **2008,** *27*, (9), 1825-1851.

8. Maurer-Jones, M. A.; Gunsolus, I. L.; Murphy, C. J.; Haynes, C. L., Toxicity of engineered nanoparticles in the environment. *Analytical Chemistry* **2013,** *85*, (6), 3036-3049.

9. Gottschalk, F.; Sonderer, T.; Scholz, R. W.; Nowack, B., Modeled environmental concentrations of engineered nanomaterials (TiO_2, ZnO, Ag, CNT, Fullerenes) for different regions. *Environmental Science & Technology* **2009,** *43*, (24), 9216-9222.

10. Judy, J. D.; Bertsch, P. M., Bioavailability, toxicity, and fate of manufactured nanomaterials in terrestrial ecosystems. *Advances in Agronomy* **2014,** *123*, 1-64.

11. Dinesh, R.; Anandaraj, M.; Srinivasan, V.; Hamza, S., Engineered nanoparticles in the soil and their potential implications to microbial activity. *Geoderma* **2012,** *173–174*, (0), 19-27.

12. Djurišić, A. B.; Leung, Y. H.; Ng, A.; Xu, X. Y.; Lee, P. K.; Degger, N., Toxicity of metal oxide nanoparticles: Mechanisms, characterization, and avoiding experimental artefacts. *Small* **2015,** *11*, (1), 26-44.

13. Torsvik, V.; Øvreås, L., Microbial diversity and function in soil: from genes to ecosystems. *Current opinion in microbiology* **2002,** *5*, (3), 240-245.

14. Nannipieri, P.; Ascher, J.; Ceccherini, M.; Landi, L.; Pietramellara, G.; Renella, G., Microbial diversity and soil functions. *European Journal of Soil Science* **2003,** *54*, (4), 655-670.

15. Sondi, I.; Salopek-Sondi, B., Silver nanoparticles as antimicrobial agent: A case study on *E. coli* as a model for gram-negative bacteria. *Journal of Colloid and Interface Science* **2004,** *275*, (1), 177-182.

16. Morones, J. R.; Elechiguerra, J. L.; Camacho, A.; Holt, K.; Kouri, J. B.; Ramírez, J. T.; Yacaman, M. J., The bactericidal effect of silver nanoparticles. *Nanotechnology* **2005,** *16*, (10), 2346.

17. Gambino, M.; Marzano, V.; Villa, F.; Vitali, A.; Vannini, C.; Landini, P.; Cappitelli, F., Effects of sublethal doses of silver nanoparticles on *Bacillus subtilis* planktonic and sessile cells. *Journal of Applied Microbiology* **2015,** *118*, (5), 1103-1115.

18. Singh, R.; Shedbalkar, U. U.; Wadhwani, S. A.; Chopade, B. A., Bacteriagenic silver nanoparticles: synthesis, mechanism, and applications. *Applied Microbiology and Biotechnology* **2015,** *99*, (11), 4579-4593.

19. Xiu, Z.-m.; Zhang, Q.-b.; Puppala, H. L.; Colvin, V. L.; Alvarez, P. J., Negligible particle-specific antibacterial activity of silver nanoparticles. *Nano letters* **2012,** *12*, (8), 4271-4275.

20. Ivask, A.; ElBadawy, A.; Kaweeteerawat, C.; Boren, D.; Fischer, H.; Ji, Z.; Chang, C. H.; Liu, R.; Tolaymat, T.; Telesca, D.; Zink, J. I.; Cohen, Y.; Holden, P. A.; Godwin, H. A., Toxicity mechanisms in *Escherichia coli* vary for silver nanoparticles and differ from ionic silver. *ACS Nano* **2014,** *8*, (1), 374-386.

21. Kokalis-Burelle, N.; Kloepper, J. W.; Reddy, M. S., Plant growth-promoting rhizobacteria as transplant amendments and their effects on indigenous rhizosphere microorganisms. *Applied Soil Ecology* **2006,** *31*, (1–2), 91-100.

22. Harwood, C. R.; Cutting, S. M.; Chambert, R., *Molecular biological methods for Bacillus*. Wiley: Southern Gate Chichester, West Sussex, England, 1990.

23. Kloepper, J. W.; Ryu, C.-M.; Zhang, S., Induced systemic resistance and promotion of plant growth by *Bacillus* spp. *Phytopathology* **2004,** *94*, (11), 1259-1266.

24. Suresh, A. K.; Pelletier, D. A.; Doktycz, M. J., Relating nanomaterial properties and microbial toxicity. *Nanoscale* **2013,** *5*, (2), 463-474.

25. Kim, S.; Baek, Y.-W.; An, Y.-J., Assay-dependent effect of silver nanoparticles to *Escherichia coli* and *Bacillus subtilis*. *Applied Microbiology and Biotechnology* **2011,** *92*, (5), 1045-1052.

26. Ruparelia, J. P.; Chatterjee, A. K.; Duttagupta, S. P.; Mukherji, S., Strain specificity in antimicrobial activity of silver and copper nanoparticles. *Acta Biomaterialia* **2008,** *4*, (3), 707-716.

27. Feng, Q.; Wu, J.; Chen, G.; Cui, F.; Kim, T.; Kim, J., A mechanistic study of the antibacterial effect of silver ions on *Escherichia coli* and *Staphylococcus aureus*. *Journal of biomedical materials research* **2000,** *52*, (4), 662-668.

28. Yoon, K.-Y.; Byeon, J. H.; Park, J.-H.; Hwang, J., Susceptibility constants of *Escherichia coli* and *Bacillus subtilis* to silver and copper nanoparticles. *Science of the Total Environment* **2007,** *373*, (2), 572-575.

29. Jin, X.; Li, M.; Wang, J.; Marambio-Jones, C.; Peng, F.; Huang, X.; Damoiseaux, R.; Hoek, E. M., High-throughput screening of silver nanoparticle stability and bacterial inactivation in aquatic media: influence of specific ions. *Environmental science & technology* **2010,** *44*, (19), 7321-7328.

30. Petrus, E.; Tinakumari, S.; Chai, L.; Ubong, A.; Tunung, R.; Elexson, N.; Chai, L.; Son, R., A study on the minimum inhibitory concentration and minimum bactericidal

concentration of Nano Colloidal Silver on food-borne pathogens. *Int Food Res J* **2011,** *18*, (1), 55-66.

31. Suresh, A. K.; Pelletier, D. A.; Wang, W.; Moon, J.-W.; Gu, B.; Mortensen, N. P.; Allison, D. P.; Joy, D. C.; Phelps, T. J.; Doktycz, M. J., Silver nanocrystallites: biofabrication using *Shewanella oneidensis*, and an evaluation of their comparative toxicity on gram-negative and gram-positive bacteria. *Environmental science & technology* **2010,** *44*, (13), 5210-5215.

32. Bondarenko, O.; Ivask, A.; Käkinen, A.; Kurvet, I.; Kahru, A., Particle-cell contact enhances antibacterial activity of silver nanoparticles. *PLoS One* **2013,** *8*, (5), e64060.

33. He, X.; Pan, Y.; Zhang, J.; Li, Y.; Ma, Y.; Zhang, P.; Ding, Y.; Zhang, J.; Wu, Z.; Zhao, Y., Quantifying the total ionic release from nanoparticles after particle-cell contact. *Environmental Pollution* **2015,** *196*, 194-200.

34. McQuillan, J. S.; Shaw, A. M., Differential gene regulation in the Ag nanoparticle and Ag+-induced silver stress response in Escherichia coli: A full transcriptomic profile. *Nanotoxicology* **2014,** *8*, (sup1), 177-184.

35. Kang, F.; Alvarez, P. J.; Zhu, D., Microbial extracellular polymeric substances reduce Ag+ to silver nanoparticles and antagonize bactericidal activity. *Environmental Science & Technology* **2014,** *48*, (1), 316-322.

36. Haas, D.; Keel, C., Regulation of antibiotic production in root-colonizing *Pseudomonas* spp. and relevance for biological control of plant disease. *Annual Review of Phytopathology* **2003,** *41*, (1), 117-153.

37. Keel, C.; Schnider, U.; Maurhofer, M.; Voisard, C.; Laville, J.; Burger, U.; Wirthner, P.; Haas, D.; Defago, G., Suppression of root diseases by *Pseudomonas Fluorescens* Cha0 - importance of the bacterial secondary metabolite 2,4-diacetylphloroglucinol. *Mol. Plant-Microbe Interact.* **1992,** *5*, (1), 4-13.

38. Fabrega, J.; Fawcett, S. R.; Renshaw, J. C.; Lead, J. R., Silver nanoparticle impact on bacterial growth: effect of pH, concentration, and organic matter. *Environmental science & technology* **2009,** *43*, (19), 7285-7290.

39. Fabrega, J.; Renshaw, J. C.; Lead, J. R., Interactions of silver nanoparticles with *Pseudomonas putida* biofilms. *Environmental science & technology* **2009,** *43*, (23), 9004-9009.

40. Wirth, S. M.; Lowry, G. V.; Tilton, R. D., Natural organic matter alters biofilm tolerance to silver nanoparticles and dissolved silver. *Environmental science & technology* **2012,** *46*, (22), 12687-12696.

41. Radzig, M. A.; Nadtochenko, V. A.; Koksharova, O. A.; Kiwi, J.; Lipasova, V. A.; Khmel, I. A., Antibacterial effects of silver nanoparticles on gram-negative bacteria:

Influence on the growth and biofilms formation, mechanisms of action. *Colloids and Surfaces B: Biointerfaces* **2013,** *102*, 300-306.

42. Park, H.-J.; Park, S.; Roh, J.; Kim, S.; Choi, K.; Yi, J.; Kim, Y.; Yoon, J., Biofilm-inactivating activity of silver nanoparticles: A comparison with silver ions. *Journal of Industrial and Engineering Chemistry* **2013,** *19*, (2), 614-619.

43. Yang, Y.; Alvarez, P. J., Sublethal concentrations of silver nanoparticles stimulate biofilm development. *Environmental Science & Technology Letters* **2015,** *2*, (8), 221-226.

44. Hartmann, T.; Mühling, M.; Wolf, A.; Mariana, F.; Maskow, T.; Mertens, F.; Neu, T. R.; Lerchner, J., A chip-calorimetric approach to the analysis of Ag nanoparticle caused inhibition and inactivation of beads-grown bacterial biofilms. *Journal of microbiological methods* **2013,** *95*, (2), 129-137.

45. Wang, P.; Menzies, N. W.; Dennis, P. G.; Guo, J.; Forstner, C.; Sekine, R.; Lombi, E.; Kappen, P.; Bertsch, P. M.; Kopittke, P. M., Silver Nanoparticles Entering Soils via the Wastewater–Sludge–Soil Pathway Pose Low Risk to Plants but Elevated Cl Concentrations Increase Ag Bioavailability. *Environmental Science & Technology* **2016**.

46. Thuptimdang, P.; Limpiyakorn, T.; McEvoy, J.; Prüß, B. M.; Khan, E., Effect of silver nanoparticles on *Pseudomonas putida* biofilms at different stages of maturity. *Journal of hazardous materials* **2015,** *290*, 127-133.

47. Gajjar, P.; Pettee, B.; Britt, D. W.; Huang, W.; Johnson, W. P.; Anderson, A. J., Antimicrobial activities of commercial nanoparticles against an environmental soil microbe, *Pseudomonas putida* KT2440. *J Biol Eng* **2009,** *3*, (9), 1-13.

48. Dams, R.; Biswas, A.; Olesiejuk, A.; Fernandes, T.; Christofi, N., Silver nanotoxicity using a light-emitting biosensor *Pseudomonas putida* isolated from a wastewater treatment plant. *Journal of hazardous materials* **2011,** *195*, 68-72.

49. Guzman, M.; Dille, J.; Godet, S., Synthesis and antibacterial activity of silver nanoparticles against gram-positive and gram-negative bacteria. *Nanomedicine-Nanotechnology Biology and Medicine* **2012,** *8*, (1), 37-45.

50. Pal, S.; Tak, Y. K.; Song, J. M., Does the antibacterial activity of silver nanoparticles depend on the shape of the nanoparticle? A study of the gram-negative bacterium *Escherichia coli*. *Applied and Environmental Microbiology* **2007,** *73*, (6), 1712-1720.

51. Dimkpa, C. O.; Calder, A.; Gajjar, P.; Merugu, S.; Huang, W.; Britt, D. W.; McLean, J. E.; Johnson, W. P.; Anderson, A. J., Interaction of silver nanoparticles with an environmentally beneficial bacterium, *Pseudomonas chlororaphis*. *Journal of hazardous materials* **2011,** *188*, (1), 428-435.

52. Badireddy, A. R.; Farner Budarz, J.; Marinakos, S. M.; Chellam, S.; Wiesner, M. R., Formation of silver nanoparticles in visible light-illuminated waters: mechanism and

possible impacts on the persistence of AgNPs and bacterial lysis. *Environmental Engineering Science* **2014,** *31*, (7), 338-349.

53. Dorobantu, L. S.; Fallone, C.; Noble, A. J.; Veinot, J.; Ma, G.; Goss, G. G.; Burrell, R. E., Toxicity of silver nanoparticles against bacteria, yeast, and algae. *Journal of Nanoparticle Research* **2015,** *17*, (4), 1-13.

54. Gozdziewska, M.; Cichowicz, G.; Markowska, K.; Zawada, K.; Megiel, E., Nitroxide-coated silver nanoparticles: synthesis, surface physicochemistry and antibacterial activity. *RSC Advances* **2015,** *5*, (72), 58403-58415.

55. Hachicho, N.; Hoffmann, P.; Ahlert, K.; Heipieper, H. J., Effect of silver nanoparticles and silver ions on growth and adaptive response mechanisms of *Pseudomonas putida* mt-2. *FEMS microbiology letters* **2014,** *355*, (1), 71-77.

56. Matzke, M.; Jurkschat, K.; Backhaus, T., Toxicity of differently sized and coated silver nanoparticles to the bacterium *Pseudomonas putida*: risks for the aquatic environment? *Ecotoxicology* **2014,** *23*, (5), 818-829.

57. Priester, J. H.; Singhal, A.; Wu, B.; Stucky, G. D.; Holden, P. A., Integrated approach to evaluating the toxicity of novel cysteine-capped silver nanoparticles to *Escherichia coli* and *Pseudomonas aeruginosa*. *Analyst* **2014,** *139*, (5), 954-963.

58. Soni, D.; Bafana, A.; Gandhi, D.; Sivanesan, S.; Pandey, R. A., Stress response of *Pseudomonas* species to silver nanoparticles at the molecular level. *Environmental Toxicology and Chemistry* **2014,** *33*, (9), 2126-2132.

59. Levard, C.; Hotze, E. M.; Colman, B. P.; Dale, A. L.; Truong, L.; Yang, X.; Bone, A. J.; Brown Jr, G. E.; Tanguay, R. L.; Di Giulio, R. T., Sulfidation of silver nanoparticles: natural antidote to their toxicity. *Environmental science & technology* **2013,** *47*, (23), 13440-13448.

60. Suresh, A. K.; Doktycz, M. J.; Wang, W.; Moon, J.-W.; Gu, B.; Meyer, H. M.; Hensley, D. K.; Allison, D. P.; Phelps, T. J.; Pelletier, D. A., Monodispersed biocompatible silver sulfide nanoparticles: Facile extracellular biosynthesis using the γ-proteobacterium, *Shewanella oneidensis*. *Acta biomaterialia* **2011,** *7*, (12), 4253-4258.

61. Reinsch, B.; Levard, C.; Li, Z.; Ma, R.; Wise, A.; Gregory, K.; Brown Jr, G.; Lowry, G., Sulfidation of silver nanoparticles decreases *Escherichia coli* growth inhibition. *Environmental science & technology* **2012,** *46*, (13), 6992-7000.

62. Neal, A. L.; Kabengi, N.; Grider, A.; Bertsch, P. M., Can the soil bacterium Cupriavidus necator sense ZnO nanomaterials and aqueous Zn^{2+} differentially? *Nanotoxicology* **2012,** *6*, (4), 371-380.

63. Jiang, W.; Mashayekhi, H.; Xing, B., Bacterial toxicity comparison between nano- and micro-scaled oxide particles. *Environmental Pollution* **2009,** *157*, (5), 1619-1625.

64. Li, M.; Pokhrel, S.; Jin, X.; Mädler, L.; Damoiseaux, R.; Hoek, E. M., Stability, bioavailability, and bacterial toxicity of ZnO and iron-doped ZnO nanoparticles in aquatic media. *Environmental science & technology* **2010,** *45*, (2), 755-761.

65. Rago, I.; Chandraiahgari, C. R.; Bracciale, M. P.; De Bellis, G.; Zanni, E.; Cestelli Guidi, M.; Sali, D.; Broggi, A.; Palleschi, C.; Sarto, M. S.; Uccelletti, D., Zinc oxide microrods and nanorods: different antibacterial activity and their mode of action against Gram-positive bacteria. *RSC Advances* **2014,** *4*, (99), 56031-56040.

66. Adams, L. K.; Lyon, D. Y.; Alvarez, P. J., Comparative eco-toxicity of nanoscale TiO_2, SiO_2, and ZnO water suspensions. *Water research* **2006,** *40*, (19), 3527-3532.

67. Sinha, R.; Karan, R.; Sinha, A.; Khare, S., Interaction and nanotoxic effect of ZnO and Ag nanoparticles on mesophilic and halophilic bacterial cells. *Bioresource technology* **2011,** *102*, (2), 1516-1520.

68. Kim, S. W.; An, Y.-J., Effect of ZnO and TiO_2 nanoparticles preilluminated with UVA and UVB light on *Escherichia coli* and *Bacillus subtilis*. *Applied microbiology and biotechnology* **2012,** *95*, (1), 243-253.

69. Jones, N.; Ray, B.; Ranjit, K. T.; Manna, A. C., Antibacterial activity of ZnO nanoparticle suspensions on a broad spectrum of microorganisms. *FEMS microbiology letters* **2008,** *279*, (1), 71-76.

70. Baek, Y.-W.; An, Y.-J., Microbial toxicity of metal oxide nanoparticles (CuO, NiO, ZnO, and Sb 2 O 3) to Escherichia coli, Bacillus subtilis, and Streptococcus aureus. *Science of the total environment* **2011,** *409*, (8), 1603-1608.

71. Mallevre, F.; Fernandes, T. F.; Aspray, T. J., Silver, zinc oxide and titanium dioxide nanoparticle ecotoxicity to bioluminescent *Pseudomonas putida* in laboratory medium and artificial wastewater. *Environmental Pollution* **2014,** *195*, 218-225.

72. Feris, K.; Otto, C.; Tinker, J.; Wingett, D.; Punnoose, A.; Thurber, A.; Kongara, M.; Sabetian, M.; Quinn, B.; Hanna, C., Electrostatic interactions affect nanoparticle-mediated toxicity to gram-negative bacterium *Pseudomonas aeruginosa* PAO1. *Langmuir* **2009,** *26*, (6), 4429-4436.

73. Lee, J.-H.; Kim, Y.-G.; Cho, M. H.; Lee, J., ZnO nanoparticles inhibit *Pseudomonas aeruginosa* biofilm formation and virulence factor production. *Microbiological research* **2014,** *169*, (12), 888-896.

74. García-Lara, B.; Saucedo-Mora, M. Á.; Roldán-Sánchez, J. A.; Pérez-Eretza, B.; Ramasamy, M.; Lee, J.; Coria-Jimenez, R.; Tapia, M.; Varela-Guerrero, V.; García-Contreras, R., Inhibition of quorum-sensing-dependent virulence factors and biofilm

formation of clinical and environmental *Pseudomonas aeruginosa* strains by ZnO nanoparticles. *Letters in Applied Microbiology* **2015,** *61*, (3), 299-305.

75. Dimkpa, C. O.; Hansen, T.; Stewart, J.; McLean, J. E.; Britt, D. W.; Anderson, A. J., ZnO nanoparticles and root colonization by a beneficial pseudomonad influence essential metal responses in bean (*Phaseolus vulgaris*). *Nanotoxicology* **2014**, (0), 1-8.

76. Dimkpa, C. O.; McLean, J. E.; Britt, D. W.; Anderson, A. J., Antifungal activity of ZnO nanoparticles and their interactive effect with a biocontrol bacterium on growth antagonism of the plant pathogen *Fusarium graminearum*. *Biometals* **2013,** *26*, (6), 913-924.

77. Dimkpa, C. O.; Calder, A.; Britt, D. W.; McLean, J. E.; Anderson, A. J., Responses of a soil bacterium, Pseudomonas chlororaphis O6 to commercial metal oxide nanoparticles compared with responses to metal ions. *Environmental pollution* **2011,** *159*, (7), 1749-1756.

78. Kumari, J.; Kumar, D.; Mathur, A.; Naseer, A.; Kumar, R. R.; Chandrasekaran, P. T.; Chaudhuri, G.; Pulimi, M.; Raichur, A. M.; Babu, S., Cytotoxicity of TiO_2 nanoparticles towards freshwater sediment microorganisms at low exposure concentrations. *Environmental research* **2014,** *135*, 333-345.

79. Binh, C. T. T.; Tong, T.; Gaillard, J. F.; Gray, K. A.; Kelly, J. J., Common freshwater bacteria vary in their responses to short-term exposure to nano-TiO_2. *Environmental toxicology and chemistry* **2014,** *33*, (2), 317-327.

80. Park, S.; Lee, S.; Kim, B.; Lee, S.; Lee, J.; Sim, S.; Gu, M.; Yi, J.; Lee, J., Toxic effects of titanium dioxide nanoparticles on microbial activity and metabolic flux. *Biotechnology and bioprocess engineering* **2012,** *17*, (2), 276-282.

81. Kubacka, A.; Diez, M. S.; Rojo, D.; Bargiela, R.; Ciordia, S.; Zapico, I.; Albar, J. P.; Barbas, C.; Martins dos Santos, V. A. P.; Fernández-García, M.; Ferrer, M., Understanding the antimicrobial mechanism of TiO_2-based nanocomposite films in a pathogenic bacterium. *Scientific Reports* **2014,** *4*, 4134.

82. Roumiantseva, M. L.; Andronov, E. E.; Sharypova, L. A.; Dammann-Kalinowski, T.; Keller, M.; Young, J. P. W.; Simarov, B. V., Diversity of *Sinorhizobium meliloti* from the central asian alfalfa gene center. *Applied and Environmental Microbiology* **2002,** *68*, (9), 4694-4697.

83. Galleguillos, C.; Aguirre, C.; Miguel Barea, J.; Azcón, R., Growth promoting effect of two *Sinorhizobium meliloti* strains (a wild type and its genetically modified derivative) on a non-legume plant species in specific interaction with two arbuscular mycorrhizal fungi. *Plant Science* **2000,** *159*, (1), 57-63.

84. Ma, W.; Sebestianova, S.; Sebestian, J.; Burd, G.; Guinel, F.; Glick, B., Prevalence of 1-aminocyclopropane-1-carboxylate deaminase in *Rhizobium* spp. *Antonie Van Leeuwenhoek* **2003,** *83*, (3), 285-291.

85. Bandyopadhyay, S.; Peralta-Videa, J. R.; Plascencia-Villa, G.; José-Yacamán, M.; Gardea-Torresdey, J. L., Comparative toxicity assessment of CeO_2 and ZnO nanoparticles towards *Sinorhizobium meliloti*, a symbiotic alfalfa associated bacterium: Use of advanced microscopic and spectroscopic techniques. *Journal of Hazardous Materials* **2012,** *241–242*, (0), 379-386.

86. Joshi, N.; Ngwenya, B. T.; French, C. E., Enhanced resistance to nanoparticle toxicity is conferred by overproduction of extracellular polymeric substances. *Journal of hazardous materials* **2012,** *241*, 363-370.

87. Judy, J. D.; McNear Jr, D. H.; Chen, C.; Lewis, R. W.; Tsyusko, O. V.; Bertsch, P. M.; Rao, W.; Stegemeier, J.; Lowry, G. V.; McGrath, S. P., Nanomaterials in biosolids inhibit nodulation, shift microbial community composition, and result in increased metal uptake relative to bulk/dissolved metals. *Environmental science & technology* **2015,** *49*, (14), 8751-8758.

88. Chen, C.; Unrine, J. M.; Judy, J. D.; Lewis, R. W.; Guo, J.; McNear Jr, D. H.; Tsyusko, O. V., Toxicogenomic responses of the model legume *Medicago truncatula* to aged biosolids containing a mixture of nanomaterials (TiO_2, Ag, and ZnO) from a pilot

wastewater treatment plant. *Environmental science & technology* **2015,** *49*, (14), 8759-8768.

89. Fan, R.; Huang, Y. C.; Grusak, M. A.; Huang, C.; Sherrier, D. J., Effects of nano-TiO_2 on the agronomically-relevant Rhizobium–legume symbiosis. *Science of The Total Environment* **2014,** *466*, 503-512.

90. Huang, Y. C.; Fan, R.; Grusak, M. A.; Sherrier, J. D.; Huang, C., Effects of nano-ZnO on the agronomically relevant Rhizobium–legume symbiosis. *Science of the Total Environment* **2014,** *497*, 78-90.

91. Priester, J. H.; Ge, Y.; Mielke, R. E.; Horst, A. M.; Moritz, S. C.; Espinosa, K.; Gelb, J.; Walker, S. L.; Nisbet, R. M.; An, Y.-J.; Schimel, J. P.; Palmer, R. G.; Hernandez-Viezcas, J. A.; Zhao, L.; Gardea-Torresdey, J. L.; Holden, P. A., Soybean susceptibility to manufactured nanomaterials with evidence for food quality and soil fertility interruption. *Proceedings of the National Academy of Sciences* **2012,** *109*, (37), E2451–E2456.

92. Yoon, S.-J.; Kwak, J. I.; Lee, W.-M.; Holden, P. A.; An, Y.-J., Zinc oxide nanoparticles delay soybean development: A standard soil microcosm study. *Ecotoxicology and environmental safety* **2014,** *100*, 131-137.

93. López-Moreno, M. L.; de la Rosa, G.; Hernández-Viezcas, J. Á.; Castillo-Michel, H.; Botez, C. E.; Peralta-Videa, J. R.; Gardea-Torresdey, J. L., Evidence of the

differential biotransformation and genotoxicity of ZnO and CeO_2 nanoparticles on soybean (*Glycine max*) plants. *Environmental science & technology* **2010,** *44*, (19), 7315-7320.

94. Bandyopadhyay, S.; Plascencia-Villa, G.; Mukherjee, A.; Rico, C. M.; José-Yacamán, M.; Peralta-Videa, J. R.; Gardea-Torresdey, J. L., Comparative phytotoxicity of ZnO NPs, bulk ZnO, and ionic zinc onto the alfalfa plants symbiotically associated with *Sinorhizobium meliloti* in soil. *Science of The Total Environment* **2015,** *515*, 60-69.

95. Simonin, M.; Richaume, A., Impact of engineered nanoparticles on the activity, abundance, and diversity of soil microbial communities: a review. *Environ Sci Pollut Res* **2015,** *22*, (18), 13710-13723.

96. McKee, M. S.; Filser, J., Impacts of metal-based engineered nanomaterials on soil communities. *Environmental Science: Nano* **2016,** *3*, (3), 506-533.

97. Colman, B. P.; Arnaout, C. L.; Anciaux, S.; Gunsch, C. K.; Hochella Jr, M. F.; Kim, B.; Lowry, G. V.; McGill, B. M.; Reinsch, B. C.; Richardson, C. J., Low concentrations of silver nanoparticles in biosolids cause adverse ecosystem responses under realistic field scenario. *PLoS One* **2013,** *8*, (2), e57189.

98. Shin, Y.-J.; Kwak, J. I.; An, Y.-J., Evidence for the inhibitory effects of silver nanoparticles on the activities of soil exoenzymes. *Chemosphere* **2012,** *88*, (4), 524-529.

99. Hänsch, M.; Emmerling, C., Effects of silver nanoparticles on the microbiota and enzyme activity in soil. *Journal of Plant Nutrition and Soil Science* **2010,** *173*, (4), 554-558.

100. Kumar, N.; Shah, V.; Walker, V. K., Influence of a nanoparticle mixture on an arctic soil community. *Environmental Toxicology and Chemistry* **2012,** *31*, (1), 131-135.

101. Kumar, N.; Shah, V.; Walker, V. K., Perturbation of an arctic soil microbial community by metal nanoparticles. *Journal of hazardous materials* **2011,** *190*, (1), 816-822.

102. Judy, J. D.; Kirby, J. K.; Creamer, C.; McLaughlin, M. J.; Fiebiger, C.; Wright, C.; Cavagnaro, T. R.; Bertsch, P. M., Effects of silver sulfide nanomaterials on mycorrhizal colonization of tomato plants and soil microbial communities in biosolid-amended soil. *Environmental Pollution* **2015,** *206*, 256-263.

103. Wang, P.; Menzies, N. W.; Lombi, E.; Sekine, R.; Blamey, F. P. C.; Hernandez-Soriano, M. C.; Cheng, M.; Kappen, P.; Peijnenburg, W. J.; Tang, C., Silver sulfide nanoparticles (Ag_2S-NPs) are taken up by plants and are phytotoxic. *Nanotoxicology* **2015**, (0), 1-9.

104. Ge, Y.; Schimel, J. P.; Holden, P. A., Evidence for negative effects of TiO_2 and ZnO nanoparticles on soil bacterial communities. *Environmental science & technology* **2011,** *45*, (4), 1659-1664.

105. Ge, Y.; Schimel, J. P.; Holden, P. A., Identification of soil bacteria susceptible to TiO_2 and ZnO nanoparticles. *Applied and environmental microbiology* **2012,** *78*, (18), 6749-6758.

106. Collins, D.; Luxton, T.; Kumar, N.; Shah, S.; Walker, V. K.; Shah, V., Assessing the impact of copper and zinc oxide nanoparticles on soil: a field study. *PLoS One* **2012,** *7*, (8), e42663.

107. Nogueira, V.; Lopes, I.; Rocha-Santos, T.; Santos, A. L.; Rasteiro, G. M.; Antunes, F.; Gonçalves, F.; Soares, A. M.; Cunha, A.; Almeida, A., Impact of organic and inorganic nanomaterials in the soil microbial community structure. *Science of the total environment* **2012,** *424*, 344-350.

108. Simonin, M.; Guyonnet, J. P.; Martins, J. M.; Ginot, M.; Richaume, A., Influence of soil properties on the toxicity of TiO_2 nanoparticles on carbon mineralization and bacterial abundance. *Journal of hazardous materials* **2015,** *283*, 529-535.

109. Ge, Y.; Priester, J. H.; Van De Werfhorst, L. C.; Schimel, J. P.; Holden, P. A., Potential mechanisms and environmental controls of TiO_2 nanoparticle effects on soil bacterial communities. *Environmental science & technology* **2013,** *47*, (24), 14411-14417.

110. Du, W.; Sun, Y.; Ji, R.; Zhu, J.; Wu, J.; Guo, H., TiO_2 and ZnO nanoparticles negatively affect wheat growth and soil enzyme activities in agricultural soil. *Journal of Environmental Monitoring* **2011,** *13*, (4), 822-828.

111. Martineau, N.; McLean, J. E.; Dimkpa, C. O.; Britt, D. W.; Anderson, A. J., Components from wheat roots modify the bioactivity of ZnO and CuO nanoparticles in a soil bacterium. *Environmental Pollution* **2014,** *187*, 65-72.

112. Dimkpa, C. O.; McLean, J. E.; Britt, D. W.; Anderson, A. J., Nano-CuO and interaction with nano-ZnO or soil bacterium provide evidence for the interference of nanoparticles in metal nutrition of plants. *Ecotoxicology* **2015,** *24*, (1), 119-129.

113. Calder, A. J.; Dimkpa, C. O.; McLean, J. E.; Britt, D. W.; Johnson, W.; Anderson, A. J., Soil components mitigate the antimicrobial effects of silver nanoparticles towards a beneficial soil bacterium, *Pseudomonas chlororaphis* O6. *Science of the total environment* **2012,** *429*, 215-222.

114. Whitley, A. R.; Levard, C.; Oostveen, E.; Bertsch, P. M.; Matocha, C. J.; von der Kammer, F.; Unrine, J. M., Behavior of Ag nanoparticles in soil: effects of particle surface coating, aging and sewage sludge amendment. *Environmental pollution* **2013,** *182*, 141-149.

115. Spizizen, J., Transformation of biochemically deficient strains of Bacillus subtilis by deoxyribonucleate. *Proceedings of the National Academy of Sciences* **1958,** *44*, (10), 1072-1078.

116. Lemire, J. A.; Harrison, J. J.; Turner, R. J., Antimicrobial activity of metals: mechanisms, molecular targets and applications. *Nature reviews. Microbiology* **2013,** *11*, (6), 371-84.

117. Van Nostrand, J. D.; Arthur, J. M.; Kilpatrick, L. E.; Neely, B. A.; Bertsch, P. M.; Morris, P. J., Changes in protein expression in *Burkholderia vietnamiensis* PR1301 at pH 5 and 7 with and without nickel. *Microbiology* **2008,** *154*, (12), 3813-3824.

118. Van Nostrand, J. D.; Khijniak, T. J.; Neely, B.; Sattar, M. A.; Sowder, A. G.; Mills, G.; Bertsch, P. M.; Morris, P. J., Reduction of nickel and uranium toxicity and enhanced trichloroethylene degradation to *Burkholderia vietnamiensis* PR1301 with hydroxyapatite amendment. *Environmental science & technology* **2007,** *41*, (6), 1877-1882.

119. Bååth, E., Effects of heavy metals in soil on microbial processes and populations (a review). *Water, Air, and Soil Pollution* **1989,** *47*, (3-4), 335-379.

120. Andersson, D. I.; Hughes, D., Microbiological effects of sublethal levels of antibiotics. *Nat Rev Micro* **2014,** *12*, (7), 465-478.

121. Lou, Y.; Yousef, A. E., Adaptation to sublethal environmental stresses protects *Listeria monocytogenes* against lethal preservation factors. *Applied and environmental microbiology* **1997,** *63*, (4), 1252-1255.

122. Tarkpea, M.; Eklund, B.; Linde, M.; Bengtsson, B.-E., Toxicity of conventional, elemental chlorine-free, and totally chlorine-free kraft-pulp bleaching effluents assessed by shortterm lethal and sublethal bioassays. *Environmental Toxicology and Chemistry* **1999,** *18*, (11), 2487-2496.

123. Smolders, E.; McGrath, S. P.; Lombi, E.; Karman, C. C.; Bernhard, R.; Cools, D.; Van den Brande, K.; van Os, B.; Walrave, N., Comparison of toxicity of zinc for soil microbial processes between laboratory-contamined and polluted field soils. *Environmental Toxicology and Chemistry* **2003,** *22*, (11), 2592-2598.

124. Rathnayake, I. V. N.; Megharaj, M.; Krishnamurti, G. S. R.; Bolan, N. S.; Naidu, R., Heavy metal toxicity to bacteria – Are the existing growth media accurate enough to determine heavy metal toxicity? *Chemosphere* **2013,** *90*, (3), 1195-1200.

125. Foss, M. H.; Eun, Y.-J.; Grove, C. I.; Pauw, D. A.; Sorto, N. A.; Rensvold, J. W.; Pagliarini, D. J.; Shaw, J. T.; Weibel, D. B., Inhibitors of bacterial tubulin target bacterial membranes in vivo. *Medchemcomm* **2013,** *4*, (1), 112-119.

126. Hsu, S.-h.; Lin, Y. Y.; Huang, S.; Lem, K. W.; Nguyen, D. H., Synthesis of water-dispersible zinc oxide quantum dots with antibacterial activity and low cytotoxicity for cell labeling. *Nanotechnology* **2013,** *24*, (47), 475102.

127. Lobritz, M. A.; Belenky, P.; Porter, C. B.; Gutierrez, A.; Yang, J. H.; Schwarz, E. G.; Dwyer, D. J.; Khalil, A. S.; Collins, J. J., Antibiotic efficacy is linked to bacterial cellular respiration. *Proceedings of the National Academy of Sciences* **2015,** *112*, (27), 8173-8180.

128. Bérard, A.; Mazzia, C.; Sappin-Didier, V.; Capowiez, L.; Capowiez, Y., Use of the MicroResp™ method to assess Pollution-Induced Community Tolerance in the context of metal soil contamination. *Ecological Indicators* **2014,** *40*, (0), 27-33.

129. Curlevski, N. J.; Artz, R. R.; Anderson, I. C.; Cairney, J. W., Response of soil microbial communities to management strategies for enhancing Scots pine (*Pinus sylvestris*) establishment on heather (*Calluna vulgaris*) moorland. *Plant and soil* **2011,** *339*, (1-2), 413-424.

130. Tlili, A.; Marechal, M.; Montuelle, B.; Volat, B.; Dorigo, U.; Bérard, A., Use of the MicroResp™ method to assess pollution-induced community tolerance to metals for lotic biofilms. *Environmental Pollution* **2011,** *159*, (1), 18-24.

131. Drage, S.; Engelmeier, D.; Bachmann, G.; Sessitsch, A.; Mitter, B.; Hadacek, F., Combining microdilution with MicroResp™: Microbial substrate utilization,

antimicrobial susceptibility and respiration. *Journal of microbiological methods* **2012,** *88*, (3), 399-412.

132. Arain, S.; John, G. T.; Krause, C.; Gerlach, J.; Wolfbeis, O. S.; Klimant, I., Characterization of microtiterplates with integrated optical sensors for oxygen and pH, and their applications to enzyme activity screening, respirometry, and toxicological assays. *Sensors and Actuators B: Chemical* **2006,** *113*, (2), 639-648.

133. Hutter, B.; John, G. T., Evaluation of OxoPlate for real-time assessment of antibacterial activities. *Current microbiology* **2004,** *48*, (1), 57-61.

134. Brewster, J. D., A simple micro-growth assay for enumerating bacteria. *Journal of Microbiological Methods* **2003,** *53*, (1), 77-86.

135. Hazan, R.; Que, Y.-A.; Maura, D.; Rahme, L., A method for high throughput determination of viable bacteria cell counts in 96-well plates. *BMC Microbiology* **2012,** *12*, (1), 259.

136. Hossain, M. J.; Ran, C.; Liu, K.; Ryu, C.-M.; Rasmussen-Ivey, C. R.; Williams, M. A.; Hassan, M. K.; Choi, S.-K.; Jeong, H.; Newman, M.; Kloepper, J. W.; Liles, M. R., Deciphering the conserved genetic loci implicated in plant disease control through comparative genomics of *Bacillus amyloliquefaciens* subsp. *plantarum*. *Frontiers in Plant Science* **2015,** *6*, 631.

137. Ratzlaff, K. L.; Natusch, D. F. S., Theoretical Assessment of Accuracy in Dual Wavelength Spectrophotometric Measurement. *Analytical Chemistry* **1979,** *51*, (8), 1209-1217.

138. Shaff, J.; Schultz, B.; Craft, E.; Clark, R.; Kochian, L., Geochem-EZ: a Chemical Speciation Program With Greater Power and Flexibility. In 2009.

139. Wyrzykowski, D.; Tesmar, A.; Jacewicz, D.; Pranczk, J.; Chmurzyński, L., Zinc(II) complexation by some biologically relevant pH buffers. *Journal of Molecular Recognition* **2014,** *27*, (12), 722-726.

140. Wyrzykowski, D.; Pilarski, B.; Jacewicz, D.; Chmurzyński, L., Investigation of metal–buffer interactions using isothermal titration calorimetry. *J Therm Anal Calorim* **2013,** *111*, (3), 1829-1836.

141. Pettit, L. D.; Powell, K., IUPAC stability constants database. *Chemistry international* **2006**.

142. Oginsky, E. L.; Smith, P. H.; Umbreit, W. W., The Action of Streptomycin .1. The Nature of the Reaction Inhibited. *J Bacteriol* **1949,** *58*, (6), 747-759.

143. Gullberg, E.; Albrecht, L. M.; Karlsson, C.; Sandegren, L.; Andersson, D. I., Selection of a multidrug resistance plasmid by sublethal levels of antibiotics and heavy metals. *mBio* **2014,** *5*, (5), e01918-14.

144. Baker-Austin, C.; Wright, M. S.; Stepanauskas, R.; McArthur, J. V., Co-selection of antibiotic and metal resistance. *Trends in Microbiology 14*, (4), 176-182.

145. Chen, S.; Li, X.; Sun, G.; Zhang, Y.; Su, J.; Ye, J., Heavy Metal Induced Antibiotic Resistance in Bacterium LSJC7. *International Journal of Molecular Sciences* **2015,** *16*, (10), 23390-23404.

146. Holt, K. B.; Bard, A. J., Interaction of Silver(I) Ions with the Respiratory Chain of *Escherichia coli*: An Electrochemical and Scanning Electrochemical Microscopy Study of the Antimicrobial Mechanism of Micromolar Ag^{+}. *Biochemistry* **2005,** *44*, (39), 13214-13223.

147. Gaballa, A.; Helmann, J. D., *Bacillus subtilis* CPx-type ATPases: Characterization of Cd, Zn, Co and Cu efflux systems. *Biometals* **2003,** *16*, (4), 497-505.

148. Van Nostrand, J. D.; Sowder, A. G.; Bertsch, P. M.; Morris, P. J., Effect of pH on the toxicity of nickel and other divalent metals to *Burkholderia cepacia* PR1301. *Environmental Toxicology and Chemistry* **2005,** *24*, (11), 2742-2750.

149. Bondarenko, O.; Juganson, K.; Ivask, A.; Kasemets, K.; Mortimer, M.; Kahru, A., Toxicity of Ag, CuO and ZnO nanoparticles to selected environmentally relevant test organisms and mammalian cells *in vitro*: a critical review. *Arch Toxicol* **2013,** *87*, (7), 1181-1200.

150. Anderson, T. H.; Domsch, K. H., Maintenance Carbon Requirements of Actively-Metabolizing Microbial-Populations under Insitu Conditions. *Soil Biol Biochem* **1985,** *17*, (2), 197-203.

151. Del Giorgio, P. A.; Cole, J. J.; Cimbleris, A., Respiration rates in bacteria exceed phytoplankton production in unproductive aquatic systems. *Nature* **1997,** *385*, (6612), 148-151.

152. Pradas del Real, A. E.; Castillo-Michel, H.; Kaegi, R.; Sinnet, B.; Magnin, V.; Findling, N.; Villanova, J.; Carrière, M.; Santaella, C.; Fernández-Martínez, A., Fate of Ag-NPs in sewage sludge after application on agricultural soils. *Environmental science & technology* **2016,** *50*, (4), 1759-1768.

153. Sun, T. Y.; Bornhöft, N. A.; Hungerbühler, K.; Nowack, B., Dynamic Probabilistic Modeling of Environmental Emissions of Engineered Nanomaterials. *Environmental science & technology* **2016,** *50*, (9), 4701-4711.

154. Brookes, P., The use of microbial parameters in monitoring soil pollution by heavy metals. *Biology and Fertility of soils* **1995,** *19*, (4), 269-279.

155. Bérard, A.; Mazzia, C.; Sappin-Didier, V.; Capowiez, L.; Capowiez, Y., Use of the MicroResp™ method to assess pollution-induced community tolerance in the context of metal soil contamination. *Ecological Indicators* **2014,** *40*, 27-33.

156. Vittori Antisari, L.; Carbone, S.; Gatti, A.; Vianello, G.; Nannipieri, P., Toxicity of metal oxide (CeO_2, Fe_3O_4, SnO_2) engineered nanoparticles on soil microbial biomass and their distribution in soil. *Soil Biology and Biochemistry* **2013,** *60*, 87-94.

157. Romero-Freire, A.; Aragón, M. S.; Garzón, F. M.; Peinado, F. M., Is soil basal respiration a good indicator of soil pollution? *Geoderma* **2016,** *263*, 132-139.

158. Lowry, G. V.; Espinasse, B. P.; Badireddy, A. R.; Richardson, C. J.; Reinsch, B. C.; Bryant, L. D.; Bone, A. J.; Deonarine, A.; Chae, S.; Therezien, M., Long-term transformation and fate of manufactured Ag nanoparticles in a simulated large scale freshwater emergent wetland. *Environmental science & technology* **2012,** *46*, (13), 7027-7036.

159. Brannen, P.; Kenney, D., Kodiak®—a successful biological-control product for suppression of soil-borne plant pathogens of cotton. *Journal of Industrial Microbiology and Biotechnology* **1997,** *19*, (3), 169-171.

160. Lugtenberg, B.; Kamilova, F., Plant-Growth-Promoting Rhizobacteria. *Annual Review of Microbiology* **2009,** *63*, (1), 541-556.

161. Duan, J.; Jiang, W.; Cheng, Z.; Heikkila, J. J.; Glick, B. R., The complete genome sequence of the plant growth-promoting bacterium *Pseudomonas* sp. UW4. *PLoS One* **2013,** *8*, (3), e58640.

162. Chen, C.-Y.; Nace, G. W.; Irwin, P. L., A 6× 6 drop plate method for simultaneous colony counting and MPN enumeration of *Campylobacter jejuni, Listeria monocytogenes*, and *Escherichia coli*. *Journal of Microbiological Methods* **2003,** *55*, (2), 475-479.

163. Starnes, D. L.; Unrine, J. M.; Starnes, C. P.; Collin, B. E.; Oostveen, E. K.; Ma, R.; Lowry, G. V.; Bertsch, P. M.; Tsyusko, O. V., Impact of sulfidation on the bioavailability and toxicity of silver nanoparticles to Caenorhabditis elegans. *Environmental Pollution* **2015,** *196*, 239-246.

164. Shen, M.-H.; Zhou, X.-X.; Yang, X.-Y.; Chao, J.-B.; Liu, R.; Liu, J.-F., Exposure Medium: Key in Identifying Free Ag+ as the Exclusive Species of Silver Nanoparticles with Acute Toxicity to Daphnia magna. *Scientific Reports* **2015,** *5*, 9674.

165. Glandorf, D. C. M.; Brand, I.; Bakker, P. A. H. M.; Schippers, B., Stability of rifampicin resistance as a marker for root colonization studies of *Pseudomonas putida* in the field. *Plant and Soil* **1992,** *147*, (1), 135-142.

Vita

Ricky Woodrow Lewis

Education

University of Kentucky

- Ph.D., Soil Science, 2012-present
- M.Sc., Plant and Soil Science, 2011
- B.Sc., Environmental Science, 2008

Refereed Journal Articles – Accepted

- **2015** – Chun Chen, Jason M. Unrine, Jonathan D. Judy, **Ricky W. Lewis**, Jing Guo, Dave H. McNear Jr., Olga V. Tsyusko. Toxicogenomic responses of the model legume Medicago truncatula to aged biosolids containing a mixture of nanomaterials (TiO_2, Ag and ZnO) from a pilot wastewater treatment plant. Environmental Science & Technology 49(14):8759-68

- **2015** – Jonathan D. Judy, David McNear, Chun Chen1, **Ricky W. Lewis**, Olga V. Tsyusko, Paul M. Bertsch, William Rao, John Stegemeier, Gregory V. Lowry, Steve P. McGrath, Mark Durenkamp and Jason M. Unrine. Nanomaterials in biosolids inhibit nodulation, shift microbial community composition, and result in increased metal uptake relative to bulk metals. Environmental Science & Technology 49(14):8751-8

- **2014** – Julius B. Adewopo, Christine VanZomeren, Rupesh K. Bhomia, Maya Almaraz, Allan R. Bacon, Emily Eggleston, Jonathan D. Judy, **Ricky W. Lewis**, Mary Lusk, Bradley Miller, Colby Moorberg, Elizabeth Hodges Snyder and Mary Tiedeman. "Top-Ranked Priority Research Questions for Soil Science in the 21 Century." Soil Science Society of America Journal 78.2: 337-347

- **2012** – **Ricky W. Lewis,** Guiliang Tang, and David H. McNear Jr. Morphological and genetic changes induced by excess Zn in roots of *Medicago truncatula* A17 and a Zn accumulating mutant. BMC Research Notes, 5:657

Book Chapter

- **2009** – **Ricky W. Lewis**, Venu Mendu, David H. McNear Jr., Guiliang Tang. Roles of MicroRNAs in Plant Abiotic Stress. Molecular Techniques in Crop Improvement: 357-372

Presentations

Oral Presentations

- **2015 – Ricky W. Lewis,** David H. McNear Jr., Paul M. Bertsch. High Throughput Assessment of Respiration Stress Induced by Manufactured Nanomaterials and Metal Ions in Bacillus subtilis**.** The Bill Witt Semi-Annual Graduate Student Symposium. Lexington, Kentucky

- **2014 – Ricky W. Lewis,** David H. McNear Jr., Paul M. Bertsch. Assessing Sub-lethal Responses to Metals in Plant Growth Promoting Rhizobacteria**.** University of Kentucky Spring Minisymposium. Lexington, Kentucky

- **2013 – Ricky W. Lewis,** David H. McNear Jr., Paul M. Bertsch. Toxicity of Manufactured Nanomaterials to Plant Growth Promoting Rhizobacteria. University of Kentucky Spring Minisymposium

- **2012** – **Ricky W. Lewis,** David H. McNear Jr., Paul M. Bertsch. Manufactured Nanomaterials and Plant Growth Promoting Rhizobacteria: Building a Microbial Perspective of the Nano Age. Soil Science Society of America International Annual Meeting. Cincinnati, OH.

Poster Presentations

- **2015** – **Ricky W. Lewis,** David H. McNear Jr., Paul M. Bertsch. A Combined Respiration and Viability Based Test for Assessing Sublethal Stress in Microorganisms. American Society for Microbiology 115th General Meeting. New Orleans, LA
- **2008– Ricky W. Lewis**, M. Grusak, D.J. Sherrier and D.H. McNear. The influence of soil metal concentrations on root nodule formation and function. 7th Annual Posters-at-the-Capitol, Frankfort, KY

- **2007** – **Ricky W. Lewis**, D.H. McNear, M. Grusak and D.J. Sherrier. The influence of soil metal concentrations on root nodule formation and function Soil Science Society of America International Annual Meeting, New Orleans, LA